

# Saph Pani

Enhancement of natural water systems and  
treatment methods for safe and sustainable  
water supply in India



Project supported by the European Commission within the Seventh  
Framework Programme Grant agreement No. 282911



## Deliverable D 5.3

Synthesis of modelling, monitoring and  
optimising natural treatment systems in India



|  |  |
|--|--|
| <b>Work package</b>  | WP5 Modelling and system design  |
| <b>Deliverable number</b>  | D 5.3  |
| <b>Deliverable title</b>   | Synthesis of modelling, monitoring and optimising natural treatment systems in India   |
| <b>Due date</b>  | Month 36   |
| <b>Actual submission date</b>  | Month 36   |
| <b>Start date of project</b>   | 01.10.2011   |
| <b>Participants (Partner short names)</b>  | ANNA, BRGM, DHI-WASY, FUB, HTWD, IITR, IWMI, KWB, NGRI, NIH  |
| <b>Authors in alphabetic order</b>   | Ahmed S., Alazard M., Bhola P., Boisson A., Dewandel B., Elango L., Feistel U., Fischer S., Frommen T., Ghosh N.C. , Grischek Th., Groeschke M., Grützmacher G., Hamann E., Indu S.N., Kloppmann W., Maréchal J.-C., Monninkhoff B., Perrin J., Pettenati M., Picot-Colbeaux G., Rajaveni S. P., Sandhu C., Sarah S., Schneider M., Sklorz S., Thiéry D., Zabel A. K., |
| <b>Contact for queries</b>   | Wolfram Kloppmann<br>BRGM, LAB/ISO, 3 Av. Claude Guillemin, F-45060 Orléans, France<br>Phone: +33 2 38643915<br>Email: w.kloppmann@brgm.fr   |
| <b>Dissemination level:</b><br><b>(PUBlic, Restricted to other Programmes Participants, REstricted to a group specified by the consortium, COntidential- only for members of the consortium)</b> | PU   |
| <b>Deliverable Status:</b>   | Revision 1.0   |

## Content

|       |   |    |
|-------|---|----|
| 1     | Maheshwaram MAR system percolation tank model.....                                | 1  |
| 1.1   | Abstract .....  | 2  |
| 1.2   | Introduction.....   | 2  |
| 1.3   | Existing numerical models integrating surface water-groundwater interactions..... | 4  |
| 1.4   | Conceptual model of Maheshwaram percolation tank.....                             | 6  |
| 1.5   | Implementation in the MARTHE code .....   | 8  |
| 1.6   | Test simulations .....  | 10 |
| 1.7   | Conclusion and perspective.....   | 14 |
| 1.8   | Acknowledgements .....  | 16 |
| 1.9   | References .....  | 16 |
| 2     | Maheshwaram MAR system reactive transport model .....                             | 22 |
| 2.1   | Abstract .....  | 23 |
| 2.2   | Introduction.....   | 23 |
| 2.3   | Results and Discussion .....  | 26 |
| 2.4   | Conclusions .....   | 27 |
| 2.5   | Acknowledgements .....  | 28 |
| 2.6   | References .....  | 28 |
| 3     | Chennai MAR/SAT system.....   | 30 |
| 3.2   | Abstract .....  | 31 |
| 3.3   | Introduction.....   | 32 |
| 3.4   | Description of Study area .....   | 33 |
| 3.5   | Data .....  | 34 |
| 3.6   | Geology.....  | 35 |
| 3.7   | Hydrogeology.....   | 36 |
| 3.8   | Methodology and Model description.....  | 37 |
| 3.8.1 | Surface water model.....  | 37 |
| 3.8.2 | Groundwater flow model .....  | 38 |
| 3.8.3 | Coupling Concept .....  | 40 |

|       |   |    |
|-------|---|----|
| 3.8.4 | Density-Dependent modelling .....                                 | 40 |
| 3.9   | Results and discussion .....                                      | 41 |
| 3.9.1 | Surface water model.....  | 41 |
| 3.9.2 | Groundwater flow model .....                                      | 42 |
| 3.9.3 | Managed Aquifer Recharge .....                                    | 43 |
| 3.9.4 | Density-Dependent model .....                                     | 45 |
| 3.10  | Conclusion and future work.....                                   | 46 |
| 3.11  | Acknowledgements .....  | 47 |
| 3.12  | References .....  | 47 |
| 4     | Haridwar RBF system .....   | 49 |
| 4.1   | Abstract .....  | 50 |
| 4.2   | Introduction.....   | 50 |
| 4.3   | Motivation .....  | 52 |
| 4.4   | Model set-up and Calibration.....                                 | 53 |
| 4.4.1 | Data collection, water levels and RBF well abstraction rates..... | 53 |
| 4.4.2 | Interpolation of undisturbed groundwater levels.....              | 54 |
| 4.4.3 | Model set-up.....   | 55 |
| 4.4.4 | Model boundaries .....  | 56 |
| 4.4.5 | Steady-state model calibration and particle tracking .....        | 57 |
| 4.5   | Results.....  | 58 |
| 4.6   | Conclusions .....   | 60 |
| 4.7   | References .....  | 61 |
| 5     | New Delhi RBF system .....  | 62 |
| 5.1   | Abstract .....  | 63 |
| 5.2   | Introduction.....   | 63 |
| 5.3   | Materials and Methods .....                                       | 66 |
| 5.3.1 | Sediment sampling and analyses.....                               | 66 |
| 5.3.2 | Experiments .....   | 67 |
| 5.3.3 | Modelling .....   | 70 |
| 5.4   | Results.....  | 73 |
| 5.4.1 | Sediment analyses .....   | 73 |
| 5.4.2 | Tracer Tests and Transport Parameters .....                       | 74 |
| 5.4.3 | Ammonium.....   | 76 |

|       |  |     |
|-------|--|-----|
| 5.5   | Discussion .....   | 82  |
| 5.5.1 | Sediment Characteristics.....  | 82  |
| 5.5.2 | Ammonium Transport .....   | 83  |
| 5.6   | Summary and Conclusion .....   | 85  |
| 5.7   | References .....   | 86  |
| 6     | Musi River CWL system .....  | 91  |
| 6.1   | Abstract .....   | 92  |
| 6.2   | Introduction.....  | 92  |
| 6.2.1 | Hydrodynamic characteristics of a wetland .....                                      | 93  |
| 6.2.2 | Waste water irrigation and natural treatment.....                                    | 94  |
| 6.2.3 | The concept of soil aquifer treatment (SAT) .....                                    | 95  |
| 6.2.1 | The Musi wetland: A case of wastewater impacted riverine agriculture<br>wetland..... | 95  |
| 6.3   | Study area.....  | 97  |
| 6.3.1 | Objective.....   | 98  |
| 6.4   | Distributed hydrologic modelling: Application of MIKE SHE.....                       | 99  |
| 6.4.1 | MIKE SHE model .....   | 99  |
| 6.4.2 | Musi model conceptualization.....  | 103 |
| 6.4.3 | Model setup and parameterization .....   | 105 |
| 6.4.4 | Model calibration and validation .....   | 108 |
| 6.5   | Results and Discussions.....   | 110 |
| 6.5.1 | Water table .....  | 111 |
| 6.5.2 | Water balance.....   | 113 |
| 6.5.1 | Irrigation.....  | 116 |
| 6.5.2 | Return flow.....   | 116 |
| 6.5.3 | Groundwater recharge .....   | 117 |
| 6.5.4 | Groundwater exchange with MIKE 11- Musi river and wastewater canal ..                | 118 |
| 6.6   | Conclusions and recommendations .....  | 119 |
| 6.7   | Application of the model .....   | 120 |
| 6.8   | Acknowledgements .....   | 120 |
| 6.9   | References .....   | 120 |

## 1 Maheshwaram MAR system percolation tank model

*Title:* "Modelling managed aquifer recharge capacity of crystalline aquifers in semi-arid context (South India): Implementing natural percolation tank dynamics into MARTHE code"

*Authors (BRGM, NGRI):* Picot-Colbeaux Géraldine, Thiéry Dominique, Pettenati Marie, Boisson Alexandre, Perrin Jérôme, Sarah Sarah, Dewandel Benoît, Maréchal Jean-Christophe, Ahmed Shakeel, Kloppmann Wolfram

*Journal:* to be decided

*Status:* to be submitted

## 1.1 Abstract

To cope with groundwater over-exploitation due to intensive exploitation for irrigation, managed aquifer recharge (MAR) is an attractive concept for increasing the groundwater resource. The number of recharge structures such as percolation tanks, check dams, dug-wells, is increasing in the context of the Indian crystalline basement under semi-arid climate. To assess the capacity of MAR, the three-dimensional transient groundwater numerical MARTHE code was optimized by implementing three-dimensional non-perennial surface water bodies in continuity with groundwater via an unsaturated zone. Implementation includes the spatiotemporal evolution of the natural percolation tanks (i.e., volume and geometry) linked to topography, taking into account heavy rainfalls during monsoon, evapotranspiration, infiltration, runoff, and groundwater dynamics. Part of the rain water stored in such a tanks during the monsoon season infiltrates into the soil (variably-saturated media) and reaches the aquifer whereas part is evaporated. Theoretical cases show that the new implementation is able to simulate the relation between surface water and groundwater while respecting the water balance. The three-dimensional MARTHE model will be applied to a study site in order to demonstrate its use as decision-making tool for assessing the quantitative effects of MAR on groundwater resources at the watershed scale.

*Keywords* : Numerical model, Surface water - groundwater, crystalline aquifer, MARTHE code, Managed Aquifer Recharge (MAR), percolation tank.Site description

## 1.2 Introduction

Managed aquifer recharge (MAR) in India is as old as the irrigated agriculture in the arid and semi-arid region (Sakthivadivel, 2008) in order to store rainwater both on the ground and underground. These processes were supported as early 600 A.D. by the official authorities notably the kings. These structures are called percolation tanks. Today more than 500 000 tanks are identified all over India. These tanks are thousands of years old and are used for irrigation purposes, livestock and human uses (drinking, bathing, and washing). Aquifer recharge can be ensured by infiltration from these tanks or through dug wells to provide a clean water supply throughout the year with natural filtering (DHAN Foundation, 2002).

The MAR Movement in India (Sakthivadivel, 2007), a successful example of community based effort to manage water resources, can be divided into four phases. The first phase is associated with the period before the “green revolution” (i.e. 1960) when the groundwater resources were not overexploited and where the knowledge about MAR was limited to local communities and their ancestral practices. During the second period, between 1960 and 1990, characterized by overexploitation of groundwater, scientific concepts of hydrology and hydrogeology were developed and public and government started to realize the importance of MAR to reduce groundwater levels depletion. During this period, two major studies were realized. The first provided a synthesis of research

and development works carried out in India in the field of MAR by a team of experts under the Rajiv Gandhi National Drinking Water Mission, constituted by the Ministry of Rural Areas and Development, Government of India. The second study, by the Indian Standard Organization (ISO), produced technical guidelines and specifications for MAR. The third period (1990 to date) is marked by the dramatically increasing water scarcity and by declining groundwater levels in many locations in India and the beginning of a strong action of public and government to promote and apply MAR facilities. Major events characterize this phase: determination of local communities and government to take up MAR through dug and bore wells, check dams and percolation tanks, on a mass scale; promulgation of the groundwater regulation act to implement rainwater harvesting schemes for recharge in metropolitan areas; public awareness-rising by media and non-governmental organizations. Today, the fourth period is dominated by the recent technical innovation with large scale pumping equipment and pipelines becoming available and affordable. The master plan of the Central Groundwater Board (CGWB, 2002) of India aims to build 3.9 million recharge structures (percolation tanks, check dams, trenches and defunct dug wells (Dewandel et al., 2007) nationwide over a period of 10 years. For example, the State of Andhra Pradesh has set the policy objective to increase aquifer recharge from 9 % of total rainfall under natural conditions to 15 % by the year 2020. There is a great need for scientific studies which evaluate the efficiency of these recharge structures at local to catchment scale and their impact on groundwater quantity and quality.

MAR includes a wide variety of different techniques (Gale and Dillon, 2005), through which water (e.g. stormwater, surface water or treated waste water) is intentionally introduced into an aquifer in the aim to store, treat the water or build up a hydraulic barrier against salt water intrusion. Subsurface passage is able to cope with many water-related hazards of high relevance in developing and newly industrialized countries (e.g. suspended solids, pathogens, algal toxins, Grützmacher et al., 2010). In addition, MAR gives the ability to manage highly varying flows, using the aquifer as a storage reservoir into which excess water, e.g. during monsoon periods, is infiltrated and recovered at times of higher demand (Gale et al., 2006).

The implementation of natural treatment and fresh water storage systems require an initial feasibility study in the regional context (Merritt, 1985). Groundwater models provide the unique possibility to preview the feasibility and performance of such a natural treatment system. In the regional context, such models are used to choose an optimal site, to configure an appropriate injection-recovery system and to optimize operating conditions in a way to meet fixed water quantity and quality targets (Kloppmann et al., 2009).

The need of models taking into account groundwater and surface water behavior at the scale of percolation tanks in a specific semi-arid climatic context cannot be overlooked. Yet, few tools include, through different approaches, interactions between groundwater and stored surface water, often defined as lake, wetland or reservoir.

The aim of our work is to provide a robust model adapted to the specific requirements of MAR in the semi-arid crystalline aquifer context of India illustrated by a case study in the



Maheshwaram watershed in the framework of the EU 7th Framework Programme project Saph Pani (<http://www.saphpani.eu/>)

### 1.3 Existing numerical models integrating surface water-groundwater interactions

Some of the modelling tools capable of addressing surface water – groundwater interactions are detailed in the following to provide an overview of the implemented features and their capacity of simulating and optimising the MAR systems built or planned in Indian's watershed.

**BASINS** or **GFLOW** tools integrate environmental data, analytical tools, and modelling programs under a Geographic Information System (GIS) environment. Tweed et al. (2009) integrate satellite remote sensing with on-ground field monitoring data to perform mapping and analyze water balance. This approach provides spatial and temporal datasets required for the determination of the evolution of lake-groundwater interactions over time. Zlotnik et al. (2009) provide a framework for identifying flow regimes of groundwater-dominated lakes using the concepts of gradient ratio and topo-hydrologic offset.

Mark Bakker (2004) describes two analytic solutions for steady flow problems using Mathieu functions: 1) groundwater flow to shallow elliptical lakes with leaky lake beds in a single-aquifer, 2) groundwater flow through elliptical cylinder inhomogeneities in a multi-aquifer system. The lake could be simulated by the steady influx assumption using a groundwater code (Mylopoulos et al., 2007). Boswell and Olyphant (2007) demonstrate the feasibility of using a variably-saturated groundwater flow model to evaluate the hydrologic conditions in a groundwater controlled wetland restoration site. The maximum and minimum areas of ponding could be generated.

In more sophisticated approaches, surface models or watershed models are coupled with groundwater models to create a combined tool. The integrated hydrology model (**InHM**) solves fully coupled equations for variably saturated porous media flow and overland flow (VanderKwaak, 1999). This fully coupled, integrated surface water/groundwater model was used to study hydrologic controls on lake-groundwater interaction in subhumid plains (Smerdon et al., 2007). It goes a step further in the modelling of lake-groundwater exchange, by using a numerical model able to determine the location and depth of surface water bodies (i.e., lakes and tanks) and surface-subsurface exchange fluxes, without prior definition. It is a fully coupled approach allowing for lake-groundwater interaction without defining the studied lake as a boundary condition. Yu, and Schwartz (1998) developed and applied a code called Hydrologic Model System (**HMS**) which simulates basin-scale hydrologic processes in response to weather and climatic forcing. Four modules compose HMS: a soil hydrologic model, a terrestrial hydrologic model, a ground-water hydrologic model, and a channel ground-water interaction model. No interaction between the simulated basin groundwater flow system and the interbasin regional groundwater system is included (i.e., no groundwater flow boundaries are considered). The hydrologic model is applied on climate-hydrologic simulations with explicit changes in individual rivers, lakes,

wetlands and water tables (Yu et al., 1999, 2006). Graham and Butts (2005) developed the integrated watershed model **MIKE SHE** for assessing wetland functioning which requires detailed analysis of groundwater/surface water interaction. Major processes of the hydrologic cycle are included: evapotranspiration, runoff, unsaturated flow, groundwater flow, channel flow and their interactions. Groundwater flow in saturated zone is calculated by 1) a fully implicit, three-dimensional finite-difference scheme to calculate spatial and temporal variations of the hydraulic head in the saturated groundwater zone or 2) a linear reservoir approach. However, unsaturated flow is considered only in vertical 1D. In Demetriou and Punthakey's (1999) application of MIKE SHE code for groundwater management, the effect of recycling ponds is implemented in the model as points, which leak into the aquifer with a fixed constant recharge rate and area. The analytic solutions used in GFLOW limit the application though linked with MODFLOW groundwater model. Using GFLOW and MODFLOW (Feinstein et al., 2003), this association of models has no application for problems considering a transient state or detail knowledge of the three-dimensional head and flows near the lake-ground water interface.

Approaches for modelling lake-groundwater interactions have evolved significantly from early simulations using fixed lake stages specified as constant head, towards sophisticated coupling between surface subsurface models and groundwater models or implementation of specific modules as the LAK package for MODFLOW. Meritt and Konikow (2000) and Cheng and Anderson (1993) use a module called LAK3 to simulate Lake-Aquifer Interaction using the MODFLOW code. Performance was tested on hypothetical groundwater flow systems. The relative hydraulic heads and conductances of the lakebed determine the water exchange rate between lake and adjacent aquifer. The lake is defined by several grid cells which may become "dry" or "wet" depending on the aquifer head movement. The rates of precipitation, evaporation, and runoff allow calculation of the water balance for each lake which, in turn, determines the exchanges with the aquifer. The storage capacity of the lake is determined from the lake geometry. The specification of lake cells and its associated volumes define the position and spatial extent of the lake volume in a three-dimensional grid. **MARTHE v7.0** is a complete numerical hydrosystem code designed for hydrodynamic and hydrodispersive modelling of groundwater flow and mass energy transfer in porous media (Thiéry, 1990; 1993; 1995; 2010a). This code allows the three-dimensional simulation of flow and transport under saturated conditions and in the vadose zone using a finite volume method for hydraulic calculations (Thiéry, 2010b) and integrates a hydroclimatic balance (precipitation, evapotranspiration, runoff, infiltration, recharge) using the **GARDENIA** scheme (Thiéry, 2010c). Interaction between surface, subsurface and groundwater is implemented in MARTHE v7.0 and has been applied to river basins to predict the influence of climatological changes on river flows and to anticipate floods (Thiéry and Amraoui, 2001; Habets et al., 2010; Thiéry, 2010d). Furthermore, MARTHE was applied in the context of MAR systems (Gaus et al., 2007; Klopmann et al., 2012). However in the release of MARTHE used for earlier studies, surface water is connected to the river network and is

allowed to flow out of the hydrosystem, but it cannot be stored in topographic depressions and re-infiltrate to the aquifer. **HYDRUS** is a fully interactive water, solute and heat transport, finite element solver for unsaturated and saturated porous media (Šimůnek, 1999). Ponding boundary condition was implemented as a modification of the atmospheric boundary condition in the Constructed Wetlands 2D module (**CW2D**) developed as an extension of the HYDRUS-2D (Langergraber and Šimůnek, 2005; Langergraber, 2008). When 'ponding' occurs, it is assumed that water accumulates at the soil surface and that, at the end of the loading period, the remaining water stored on the surface infiltrates into the soil profile. The water mass balance is used to calculate the reduction of the surface pressure head until all water infiltrates into the substrate and the pressure head at the surface becomes negative.

Few codes exist that have been designed and developed to fully integrate surface water and groundwater (Graham and Butts, 2005). Watershed models or surface-subsurface models are often used only to provide flux boundary conditions useful for a three-dimensional groundwater model or consider limited groundwater processes: watersheds or sub-watersheds are assumed to be isolated, storage effects are not considered, or horizontal flow systems can be simulated only in saturated conditions. Though numerical codes evolved since early simulations, in the existing groundwater codes such as MODFLOW, **FEFLOW**, or HYDRUS-3D, interactions with atmospheric or surface water are only taken into account through links to other codes. In this study, because of the semi-arid climate and the long period of over-exploitation of the crystalline aquifer, and also because irrigation and abstraction can influence natural recharge and discharge, thereby changing the flow regime in a catchment, the existing models are not appropriate.

#### 1.4 Conceptual model of Maheshwaram percolation tank

The Maheshwaram watershed is located south of Hyderabad in the State of Andhra Pradesh, India (Figure 1.A). It covers an area of 53 km<sup>2</sup> under a semi-arid climate with a wet monsoon season (Kharif) between June and October, and a dry season (Rabi) from November to May. Annual rainfall is around 750 mm with 90% of the rain occurring during the monsoon, whilst mean annual temperature is 26 °C, although daily temperatures can reach 45 °C during the dry season (Rabi). The high potential evapotranspiration rate is 1800 mm/year. The surface drainage network is dry most of the time. The geology of the Maheshwaram watershed consists of Archean granite that has been exposed to deep weathering processes. The typical weathering profile comprises (Dewandel et al., 2006):

- A thin layer of red soil (~50 cm),
- 1-3 m of sandy regolith,
- 10-15 m of laminated saprolite and clay beds (fissure filling) forming the capacitive layer of the aquifer; due to overexploitation, this layer is generally unsaturated,
- Fissured granite (15-20 m) which constitutes the transmissive aquifer with a low specific yield (Maréchal et al., 2004),

- Unfractured granite (bedrock) that constitutes the base of the aquifer.

This watershed has an impressive number wells (>900) mostly used for the irrigation due to the India's "green revolution" in the 1970's which has encouraged the access to irrigation and the use of fertilizers (Maréchal et al., 2006; Pettenati et al., 2013). This high level of groundwater exploitation has induced unbalanced state of the crystalline rock aquifer (Maréchal et al., 2006). Recently (since 2006), changes in land use have occurred because of the new Hyderabad international airport located less than 10 km away. The area is expected to become a peri-urban area within the coming years as significant housing projects are planned. But intensive groundwater exploitation for irrigation has resulted in aquifer over-exploitation (Maréchal et al., 2006) and deterioration of groundwater quality (fluoride above the maximum permissible limit of 1.5 mg/L, salinization (Perrin et al., 2012) and agricultural pollutants inputs). The increase in F-concentrations observed over the last few years (Purushotham et al., 2011) is responsible of health problems like dental fluorosis among the local children (Bouzit et al., submitted).

One of the main experimental percolation tanks relevant for MAR is located around the town of Maheshwaram near the Tummur village (Figure 1.B). A sophisticated monitoring program of groundwater levels and chemistry has been implemented around and within the Tummur percolation tank built to enhance recharge and groundwater quality in the underlying overexploited hard-rock aquifer (Boisson et al., 2013). Newly acquired detailed data complete the extensive previous studies on crystalline aquifers carried out by the Indo French Center for Groundwater Research (Maréchal et al., 2004; Dewandel et al., 2006; Perrin et al., 2009). Assessing water fluxes in this system increases indeed the understanding of the role of the weathering zone for groundwater recharge, flow and storage. A conceptual model of the Tummur tank is provided by Boisson et al. (2013) who use a water balance approach to define relationships between water level, tank area, and tank volume considering precipitation and evapotranspiration and estimated infiltration. The rainwater is stored at the surface, where artificial topographic modifications delays superficial water flow during the monsoon season. Part of the water flows into the soil and deeper, toward groundwater and another part of water is evaporated during monsoon and dry periods (Figure 1.C).

Groundwater modelling is commonly used to design operational MAR systems. The type and dimension of this system will depend on the available water and the storage capacity of the percolation tank as well as on the target pumping rates. For tank management, a major challenge is to develop a hydrosystem modelling tool able to include the spatiotemporal evolution of the tank volume and extension determined by topography, heavy monsoon rainfalls, evapotranspiration, infiltration, runoff and groundwater dynamic while respecting hydraulic mass balance. Such a modelling tool will enable the evaluation of quantitative impact of MAR on the aquifer flow. The conceptual model (Figure 1.D) will be implemented into the numerical hydrogeological MARTHE code and tested on Tummur percolation tank.

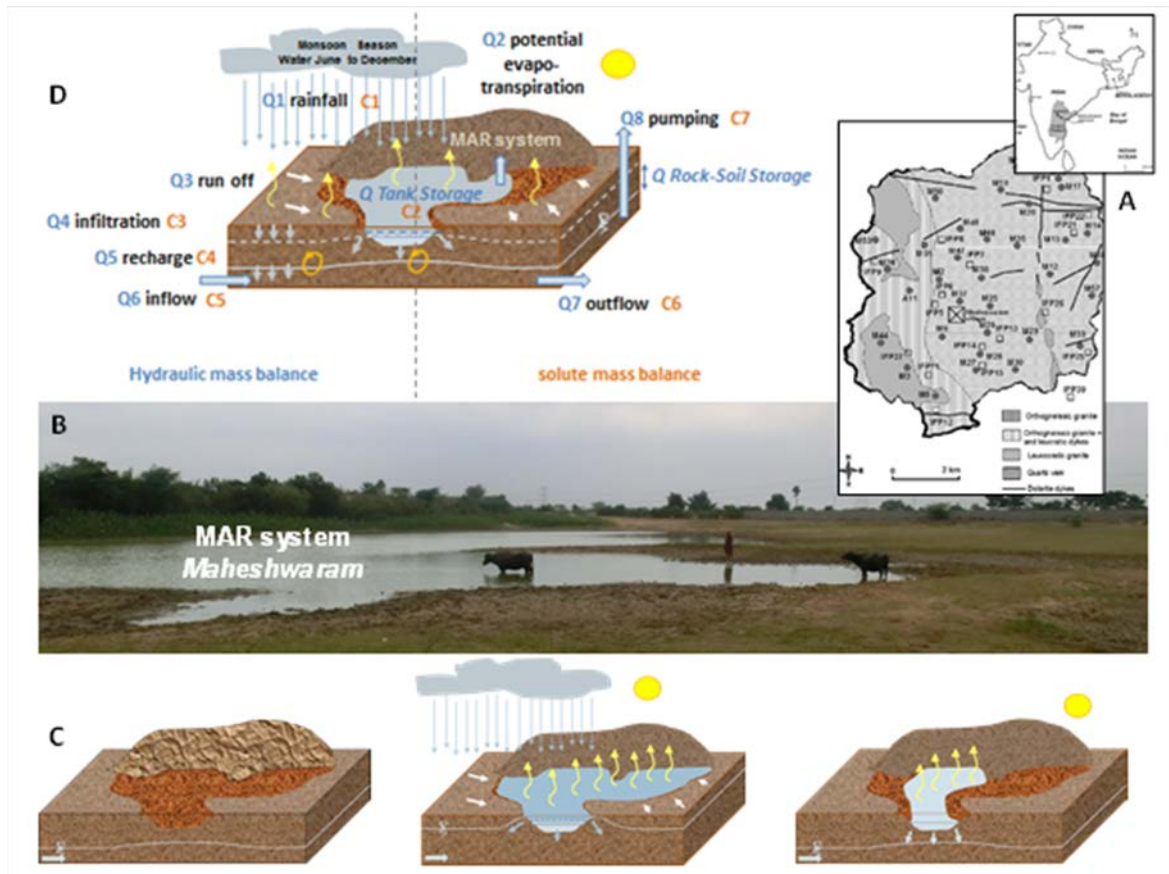


**Figure 1 Conceptual model of spatiotemporal evolution of the Tummur percolation tank studied in Maheshwaram in accordance with hydraulic balance (Q: flow rate) and solute mass balance (C: solute concentration)**

### 1.5 Implementation in the MARTHE code

In the latest release of MARTHE currently being developed, the percolation tanks, considered as lakes, are implemented at the surface of the model, above the topography (Figure 2). They do not belong to the saturated domain or to the vadose zone. There are some analogies with a river tributary. It consists of a set of cells. Each of these cells has a different bottom elevation, which corresponds to the topography of the locally outcropping aquifer surface. This bottom overlies the lakebed which is characterized by a local thickness and hydraulic conductivity. A lake is characterized by a single water elevation which varies with time. It can get partly dry or totally dry due to evaporation, infiltration and pumping. Parts of the lake get dry when the lake water level is lower than the local lakebed elevation.

A lake has interactions with:

- The climatic conditions: it receives water from rainfall over its whole surface area, and it is evaporated directly in the cells that are not dry,

- The river network: it may receive water from upstream river tributaries, and overflow into downstream tributaries,
- The surface runoff: the effective rainfall, calculated in the model cells located upstream of the lake, flows into the lake,
- The groundwater or the vadose zone: the exchanges occur where the lake is not dry. The exchange scheme is quite similar to the river exchange scheme. In the simpler cases the exchange flow is computed, using Darcy's law (Equation 1). In cells where in the underlying aquifer the hydraulic head is lower than the lakebed, a different scheme is used when the vadose zone is not simulated explicitly (Equation 2). Where the lake is dry, evaporation may apply to the underlying vadose zone or to the aquifer according to its depth.
- The anthropic injection of water or the pumping rate inside the lake: the actual pumping is decreased or nil when the lakes gets dry.

$$Q_{Exch} = Cell\_Area \cdot K_B \cdot \frac{(H_L - H_{Aq})}{Thickn} \quad \text{Eq. 1}$$

$$Q_{Percol} = Cell\_Area \cdot K_B \cdot \frac{(H_L - H_B)}{Thickn} \quad \text{Eq. 2}$$

With :

$K_B$  = Lakebed hydraulic conductivity

$Thickn$  = Lakebed thickness

$H_L$  = Absolute lake level

$H_{Aq}$  = Hydraulic head water table level) in the underlying aquifer

$H_B$  = Lake bottom elevation

$Cell\_Area$  = Cell surface area

$Q_{Exch}$  = Exchange flow from the lake to the aquifer

$Q_{Percol}$  = Percolation flow from the lake to the unconnected aquifer level

The calculation process is iterative due to the numerous nonlinearities: evaporation and infiltration depend on the lake surface area, and/or on the lake elevation, which in turn depends on the volume, which depends on rainfall, evaporation, infiltration etc. For each iteration the model estimates the evaporative flow and the exchange flow in each cell. Then, for each lake, the non-linear equation of the conservation of flow (Equation 3) is solved for the lake level, using a Newton-Raphson technique.

$$\text{Storage} = \text{Rain} - \text{Evap} + \text{Runoff} + \text{Upstream} - \text{Downstream} + \text{Inject} - \text{Pumping} \quad \text{Eq. 3}$$

The mass transport, which in MARTHE is fully coupled with flow in the vadose zone, the groundwater and the river network, will also be coupled with the lakes interactions. Each lake is characterized by a single water elevation resulting from rainfall, evaporation, runoff, aquifer exchange, rivers exchange. Resulting from all those components, a lake will have a single concentration for a given dissolved chemical species. This hypothesis, which is a simplification of the real processes, is valid when the lake is well mixed.

The flow and transport calculations may be performed in steady state or in transient state. When the calculations are carried out in transient state, the time step may be constant or adapted to the flow variations. Typically a time step of the order of magnitude of one day will be used, but time steps varying from some minutes to some weeks are allowed.

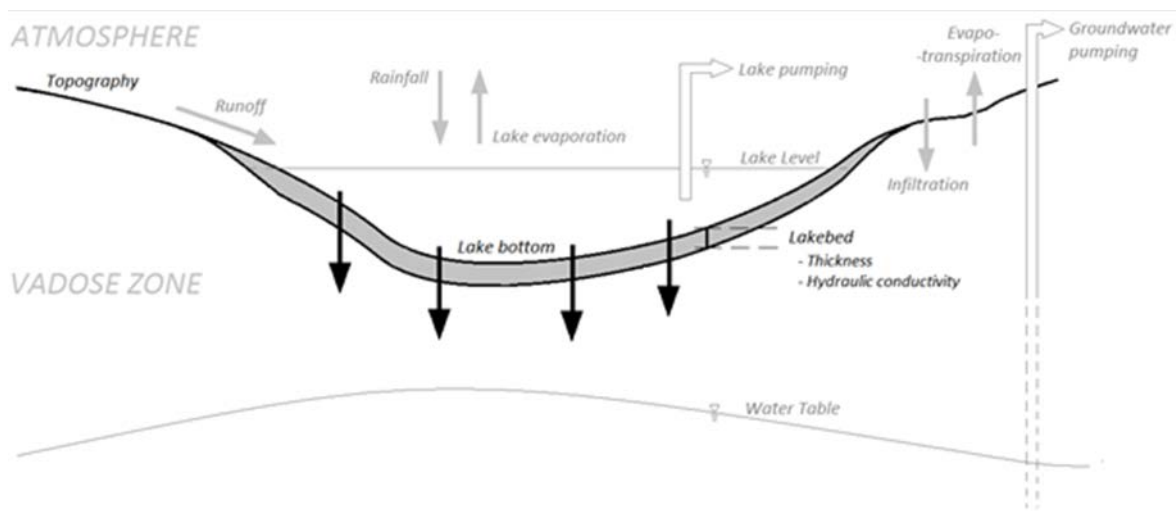


**Figure 2 Concept used for implementing managed aquifer recharge by percolation tank (designed as lake) and groundwater interactions**

## 1.6 Test simulations

The numerical code was verified with respect to two simple analytical solutions, and by comparison with a hypothetical case representing the filling of a lake during a heavy rainfall period, followed by a drying period due to evaporation and percolation.

Two theoretical cases were then tested and compared with analytical solutions:

Natural drainage of a lake into a confined aquifer, following a sudden rise of the lake: Cooper *et al.* (1967) solution.

- Pumping in a lake initially at the same level as the aquifer: Papadopoulos and Cooper (1967) solution.
- The common characteristics of the two theoretical cases are given in Table 1.

For the natural drainage case (Fig. 3A), the lake has a radius of 228.9 m. Its level is suddenly raised by 1 meter. For the pumping case (Fig. 3B), the lake has a radius of 121.9 m, and the pumping rate is 0.1311 m<sup>3</sup>/s.

The hypothetical case refers to a circular lake having a maximum diameter of 120 meters. At the beginning of the simulation the lake is empty and the aquifer water table is 100 cm below the lowest elevation of the lake bottom. During a period of two months, corresponding to a heavy rainfall period, the net rainfall is 40 mm/day, and then the rainfall stops and the evaporation is 10 mm/day during the following 10 months of the dry period. Figure 4 shows that the lake fills during the heavy rainfall period (After 5 days and after 30 days).

After 30 days the “island” in the middle of the lake has completely disappeared. During the heavy rainfall period the lake area and volume increase (Figure 5d.) then decrease due to evaporation and infiltration (Figure 5a.). The aquifer water table rises and merges into the lake before decreasing again (Figure 5b.). The exchange flow between lake and aquifer (Figure 5c.) is however always directed from the lake to the aquifer because, in this example, the lake level is always higher than the aquifer water table.



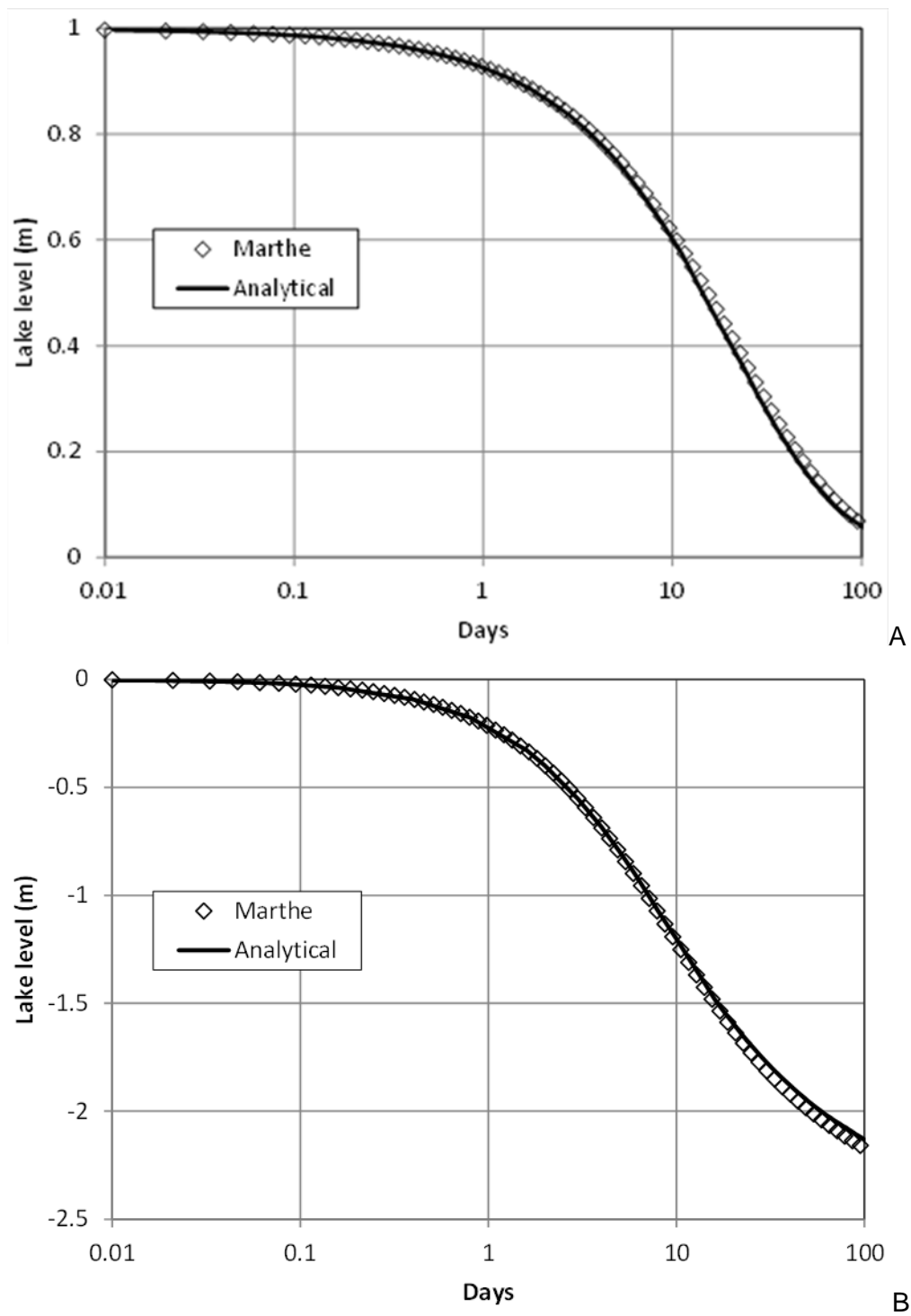


**Figure 3** MARTHE simulation results compared to analytical solution for the lake natural drainage case (A.) and for the lake pumping case (B.).

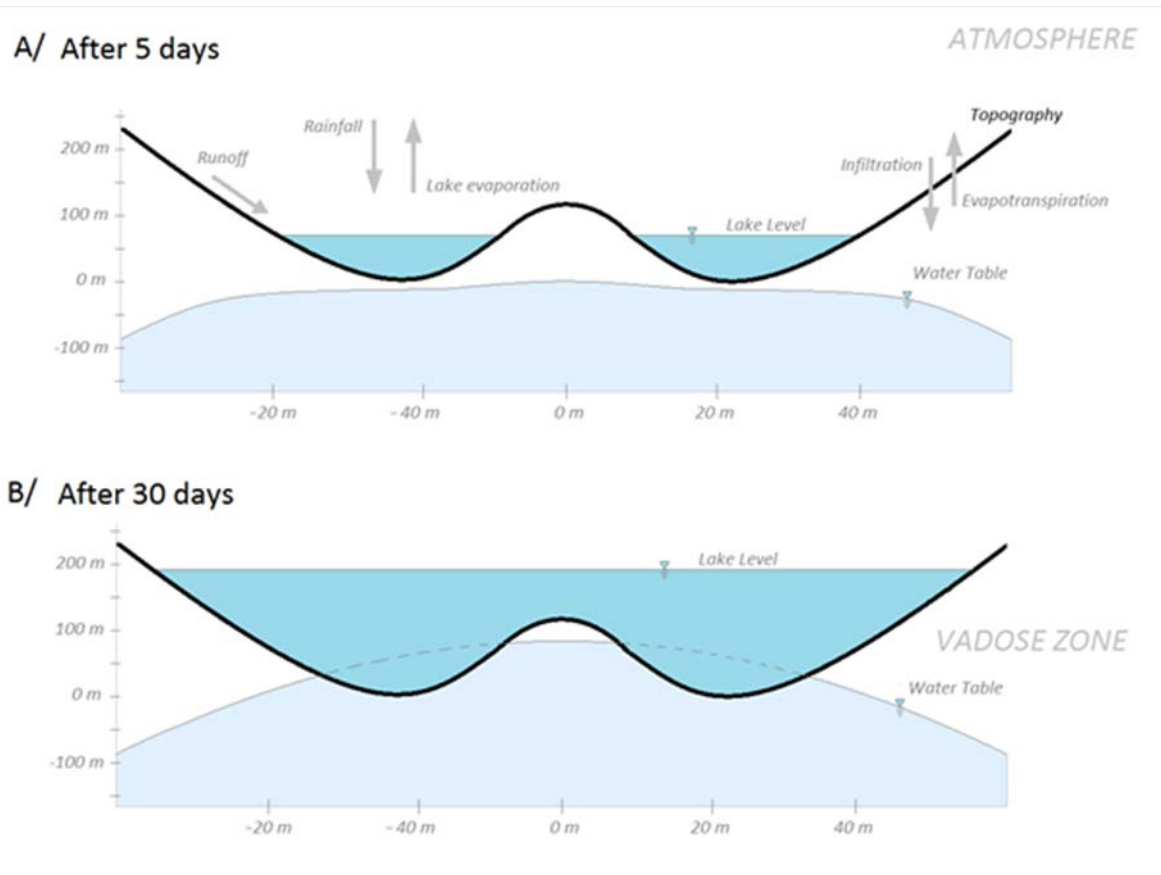


Figure 4 MARTHE simulation results of a hypothetical case representing the filling of a percolation tank (considered as lake) during a heavy rainfall period, followed by a drying period due to evaporation and percolation. Results after 5 days (A.) and 30 days (B.)

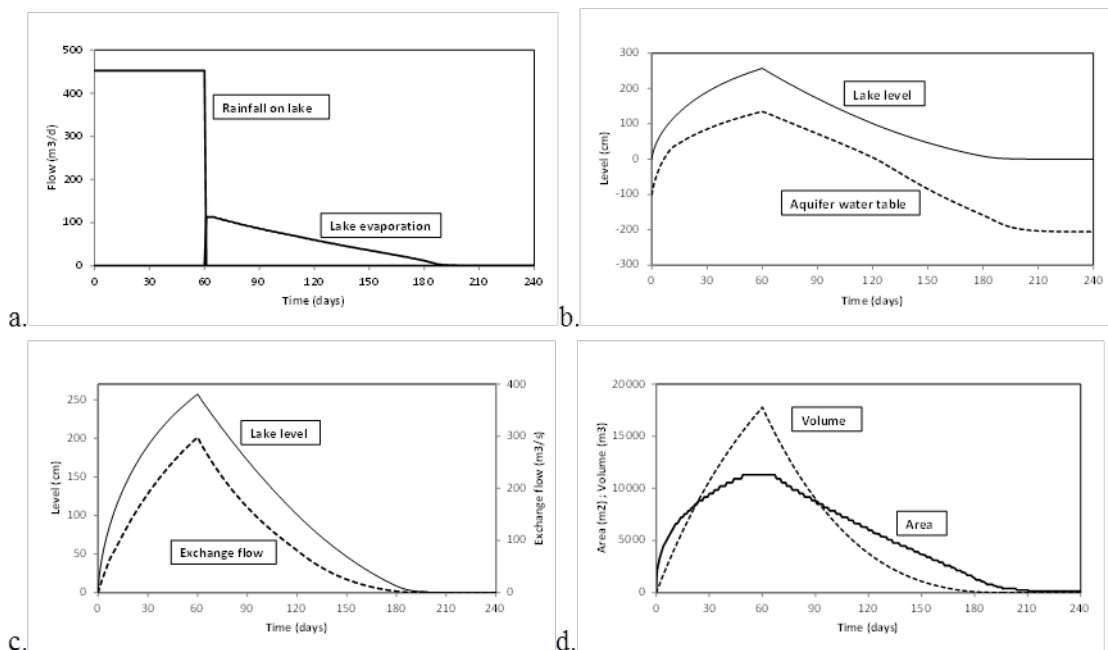


Figure 5 MARTHE simulation results of a hypothetical case representing the filling of a lake during a heavy rainfall period, followed by a drying period due to

evaporation and percolation (a. rainfall-evaporation, b. lake and water table levels, c. exchange flow, d lake volume and lake area).

**Table 1 Common characteristics of the two theoretical cases.**

| Parameter                            | Value                 |
|--------------------------------------|-----------------------|
| Lake geometry                        | Circular              |
| Aquifer thickness (m)                | 0.305                 |
| Aquifer extent : infinite            | Infinite              |
| Aquifer hydraulic conductivity (m/s) | $5.376 \cdot 10^{-2}$ |
| Lakebed thickness (m)                | 0.0152                |
| Lakebed hydraulic conductivity (m/s) | $3.53 \cdot 10^{-6}$  |
| Confined storage coefficient [-]     | $10^{-3}$             |
| Initial lake elevation (m)           | 0                     |
| Initial aquifer hydraulic head (m)   | 0                     |

## 1.7 Conclusion and perspective

We implemented into the three-dimensional finite-difference groundwater model MARTHE first published in 1990, a new feature allowing for interaction between surface water bodies and groundwater, adapted to the use of MAR in the Indian context. Implementation will:

- Increase our understanding of the recharge capacity measured on experimental percolation tanks,
- Assess the quantitative and qualitative effects of monsoon water recharge on an overexploited semi-urban aquifer,
- Evaluate the impact on groundwater recharge of future MAR implementation at basin scale.

An appropriate experimental site within the Maheshwaram watershed including an ephemeral percolation tank was selected for future modelling application. The Maheshwaram catchment has been investigated through numerous studies (geology, hydrogeology, GIS, geochemistry...) over the last two decades. A conceptual hydrogeological model exists at basin scale for the hydrology of such a watershed composed by fractured crystalline bedrock and a thick weathering zone. A three-dimensional groundwater flow model using MARTHE has been established (Engerrand, 2002; Engerrand and Ledoux, 2003) and calibrated for the 2001-2004 period, with a long initialization beginning in 1920. The model includes detailed pumping rates and return flow from irrigated land and meteorological evolution (rainfall and evapotranspiration). Scenarios for forecasting were simulated as support to decision-making for water

management (Petrelluzzi, 2004). However the model is not yet updated with the last data acquired on the Maheshwaram watershed and does not include yet existing natural percolation ponds.

Further steps comprise detailed modelling at percolation tank scale and then extrapolation of MAR implementation at watershed scale (Figure 6):

- 1) The specific properties of hard-rock aquifers acquired on the Tumulur percolation tank in the Maheshwaram watershed will be implemented in a three-dimensional MARTHE model in order to assess the impact of MAR structures on the water cycle at the local scale. Modelling will be optimized with a 3 years time serie of water levels (natural percolation pond and groundwater) and constrained by climatic records (rainfall and evapotranspiration). Water balance computation will quantify the different water fluxes and storage changes.

- 2) The updating of the existing numerical model MARTHE representing the experimental site, Maheshwaram, with recent studies increasing the hydrogeological system knowledge (Dewandel et al., 2010; Negrel et al., 2011; Perrin et al., 2011b; Dewandel et al., 2011; Dewandel et al., 2012). The main purpose of this exercise is to perform a hydrogeological 3D meshed model representing initial state of the watershed (MAR site implementation). Integrating theoretical percolation pond into the basin-scale groundwater flow model, the effects of MAR at basin scale will be established in relation with climatic forecast. Running several scenarios with MAR facilities at different potential locations will define a decision-support system for optimizing, or for identifying general recommendations on the implementation of MAR structures under the specific conditions met in India. Their efficiency in sustaining the water table and their positive impacts on the groundwater balance at the watershed scale will be simulated.

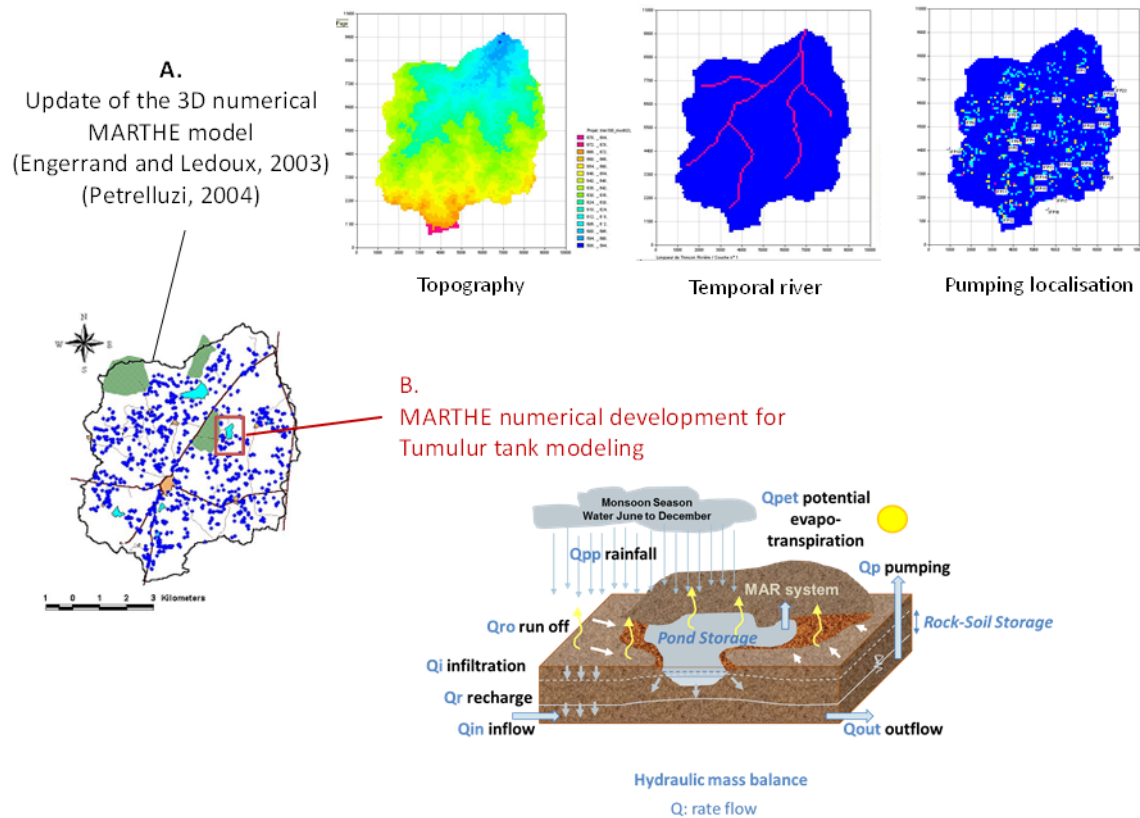


**Figure 6 Modelling methodology to evaluate the impact of MAR implementation through percolation tanks on groundwater recharge at watershed scale (A.) and local scale (B.).**

## 1.8 Acknowledgements

This study was carried out within the Saph Pani Project and co-financed by the European Commission within the Seventh Framework Programme Grant agreement No. 282911 and the Research Division of BRGM.

## 1.9 References

- Bakker, M. (2004). "Modelling groundwater flow to elliptical lakes and through multi-aquifer elliptical inhomogeneities." *Adv. in Water Resour.*, 27, 497–506.
- Boisson, A., Villesseche, D., Baisset, M., Perrin, J., Viossanges, M., Kloppmann, W., Chandra, S., Dewandel, B., Picot-Colbeaux, G., Rangarajan, R., Maréchal, J-C., Ahmed, S., (2013). "Questioning the impact and sustainability of percolation tanks as aquifer recharge structures in semi-arid crystalline context", *Proc., Int. Symp. on Managed Aquifer recharge ISMAR 8, Beijing, China, (submitted).*

- Boswell, J. S., and Olyphant, G. A. (2007). "Modelling the hydrologic response of groundwater dominated wetlands to transient boundary conditions: Implications for wetland restoration." *J. Hydrol.*, 332, 467– 476
- Bouzit, M., Fatima, S., Pauwels, H., Ahmed, S., Perrin, J., (submitted). "Fluoride Groundwater Contamination: Impact of Land-use on Prevalence of Dental Fluorosis (Maheshwaram Watershed, India)." Fluoride
- CGWB (2002). "Master plan for artificial recharge to ground water in India." Available via the website of Central Ground Water Board (CGWB), Ministry of Water Resources, Govt. of India, <http://cgwb.gov.in/documents/MASTER%20PLAN%20Final-2002.pdf> (May 30, 2013)
- Cheng, X., and Anderson, M.P. (1993). "Numerical simulation of ground-water interaction with lakes allowing for fluctuating lake levels", *Ground Water*, v. 31, no. 6, p. 929-933.
- Cooper, H.H., Bredehoeft, J.D. and Papadopoulos, S.S. (1967). "Response of a finite-diameter well to an instantaneous charge of water." *Water Resour. Res.*, 3(1), 263-269.
- Demetriou, C., and Punthakey, J.F. (1999). "Evaluating sustainable groundwater management options using the MIKE SHE integrated hydrogeological modelling package." *Environ. Modell. Softw.*, 14, 129–140.
- Dewandel B., Maréchal, J.C., Bour. O., Ladouche. B., Ahmed, S., Chandra, S., Pauwels, H. (2012). "Upscaling and regionalizing hydraulic conductivity and effective porosity at watershed scale in deeply weathered crystalline aquifers." *J. Hydrol.*, (416–417), 83–97.
- Dewandel, B., Lachassagne, P., Zaidi, F.K., Chandra, S. (2011). "A conceptual hydrodynamic model of a geological discontinuity in hard rock aquifers: example of a quartz reef in granitic terrain in South India." *J. Hydrol.* (405), 474–487.
- Dewandel, B., Perrin, J., Ahmed, S., Aulong, S., Hrkal, Z., Lachassagne, P., Samad, M., Massuel, S. (2010). "Development of a tool for managing groundwater resources in semi-arid hard rock regions. Application to a rural watershed in south India" *Hydrol. Process.*, (24): 2784–2797.
- Dewandel, B., Gandolfi, J.-M., Zaidi, F., K., Ahmed S., and Subrahmanyam, K. (2007). "A decision support tool with variable agroclimatic scenarios for sustainable groundwater management in semi-arid hard-rock areas." *Curr. Sci.*, 92(8), 1093-1102.
- Dewandel, B., Lachassagne, P., Wyns, R., Maréchal, J.C., Krishnamurthy, N.S. (2006). "A generalized 3-D geological and hydrogeological conceptual model of granite aquifers controlled by a single or multiple weathering". *J. Hydrol.* 330, 260-284.
- DHAN Foundation. (2002). "Revisiting Tanks in India" National Seminar on Conservation and development of Tanks, New Delhi, India.

- Engerrand, C., (2002) "Hydrogeology of the weathered–fissured hard rock aquifers located in monsoon areas: hydrogeological study of two watersheds in Andhra Pradesh (India)." Doctoral thesis report, University Pierre et Marie Curie - Paris VI (France), 203p.
- Engerrand, C. and Ledoux, E. (2003). "Modelisation of groundwater aquifer flow in Maheshwaram watershed, RR dist, AP., India." Technical report, Ecole des Mines de Paris.
- Feinstein, D., Dunning, C., Hunt, R.J., Krohelski, J. (2003). "Stepwise use of GFLOW and MODFLOW to determine relative importance of shallow and deep receptors." *Ground Water*, 41 (2), 190-9.
- Gale, I., and Dillon P. (2005). "Strategies for Managed Aquifer Recharge (MAR) in semi-arid areas." NESCO-IHP, Paris.
- Gale, I. N., Macdonald, D. M. J., Calow, R. C., Neumann, I., Moench, M., Kulkarni, H., Mudrakartha, S. and Palanisami, K. (2006). "Managed Aquifer Recharge: an assessment of its role and effectiveness in watershed management." British Geological Survey Commissioned Report, CR/06/107N. 80pp.
- Gaus, I., Cikurel, H., Picot, G., Aharoni, A., Guttman, Y., Azaroual, M., Kloppmann, W. (2007). "Alternative SAT of secondary effluents using a combination of UF and short term SAT for increasing infiltration rates at the Shafdan site (Israel )" *Proc., Int. Symp. on Managed Aquifer recharge ISMAR 6*, Phoenix, USA, 544-557.
- Graham, D.N., and M. B. Butts (2005). "Flexible, integrated watershed modelling with MIKE SHE. In *Watershed Models*", Eds. V.P. Singh & D.K. Frevert Pages 245-272, CRC Press. ISBN: 0849336090.
- Grützmacher, G., Wessel, G., Klitzke, S., Chorus, I. (2010). "Microcystin Elimination During Sediment Contact." *Environ. Sci. Technol.* 44(2), 657-662.
- Habets, F., Gascoin, S., Korkmaz, S., Thiéry, D., Zribi, M., Amraoui, N., Carli, M., Ducharne, A., Leblois, E., Ledoux, E., Martin, E., Noilhan, J., Ottlé, C., and Viennot, P., (2010). "Multi-model comparison of a major flood in the groundwater-fed basin of the Somme River (France)", *Hydrol. Earth Syst. Sci.*, 14, 99–117.
- Kloppmann, W., Aharoni, A., Chikurel, H., Dillon, P., Gaus, I., Guttman, Y., Kraitzer, T., Kremer, S., Masciopinto, C., Pavelic, P., Picot-Colbeaux, G., Pettenati, M., Miotlinski, K. (2012). "Use of groundwater models for prediction and optimisation of the behaviour of MAR sites." in "Water Reclamation Technologies for Safe Managed Aquifer Recharge – ch. 18", Chapter book: IWA Publishing C.Kazner, T.Wintgens, P.Dillon Editors, ISBN 9781843393443.
- Kloppmann, W., Chikurel, H., Picot, G., Guttman, J., Pettenati, M., Aharoni, A., Guerrot, C., Millot, R., Gaus, I., and Wintgens, T. (2009). "B and Li isotopes as intrinsic tracers for injection tests in aquifer storage and recovery systems." *Appl. Geochem.* 24, 1214-1223.

- Langergraber, G. (2008). "Modelling of processes in subsurface flow constructed wetlands – A review." *Vadoze Zone J.*, 7(2), 830-842.
- Langergraber, G., and Šimůnek, J. (2005). "Modelling variably-saturated water flow and multi-component reactive transport in constructed wetlands." *Vadose Zone J.*, 4(4), 924-938.
- Maréchal, J.C., Dewandel, B., Ahmed, S., Galeazzi, L., Zaidi, F.K. (2006) "Combined estimation of specific yield and natural recharge in a semi-arid groundwater basin with irrigated agriculture." *J.Hydrol.*, 329(1), 281-293.
- Maréchal, J.C., Dewandel, B. & Subrahmanyam, K. (2004) "Use of hydraulic tests at different scales to characterize fracture network properties in the weathered-fractured layer of a hard rock aquifer." *Water Resour. Res.*, 40(11), W11508, doi:10.1029/2004WR003137.
- Maréchal, J.C., Wyns, R., Lachassagne, P., Subrahmanyam, K. & Touchard, F. (2003) "Anisotropie verticale de la perméabilité de l'horizon fissuré des aquifères de socle : concordance avec la structure géologique des profils d'altération." *C.R. Geoscience*, 335(5), 451-460.
- Merritt, M.L. (1985). "Subsurface storage of freshwater in south Florida-A digital model analysis of recoverability." U.S. Geological Survey Water-Supply Paper 2261, 44 p.
- Merritt, M. L., and Konikow, L. F. (2000). "Documentation of a Computer Program to Simulate Lake-Aquifer Interaction Using the MODFLOW Ground-Water Flow Model and the MOC3D Solute-Transport Model." U.S. Geological Survey, Water-Resources Investigations Report 00-4167, 146p.
- Mylopoulos, N., Mylopoulos, Y., Veranis, N., Tolikas, D. (2007). "Groundwater modelling and management in a complex lake-aquifer system." *Water. Resour. Manage.*, 21, 469–494.
- Negrel, P., H. Pauwels, Dewandel, B., Gandolfi, J.M., Mascré, C., Ahmed, S. (2011). "Understanding groundwater systems and their functioning through the study of stable water isotopes in a hard-rock aquifer (Maheshwaram watershed, India)." *J. Hydrol.* 397(1-2), 55-70.
- Papadopoulos, I. S. and Cooper, H. H. Jr. (1967) "Drawdown in a well of large diameter." *Water Resour. Res.*, 3(1), 241–244.
- Perrin, J., Ferrant, S., Massuel, S., Dewandel, B., Maréchal, J.C., Ahmed, S., Aulong, S. (2012). "Assessing water availability in a semi-arid watershed of southern India using a semi-distributed model". *J. Hydrol.* 460(46), 143–155.
- Perrin, J., Ahmed, S., Hunkeler, D. (2011). "The effects of geological heterogeneities and piezometric fluctuations on groundwater flow and chemistry in a hard-rock aquifer, southern India" *Hydrog. J.*, (19-6): 1189-1201.
- Perrin, J., Mascré, C., Massuel, S., Ahmed, S. (2009). "Tank management in Andhra Pradesh, India: percolation vs. irrigation". IAHS special publication, Joint Int. Conf., Hyderabad. India.



- Petrelluzzi, E. (2004) "Mise au point d'une méthodologie de modélisation des aquifères de socle." Mémoire Master 2 : Sciences de l'Univers, Ecologie, Environnement - Parcours Hydrologie Hydrogéologie.
- Pettenati, M., Perrin, J., Pauwels, H., Ahmed, S. (2013). "Simulating fluoride evolution in groundwater using a multicomponent transient transport model: application to a crystalline aquifer of southern india." *Appl. Geochem.* 29, 102-116.
- Purushotham, D., M. R. Prakash, Rao, M. R.; Narsing, A. (2011). "Groundwater depletion and quality deterioration due to environmental impacts in Maheshwaram watershed of R.R. district, AP (India)." *Env. Earth Sci.* 62(8), 1707-1721.
- Sakthivadivel, R. (2008). "Decentralized artificial recharge movements in India: potential and issues". Conference Papers from International Water Management Institute.
- Sakthivadivel, R. (2007). "The Groundwater Recharge Movement in India." Chap. 10 in *The agricultural Groundwater Revolution: Opportunities and Threats to Development*. Giordano, M. and Villholth, K. G., eds., CABI, 195-210.
- Šimůnek, J., Šejna, M., and van Genuchten, M. Th. (1999). "The Hydrus-2D software package for simulating two-dimensional movement of water, heat, and multiple solutes in variably saturated media." Version 2.0, IGWMC - TPS - 53, International Ground Water Modelling Center, Colorado School of Mines, Golden, Colorado, 251 pp.
- Smerdon, B. D., Mendoza, C. A., and Devito, K. J. (2007). "Simulations of fully coupled lake-groundwater exchange in a subhumid climate with an integrated hydrologic model." *Water Resour. Res.*, Vol. 43, W01416, doi:10.1029/2006WR005137.
- Thiéry, D. (2010a). "Groundwater Flow Modelling in Porous Media Using MARTHE", in "Modelling Software Volume 5, Chapter 4, pp. 45-60 • Environmental Hydraulics Series". Tanguy J.M. (Ed.) – Editions Wiley/ISTE London. ISBN: 978-1-84821-157-5.
- Thiéry, D. (2010b). "Presentation of the Finite Volume Method", in "Numerical Methods Volume 3, chapter 8.6, pp. 195-211 • Environmental Hydraulics Series". Tanguy J.M. (Ed.) – Editions Wiley/ISTE London. ISBN: 978-1-84821-155-1.
- Thiéry, D. (2010c). "Reservoir Models in Hydrogeology", in "Mathematical Models Volume 2, chapter 13, pp. 409-418 • Environmental Hydraulics Series". Tanguy J.M. (Ed.) – Editions Wiley/ISTE London. ISBN: 978-1-84821-154-4.
- Thiéry, D. (2010d). "Interaction between Surface and Subsurface Flows: Somme Basin", in "Practical Applications in Engineering: Volume 4, chapter 13, pp. 143-156 • Environmental Hydraulics Series". Tanguy J.M. (Ed.) – Editions Wiley/ISTE London. ISBN: 978-1-84821-156-8.
- Thiéry, D., Amraoui, N. (2001). "Hydrological modelling of the Saone basin sensitivity to the soil model" *Phys. Chem. Earth, Pt B*, 26(5–6), 467-472.
- Thiéry, D. (1995). "Modélisation 3D du transport de masse avec le logiciel MARTHE version 5.4". Report BRGM R 38149 DR/HYT 95, 171 p.

- Thiéry, D. (1993). "Modélisation des aquifères complexes - Prise en compte de la zone non saturée et de la salinité. Calcul des intervalles de confiance". *Revue Hydrogéologie* 4, 325-336.
- Thiéry, D. (1990). "Software MARTHE. Modelling of Aquifers with a Rectangular Grid in Transient state for Hydrodynamic calculations of heads and flows. Release 4.3". Report BRGM 4S/EAU n° R32548.
- Tweed, S., Leblanc, M., Cartwright, I. (2009). "Groundwater–surface water interaction and the impact of a multi-year drought on lakes conditions in South-East Australia." *J. Hydrol.*, 379, 41–53.
- VanderKwaak, J. E. (1999). "Numerical simulation of flow and chemical transport in integrated surface-subsurface hydrologic systems." Ph.D. thesis, 217 pp., Univ. of Waterloo, Ontario, Canada.
- Yu, Z., Schwartz, F.W. (1998). "Application of integrated basin-scale hydrologic model to simulate surface water and ground-water interactions in Big Darby Creek Watershed Ohio." *J. Am. Water Resour. Assoc.* 34, 409–425.
- Yu, Z., Lakhtakia, M.N., Yarnal, B., White, R.A., Miller, D.A., Frakes, B., Barron, E.J., Duffy, C., Schwartz, F.W. (1999). "Simulating the river-basin response to atmospheric forcing by linking a mesoscale meteorological model and hydrologic model system." *J. Hydrol.*, 218, 72–91.
- Yu, Z., Pollard, D., Cheng, L. (2006). "On continental-scale hydrologic simulations with a coupled hydrologic model." *J. Hydrol.*, 331, 110– 124.
- Zlotnik, V. A., Olaguera, F., Ong, J. B. (2009). "An approach to assessment of flow regimes of groundwater-dominated lakes in arid environments." *J. Hydrol.*, 371, 22–30.

## 2 Maheshwaram MAR system reactive transport model

*Title:* "Water quality evolution during managed aquifer recharge (MAR) in Indian crystalline basement aquifers: reactive transport modelling in the critical zone"

*Authors (BRGM, NGRI):* Pettenati Marie, Picot-Colbeaux Géraldine, Thiéry Dominique, Boisson Alexandre, Alazard Marina, Perrin Jérôme, Dewandel Benoît, Maréchal Jean-Christophe, Ahmed Shakeel4, Kloppmann Wolfram

*Journal:* Procedia: Earth and Planetary Science

*Status:* accepted

## 2.1 Abstract

The present study investigates the role of MAR (Managed Aquifer Recharge) on groundwater quality overexploited crystalline aquifers in semi-arid context (South India). A 1D transient reactive transport model was conceived to simulate the infiltration of a recharge tank through the critical zone. The model takes into account hydrodynamics, evaporation, kinetic weathering of minerals (precipitation/dissolution), adsorption, cationic exchange. Results show the beneficial effect of MAR on groundwater quality, in particular on Fluoride accumulation, a widespread problem in the Indian context, strongly depending on seasonal climatic variations.

*Keywords:* MAR; overexploited crystalline aquifers, Fluoride accumulation, critical zone, reactive transport modelling.

## 2.2 Introduction

The overexploitation of crystalline aquifers in India due to the green revolution in the 1970s, has led to not only to a general water level drawdown but also to the degradation of water quality [1]. In the Maheshwaram watershed (Andhra Pradesh, Southern India), groundwater is largely used for irrigation. Fluoride (F<sup>-</sup>) progressively accumulated in the irrigation return flow (IRF) because of strong evaporation in the paddy fields together with mineral dissolution of primary minerals containing F<sup>-</sup> (fluorapatite, biotite, epidote) [2,3]. This accumulation is enhanced by calcite precipitation reducing Ca<sup>2+</sup> activity and also by Ca<sup>2+</sup> removal through cation exchange with Na<sup>+</sup> on clay minerals, thus hindering fluorite (CaF<sub>2</sub>) precipitation the only mechanism efficiently controlling F<sup>-</sup> concentrations [4]. High concentrations of F<sup>-</sup> are therefore typically accompanied by a Na-HCO<sub>3</sub><sup>-</sup> water type [5] and areas of alkaline soils increase in India due to poorly managed irrigation projects [7,8,9].

Managed Aquifer Recharge (MAR) through percolation tanks is often presented as a promising technique to increase groundwater availability and eventually enhance water quality, but is rarely estimated (Boisson et al., 2014). Currently there are three percolation tanks located within the Maheshwaram watershed and the monitored one, is close to Tumulur village (Fig. 1), has been monitored over 2 years. Instrumentation monitoring equipment of the Tumulur tank is described in detail by [10].

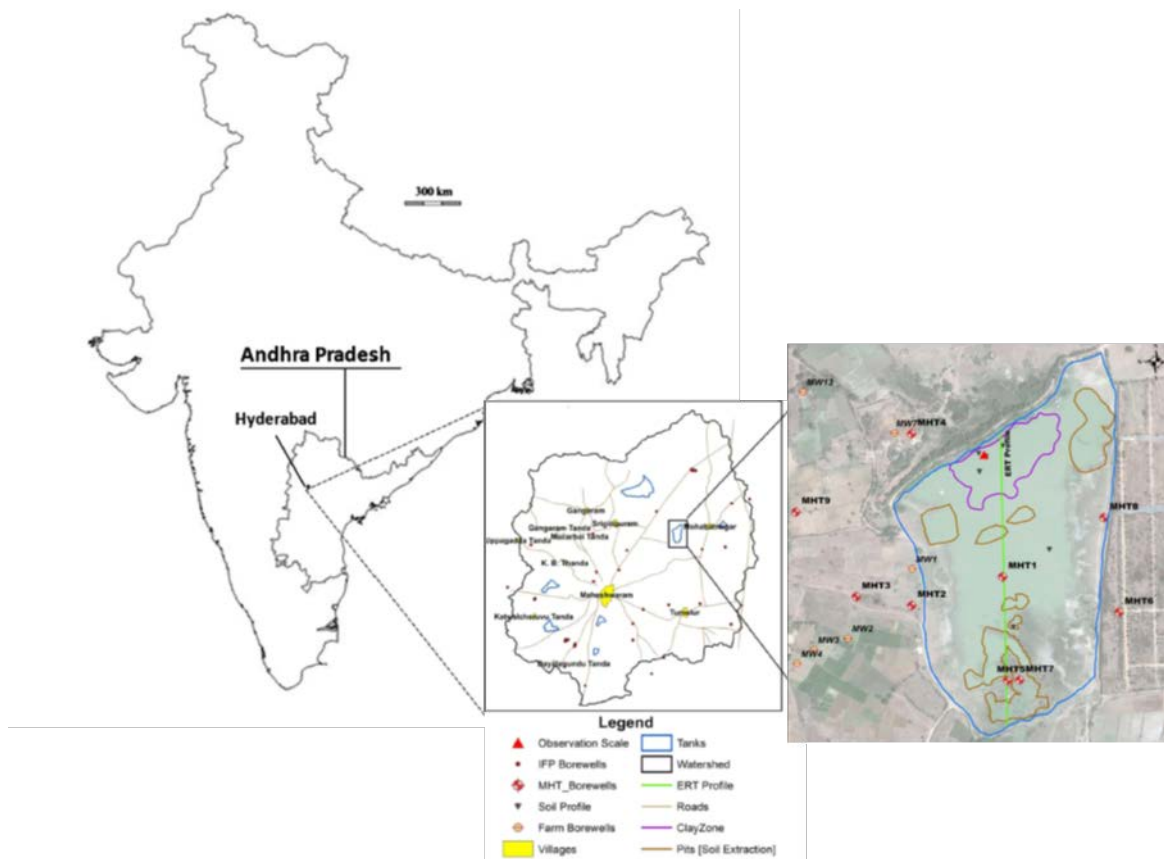


**Figure 1 Location of the Maheshwaram watershed and Recharge tank near the Tumulur village**

The aim of the geochemical modelling presented here is to quantify the water-rock interactions processes during the recharge and to investigate the corresponding impact on groundwater quality at the watershed scale. Results of hydrogeological models, including recharge scenarios are used to establish water budget as input to the reactive transport model [10]. The global objective is to evaluate the beneficial or adverse effect of managed recharge upon soil salinization and fluoride accumulation under the particular conditions of the Maheshwaram aquifer. The geochemical model of solute recycling developed for paddy field irrigation [3] using a 1D PHREEQC reactive-transport column [11] was adapted to the MAR problem, on the basis of new monitoring data in order to test the conceptual geochemical model of MAR (Fig. 2).

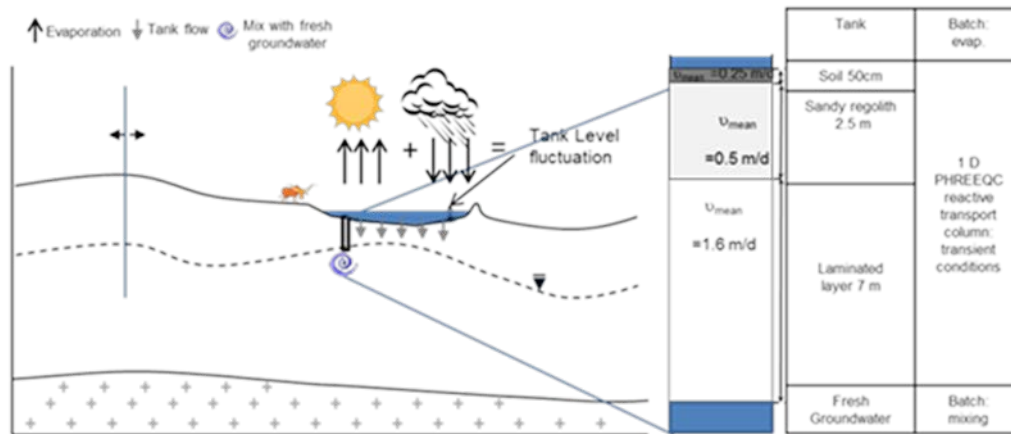


**Figure 2 Conceptual model of hard-rock aquifer in southern India with Managed Aquifer Recharge (MAR) through an infiltration tank used for the development of a 1D Phreeqc reactive column model.  $v_{mean}$  is the mean pore flow velocity.**

Reactive transport modelling is performed during 110 days using a 1D PHREEQC column with calculated pore flow velocity (Fig. 3). The reactive transport model takes into account:

- The mineral composition of the 3 distinct layers of altered biotite granite determined by XRD analysis [3],
- Cation Exchange Capacity (CEC) of the weathering profile determined by cobalt hexamine chloride solution [3],
- Initial groundwater composition determined using ion chromatography and ICP-MS [3].

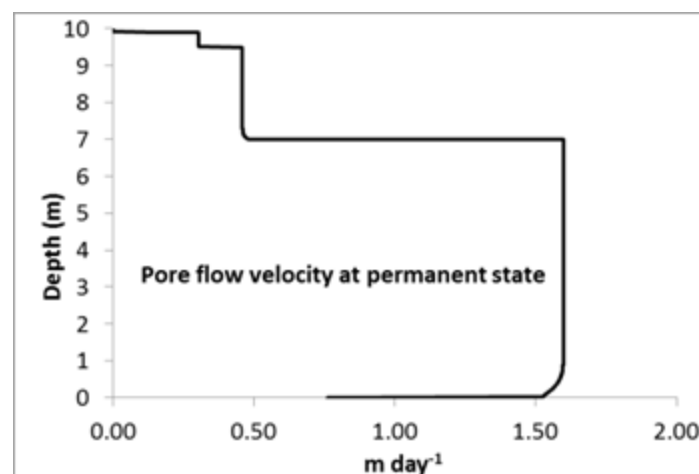


**Figure 3 Simulated steady-state pore flow velocity with 2 D variably saturated model.**

The processes integrated in the reactive transport model are:

- The thermo-kinetic dissolution of primary aluminosilicate phases based on [16] and [17] formulation (Transition State Theory, TST; [18]),

- The possible precipitation of secondary mineral phases [19],
- The adsorption on Fe hydroxides following the [20] theory, [21] and [22] for surface site characteristics,
- The cationic exchange processes.

The groundwater geochemistry is calculated with batch reaction at a daily time step mixing the solution taken at the outlet of the column with the evolving groundwater composition. The ratio of mixing (MAR water volume/aquifer volume) is fixed to 0.01%.

### 2.3 Results and Discussion

Fig. 4 shows the results of modelling in terms of solute evolution (chloride and fluoride) in Maheshwaram groundwater for several climatic conditions (dry and monsoon periods) and land uses contexts. Perrin et al. [1] has shown that the observed increasing TDS can be reproduced with the help of a solute recycling model (SRM) since the start of irrigation pumping. Pettenati et al. [3] used a geochemical reactive transport model to simulate the impact of IRF on groundwater chemistry and F- accumulation. This model including water/rock interaction in the Critical Zone and climatic parameters highlights the joint effect of dissolution of F--bearing minerals (fluorapatite/allanite/biotite) and of evaporation as principal trigger of F- enrichment in the return flow and the aquifer.

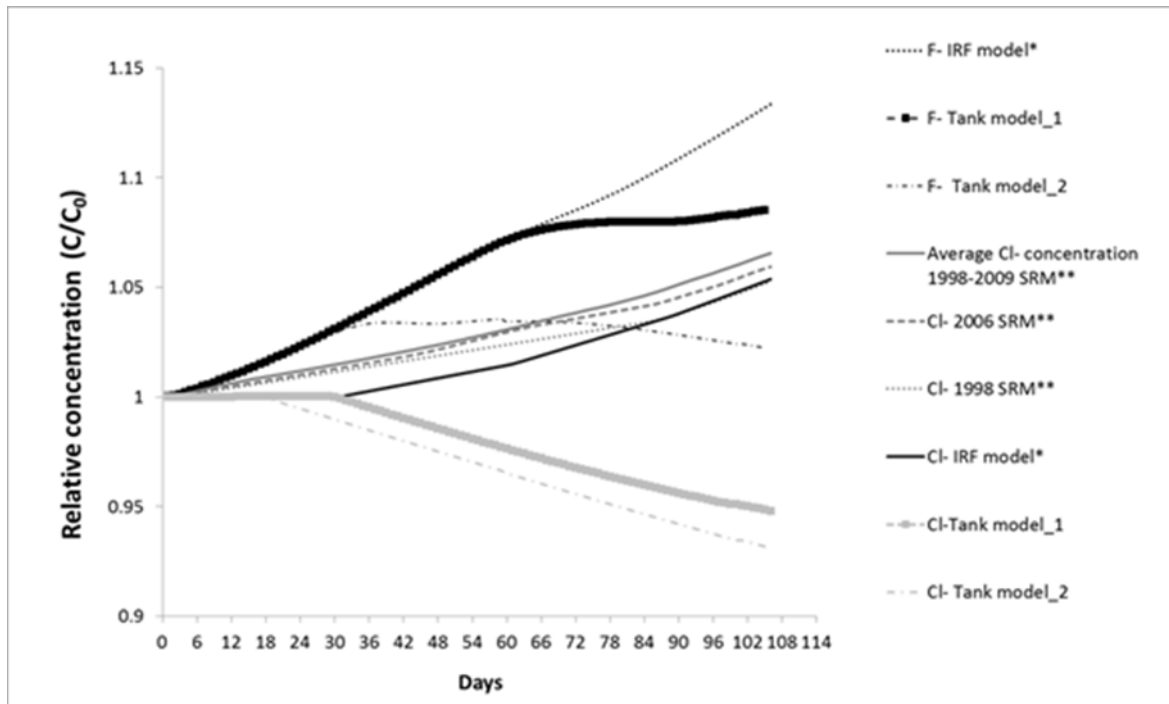


**Figure 4 Comparison between the relative aquifer solute concentration of chloride (Cl<sup>-</sup>) simulated by the solute recycling model SRM ([1]\*\*) and by the PHREEQC model for chloride (Cl<sup>-</sup>) and fluoride (F<sup>-</sup>) over one cycle of paddy field irrigation (dry season, [3]\*) and one cycle of Tank infiltration (Tank model\_1 = dry conditions 01/2006 to 04/2006; Tank model\_2 = monsoon conditions 07/2012 to 10/2012)..**

Based on these previous works, the MAR model applied to the critical zone shows that tank infiltration can have a beneficial effect on the decrease of aquifer fluoride concentration (F- Tank model\_2) under monsoon period (tank filling). As illustrated by the decreasing concentration of non-reactive chloride, this effect is due to a dilution effect compensating the evaporation processes. But results obtained considering another dry period (tank drainage) illustrate that, even if F- accumulation is delayed (F- Tank model\_1) compared to the IRF model (paddy field context) there is still an increase of F- over the duration of managed recharge. This tendency is due to a higher degree of evaporation over the dry period combined with the weathering of F--bearing matrix minerals within the critical zone during tank water percolation. Added value of modelling for each NWTS/study site

## 2.4 Conclusions

This research investigated the role of managed aquifer recharge under variable climatic conditions and its impact on groundwater chemistry. Based on a previous model which reproduced satisfactorily the solute behavior in Maheshwaram groundwater, the reactive transport model of the Tumulur tank infiltration through the critical zone helps to



understand the evolution of Fluoride enrichment or depletion in groundwater when MAR is implemented in a watershed. Results of the first scenarios simulation show that the beneficial effect of MAR may be variable over the year being strongest during monsoon whereas during the dry period, F accumulation occurs.

## 2.5 Acknowledgements

This research was conducted within the framework of the Saph Pani project and co-financed by the European Commission within the Seventh Framework Programme Grant agreement No. 282911 and the Research Division of BRGM.

## 2.6 References

1. Perrin, J., Mascré, C., Pauwels, H., Ahmed, S. Solute recycling: an emerging threat to groundwater resources in southern India? *J. Hydrol.* 2011; **398**, 144–154.
2. Pauwels, H., Negrel, P., Bouzit, M., Aquilina, L., Labasque, T., Perrin, J., Fatima, S. Vulnerability of over-exploited groundwater to fluoride contamination, in WRI 13 – Balkema. 2010; 415-418.
3. Pettenati, M., Perrin, J., Pauwels H., Ahmed, S. Simulating fluoride evolution in groundwater using a reactive multicomponent transient transport model: application to a crystalline aquifer of Southern India. *Appl. Geochem.* 2013; **29**, 102-116.
4. Jacks, G., Bhattacharya, P., Chaudhary, V., Singh, K.P. Controls on the genesis of some high-fluoride groundwaters in India. *Appl. Geochem.* 2005; **20**, 221-228.
5. Rao, N. S. The occurrence and behavior of fluoride in the groundwater of the Lower Vamsadhara River Basin, India. *Hydrol. Sci. J.* 1997; **42(6)**, 877-892.
6. Saxena, V. K., Ahmed, S. Inferring the chemical parameters for the dissolution of fluoride in groundwater. *Environ. Geol.*, **43** (Handa 1975). 2003; 731-736.
7. Srinivasulu, A., Satyanarayana, T.V., Hema Kumar, H.V. Subsurface drainage in a pilot area in Nagajuna Sagar right canal command, India. *Irrig. Drain. Syst.* 2005; **19**, 61-70.
8. Jacks, G., Harikumar, P.S., Bhattacharya, P. Fluoride mobilisation in India. in: Goldschmidt Conf. Abstr., June 21-26, 2009, Davos, Switzerland, A578.
9. Purushotham, D., Prakash, M.R., Narsing Rao, A. Groundwater depletion and quality deterioration due to environmental impacts in Maheshwaram watershed of R.R. district, AP (India). *Environ. Earth Sci.* 2011 ; **62**, 1707-1721.
10. Boisson, A., Villesseche, D., Baisset, M., Perrin, J., Viossanges, M., Kloppmann, W., Chandra, S., Dewandel, B., Picot-Colbeaux, G., Rangarajan, R., Maréchal, J.C., Ahmed, S. Questioning the impact and sustainability of percolation tanks as aquifer recharge structures in semi-arid crystalline context. *Environmental Earth Sciences.* 2014 ; DOI 10.1007/s12665-014-3229-2

11. Parkhurst, D.L., Appelo, C.A.J. User's Guide to PHREEQC (Version 2)- a computer program for speciation, batch-reaction, one dimensional transport, and inverse geochemical calculation. USGS Water Res. Invest. Rept. 99-4259, 312 p.
12. Thiéry, D. "Software MARTHE. Modelling of Aquifers with a Rectangular Grid in Transient state for Hydrodynamic calculations of heads and flows. Release 4.3". 1990; Report BRGM 4S/EAU n° R32548.
13. Thiéry, D. Groundwater Flow Modelling in Porous Media Using MARTHE, in "Modelling Software Volume 5 Chapter 4, pp. 45-60 • Environmental Hydraulics Series". 2010; Tanguy J.M. (Ed.) – Editions Wiley/ISTE London. ISBN: 978-1-84821-157-5.
14. Thiéry, D. Presentation of the Finite Volume Method, in "Numerical Methods Volume 3; chapter 8.6, pp. 195-211 • Environmental Hydraulics Series". 2010; Tanguy J.M. (Ed.) – Editions Wiley/ISTE London. ISBN: 978-1-84821-155-1.
15. Thiéry, D. Reservoir Models in Hydrogeology, in "Mathematical Models Volume 2, chapter 13, pp. 409-418 • Environmental Hydraulics Series". 2010; Tanguy J.M. (Ed.) – Editions Wiley/ISTE London. ISBN: 978-1-84821-154-4.
16. Palandri, J.L., Kharaka, Y.K.. A compilation of rate parameters of water-mineral interaction kinetics for application to geochemical modelling. USGS Open-File Rept. 2004-1068, 61 p.
17. Chaïrat, C., Schott, J., Oelkers, E.H., Lartigue, J-E., Harouiya, N. Kinetics and mechanism of natural fluorapatite dissolution at 25°C and pH from 3 to 12. *Geochim. Cosmochim. Acta.* 2007; **71**, 5901-5912.
18. Aagaard, P., Helgeson, H.C. Thermodynamic and kinetic constraints on reaction rates among minerals and aqueous solutions: 1. Theoretical considerations. *Am. J. Sci.* 1982; **282**, 237-285.
19. White, A.F., Schulz, M.J., Lowenstern, J.B., Vivit, D.V., Bullen, T.D. The ubiquitous nature of accessory calcite in granitoid rocks: Implications for weathering, solute evolution, and petrogenesis. *Geochim. Cosmochim. Acta.* 2005; **69**, 1455-1471.
20. Dzombak, D.A, Morel, F.M.M.. Surface complexation modelling. Hydrous ferric oxide. 1990; John Wiley & Sons, 393 p.
21. Wilkie, J.A., Hering, J.G. Adsorption of arsenic onto hydrous ferric oxide: effect of adsorbate/adsorbent ratios and co-occurring solutes. *Colloids & Surf.* 1996; **107**, 97-110.
22. Sujana, M.G., Soma, G., Vasumathi, N., Anand, S., 2009. Studies on fluoride adsorption capacities of amorphous Fe/Al mixed hydroxides from aqueous solutions. *J. Fluorine Chem.* **130**, 749-754.

### 3 Chennai MAR/SAT system

*Title:* Finite element modelling of groundwater flow in a multilayered aquifer in North of Chennai, Tamil Nadu, India

*Authors:* (Anna University, DHI-WASY): Rajaveni S. P., Indu S.N., Zabel A. K., Sklorz S., Bholá P., Monnikhoff B., Elango L.

*Journal:* to be decided

*Status:* to be submitted

### 3.2 Abstract

Managed Aquifer Recharge (MAR) is a major option for remediating groundwater over-abstraction, the resulting seawater intrusion into coastal aquifer through temporary storage of excess runoff in the aquifer reservoirs. MAR, combined to Soil Aquifer Treatment (SAT) is part of Natural Water Treatment systems (NWT) that are increasingly implemented and investigated under the specific conditions of the Indian subcontinent. The greater Chennai area heavily relies on groundwater abstraction, together with surface water reservoirs, to ensure urban water supply and irrigation. This has resulted in groundwater overexploitation and seawater intrusion and MAR systems are being implemented as remediation strategy. The present study developed a groundwater flow model of the Arani-Koratalaiyar (A-K) basin, north of Chennai and simulated groundwater flow under transient conditions. Differential Global Positioning System was used to measure topographical elevation and groundwater level. Aquifer thickness and the number of the aquifers were identified from borehole data, from which a 3D FEFLOW model was conceptualized. The aquifer properties such as hydraulic conductivity and specific yield were taken from pumping tests conducted by UNDP in the year of 1987. Initially steady state conditions were simulated, using the 1st of March 1996 to calibrate the aquifer properties. After the successful calibration, the model was run in transient conditions for a period from January 1996 to December 2010. The boundary conditions (BC) on the coastal side have been assigned with a constant head BC, the river crossing parts in the western side and south western side of Palar river is taken as time varying head BC and all other sides were considered as no flow. The Arani and Koratalaiyar River were defined as fluid-transfer BC. Time varying parameters of groundwater recharge were estimated from rainfall and groundwater pumping was calculated from crop water requirement. In addition to the crop water requirements, groundwater has been withdrawn from single wells located in 5 well fields. Transient simulation results show good correlation between observed and simulated groundwater level. The model results show particularly strong dependencies between groundwater potentials and river recharge rates, from which it was concluded that the use of a dynamically coupled approach between the surface water and groundwater components is required to analyse the effect of potential measures within the basin. Therefore, the model is coupled to a hydrodynamic surface water model, including rainfall-runoff processes. A scenario with additional check dams was simulated and analysed using the coupled model. The results indicated a local increase of groundwater levels, at the locations where additional check dams were implemented. In parallel to the coupling, a density-dependent component was added to the uncoupled 3D-groundwater model. Mesh refinements were necessary in the coastal region (high density gradient area) to obtain stable results, and a saltwater front was successfully represented. The model results help to understand the aquifer properties and to investigate the dynamic behaviour of groundwater level. In future, the simulated model can be used to predict groundwater level fluctuations and to determine the status of saltwater intrusion under various hydrological stress conditions.

*Keywords:* FEFLOW, numerical model, groundwater, A-K basin, coastal aquifer

### 3.3 Introduction

Chennai is the largest city in South India located in the eastern coastal plains. Water supply to the Chennai city is met by reservoirs, collecting surface water, and by groundwater. Most of the groundwater is pumped to the city from the well fields located in the Araniyar and Korttalaiyar River (A-K River) catchment north of Chennai (Figure 1). Severe pumping for supply to the Chennai city and for local irrigational needs has also resulted in seawater intrusion in well fields nearest to the coast hydraulically connected with the sea. The average rainfall on the basin is 7-9 billion m<sup>3</sup>/year, which corresponds to 950-1250 mm/year. Even though the annual rainfall is moderate, extreme cases of very high daily rainfall were recorded in past in the Chennai basin. Severe rainfall during short periods of time combined with high percentage of impervious areas in this region is the major source of flooding. Thus, the Chennai region on one hand is affected by floods and on the other by severe shortage of water.

The overall objective of the Chennai study within the Indo-European Saph Pani project, conducted within the EU's Seventh Framework Programme for Research (FP7), is the development of technical recommendations for implementing Managed Aquifer Recharge (MAR) systems in Chennai that utilize excess monsoon water to counteract seawater intrusion and groundwater overexploitation. The main aim for modelling groundwater flow in the A-K River catchment is to undertake a comprehensive assessment of MAR options at basin scale and to develop recommendations and a management plan for implementing MAR systems.

Numerical modelling of groundwater flow was previously carried out in the south Chennai coastal aquifer by Sivakumar et al. (2006) to simulate the effect of pumping and the changes in rainfall pattern. Excess pumping of groundwater in the coastal areas of Chennai such as Thiruvanmiyur, Besant Nagar and Palavakkam was identified by numerical modelling by Gnanasundar and Elango (2000). The feasibility of controlling the overland flow to provide augmentation of the groundwater resources in the Arani-Korttalaiyar basin proved successful by modelling (Anuthaman 2009). Ganesan and Thayumanavan (2009) developed a 3D MODFLOW/MT3D flow and transport model for the coastal aquifer north/northeast of Chennai. The optimal pumping and injection rates stated in this study may provide useful information for an improved and extended numerical model. After the 2004 tsunami that hit the Chennai coast, solute transport modelling was carried out by Sivakumar and Elango (2010) which helped to understand the salinisation process of the groundwater by the tsunami. The time required for remediation was also determined by numerical modelling. Sundaram et al. (2008) investigated the vulnerability of the coastal aquifers in Pondicherry (approx. 120 km south of Chennai) in terms of seawater intrusion using GIS methods and evaluated the effects of MAR techniques on the dynamics of the freshwater-seawater interface in the region.

The objective of this study was to setup a transient 3D groundwater model of the coastal aquifer located in north of Chennai, Tamil Nadu, India. The groundwater model represents surface-groundwater interactions, as well as freshwater-seawater dynamics. The model will serve as a tool for simulating MAR options and for analysing their impact on saltwater intrusion. Check dams were implemented as MAR structures and simulated for understanding the groundwater level changes.

### 3.4 Description of Study area

The study area comprises of two non perennial river basins Arani - Koratalaiyar (A-K) which are flowing through the north of Chennai. The eastern side of the study area is occupied by the Bay of Bengal. The Arani River originates from the flanks of Andhra Pradesh. The Koratalaiyar River passes through the Kesavaram anicut and flows into the sea at Ennore. The rivers generally flow only for few days during the north east monsoon. The total surface area of the A-K basin is about 1000 km<sup>2</sup> of which some 275 km<sup>2</sup> is underlain by a buried channel system which is part of the Palar River.

A very dry period occurs in this region during April to May when the temperature rises above 45 °C. A colder (winter) period occurs during November to January, experiencing an average temperature of 25 °C. The average annual rainfall is around 1200 mm/year, 35% falling in the south west monsoon (June - September) and 60% during the north east monsoon (October – December).

This area comprises landforms of fluvial, marine and erosional sediments. It includes alluvial planes, beach ridges, mudflats and paleo channels in the eastern region. Agriculture is the major activity and the main crops cultivating in this area are rice, pulses, groundnut, sesame, sugarcane and vegetables respectively (CGWB, 2007). Five well fields have been constructed to supply Chennai with water (Figure 1).

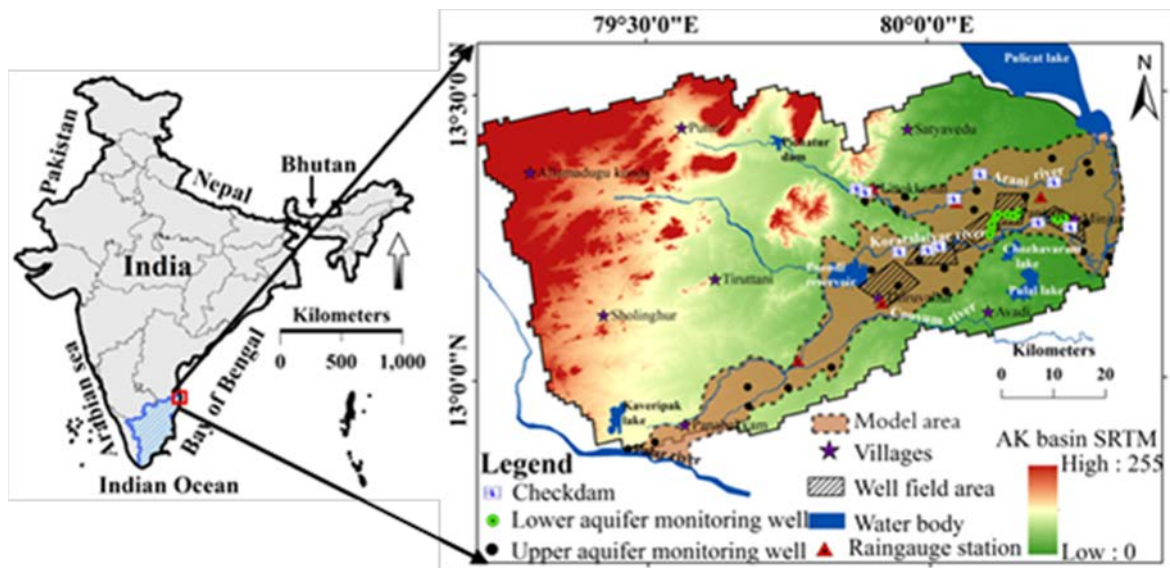


**Figure 1 Study area**

### 3.5 Data

The data used for the modelling, such as, aquifer types, borehole lithologs, rainfall and long term groundwater level observations were collected from various departments of the Government of Tamil Nadu, India. The base map was prepared from toposheets obtained from Survey of India (Figure 1). A Differential Global Positioning System (DGPS) survey was carried out to improve the topographical information at about 45 locations. The model area has a maximum elevation of 120 m amsl (above mean sea level). Geology map of the study area was derived from the geological map procured from the Geological Survey of India (GSI). To understand the subsurface geological formation of the area, lithologs and aquifer types were collected from the Chennai Metropolitan Water Supply and Sewerage Board (MWSSB). The groundwater level data from January 1996 to December 2010 was collected from the Public Works Department (PWD). Aquifer thickness of the model area was derived from Charalambous and Garratt (2009) and it was updated by the available litholog data. Also, rainfall data from January 1985 to December 2010 in 5 rain gauge stations were collected from PWD (location shown in Figure 1).

For the surface water modelling using MIKE 11, the basic input data required is river geometry and boundary conditions. The MIKE 11 cross-sections were mainly generated from the digital elevation model of 30 m resolution using GIS routines. For the rivers, a cross section profile of 500 m width was generated at every 5 km stretch. Six additional and more detailed profiles were surveyed on-field in the Koratalaiyar River.

Basic data requirements for the rainfall-runoff model (NAM) include catchment area, precipitation, potential evapotranspiration, and stream discharge. Daily evaporation was calculated based on the FAO Penman-Monteith method. Daily rainfall was obtained from eight rainfall stations located in the basin. Discharge and water level data for one gauge station is available on the website of the Chennai Metropolitan Water Supply and Sewerage Board at the Poondi reservoir.

### 3.6 Geology

Geologically, the basin is underlain by formations ranging in age from Archaean to Recent. Geological succession of the study area is tabulated below in Table 1. Crystalline rocks of Archean age comprising Charnockites, gneisses and associated rocks are restricted to the western part (Figure 2). Upper Gondwana series of Gondwana shale and clay are overlain by crystalline rocks. Tertiary formation is underlain by Gondwana series of massive pile of lacustrine and fluvial deposits. The central and eastern parts are underlain by a thick pile of Gondwana shales, clays and sandstones below the recent alluvial deposits. The area is predominated by sand which may be parts of coastal, alluvial and aeolian deposits. The total area for modelling mainly contains sand and silt. The north west and southern east part of the area is covered by laterite, sandstone and conglomerate. Most of this model area is exposed by Quaternary deposits, which consists of laterite and alluvium deposit (UNDP, 1987). Alluvium deposits contain sand and silt, sandy clay, gravel and pebbles occur along the Arani and Koratalaiyar river courses.

**Table 1 Geological succession of the study area (after UNDP,1987)**

|   |                         |  |
|---|-------------------------|--|
| ↑ | Quaternary (Up to 45 m) | Fine to coarse sand gravel, laterite, clay and clayey sand |
|   | Tertiary (45-50 m)      | Shale, clay and friable sandstone                          |
|   | Upper Gondwana          | Gondwana shale and clay                                    |
|   | Archean                 | Crystalline rocks  |



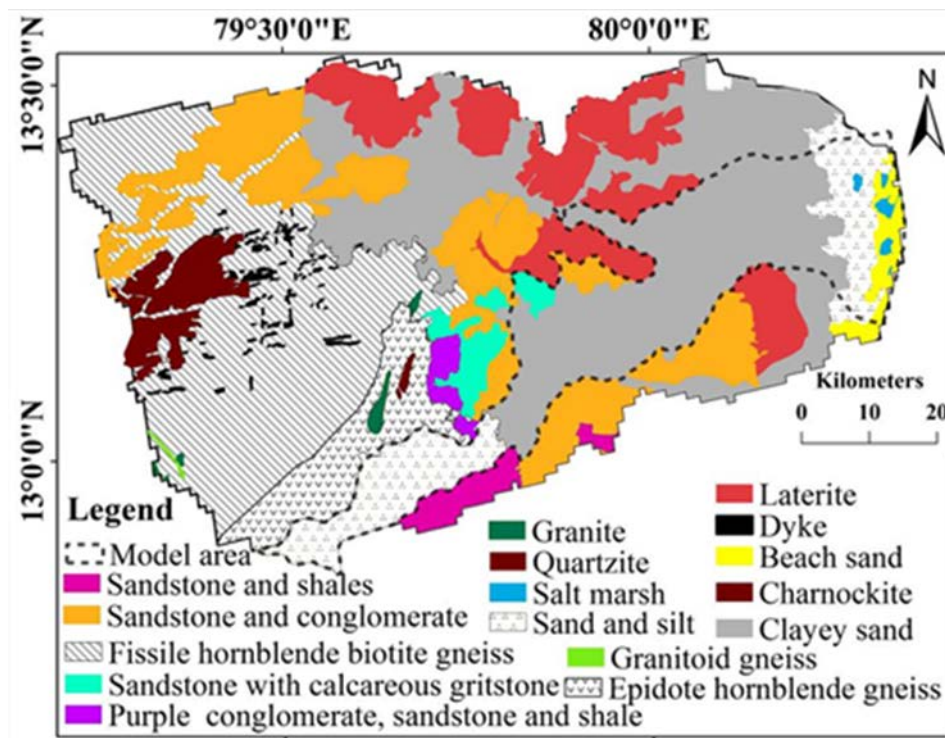


**Figure 2. Geology map of the Arani – Koratalaiyar river basin**

### 3.7 Hydrogeology

The main aquifer in the area is undoubtedly the Quaternary alluvium; predominantly fine grained, reflecting such a buried channel system; this constitutes the most important aquifer in the area (Anuthaman, 2009). Here the alluvium is up to 50 m thick, and much of it is sandy, though clays are sufficiently persistent in places to make its lower part behave like a confined aquifer. In addition, a significant amount of exploitable groundwater is located in the quaternary deposits. It is assumed that these aquifers area partly alluvial and partly of marine littoral origin. In both cases the saturated thicknesses are estimated to be small and their proximity to the sea limits the productive potential. UNDP (1987) identified a buried channel with highly permeable alluvial aquifers favorable for groundwater extraction through geological survey. Based on the borehole studies, the maximum depth of 50 m in the A-K basin show the thickness of the coastal alluvium as 35 m. The thick clay lenses form a semi-confined aquifer system. Two aquifer systems are found around 25 km from the coast, with an unconfined aquifer at the upper and a semi-confined aquifer at the lower. These two aquifers are either separated by an aquitard or the hydraulic conductivity of upper aquifer is of considerably lower than the lower aquifer. The two aquifers merge and become a single aquifer at a distance of about 30 km from the coast. The groundwater levels in the unconfined aquifer ranges from 2 to 6 m bgl (below ground level) and in the semi-confined aquifer it ranges from 14 to 20 m bgl. A west to east geological cross section in the area is given in Figure 3. In general the regional groundwater flow is towards the sea; however there may be variations in local hydraulic heads due to the difference in pumping pattern. The groundwater recharge

relies mainly on rainfall which feeds the non-perennial streams at the same time. The open/dug wells in this area are up to 25 m deep and bore wells up to 120 m deep. The water from these wells is used for domestic and irrigational purposes.

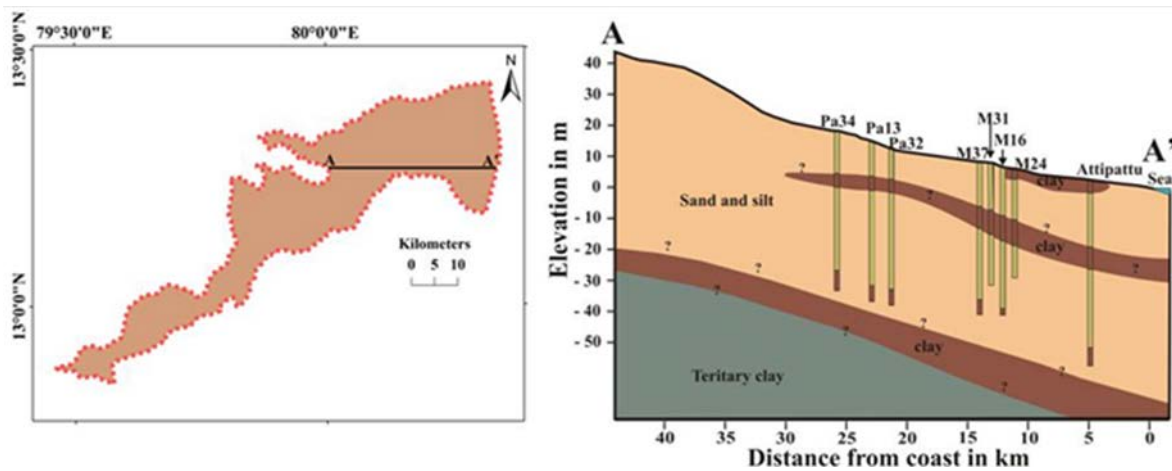


**Figure 3. Subsurface geology of the area shown by a west – east cross section (A-A')**

### 3.8 Methodology and Model description

The model concept used in the present study, to generate the catchment scale model, is as follows:

1. A rainfall-runoff model (NAM) to produce surface water inflow at the sub-catchment scale for the boundary conditions into the surface water system as well as the infiltration into the subsoil, integrated in the 1D surface water model.
2. A 1D surface water model (MIKE 11) for the two rivers Arani and Koratalaiyar.
3. A 3D groundwater model (FEFLOW) for the alluvial aquifers of A-K basin
4. Coupling of the 3D groundwater model to the MIKE 11 model using the coupling interface lfmMIKE11 (Monninkhoff 2011), to describe the interaction between the ground- and surface water in detail.
5. An additional density component will be added to the coupled 3D groundwater model, to account for the fresh- and seawater interactions.

#### 3.8.1 Surface water model

##### 3.8.1.1 Rainfall-runoff model (NAM)

NAM is the abbreviation of the Danish "Nedbør-Afstrømnings-Model", meaning precipitation-runoff-model. It is a deterministic, lumped and conceptual rainfall-runoff model that operates by continuously accounting for the moisture content in four different and mutually interrelated storages that represent overland flow, interflow, base flow and precipitation, respectively (DHI 2012). It forms a part of the rainfall-runoff module, which can be applied independently or used to represent one or more contributing catchments that generate lateral inflows to a river network.

A NAM model was set up for the A-K basin and parameters were calibrated on a transient state approach for a time period of eight years (2004 - 2011). Apart from the discharge at

the gauge station, the model was also calibrated on the range of minimum and maximum annual recharge.

#### 3.8.1.2 Surface water model (MIKE 11)

MIKE 11 is a dynamic, user-friendly 1D modelling tool for the simulation of flows, water quality and sediment transport in estuaries, rivers, irrigation systems, channels and other water bodies (DHI 2012).

In the present study, a MIKE 11 model was setup and used to predict water levels, which serve as input to the FEFLOW groundwater model. The NAM model described above is completely integrated in MIKE 11. The model for the A-K basin consists of two main rivers (Arani and Koratalaiyar) and a total of eight check dams along the river courses.

#### 3.8.2 Groundwater flow model

A three dimensional unsaturated groundwater flow model was created in FEFLOW for this alluvial aquifer. A detailed study was carried out in the A-K basin by various data such as drainage, geology and lithologs, in order to demarcate the model boundary. Based on this groundwater potential zones comprising of aquifers in alluvial deposits were considered for carrying out groundwater modelling. The model area covers 1456 km<sup>2</sup> which is discretized in the groundwater model by approximately 1 million triangular elements. The mesh is refined along the river course and around the well field areas to avoid instabilities. This aquifer system is conceptualized into 8 layers in the model. The eastern side of the model area is bounded by Bay of Bengal which is considered as constant head boundary condition. The northern and southern boundaries of this area are watershed boundaries, the groundwater flow from these boundaries is negligible and they are considered as no flow boundary. The Palar River is flowing in the south western boundary and the Arani and Koratalaiyar rivers are crossing in the western side of the model boundaries, which were assigned as time varying head boundary conditions of 1st kind (Dirichlet) flow BC. The Arani and Korttalaiyar river were defined as a fluid-transfer BC (3rd kind BC).

##### 3.8.2.1 *Aquifer characteristics*

The hydraulic conductivity of the single aquifer varies from 35 m/day to 100 m/day and the conductivity of the lower semi-confined aquifer, which was taken from the pumping test conducted by UNDP (1987), varies from 30 m/day to 250 m/day. The hydraulic conductivity and the thickness of lower aquifer is higher compared to the upper aquifer. Hence, the lower semi-confined aquifer is the major aquifer near the coastal side.

##### 3.8.2.2 *Groundwater recharge*

Sources of groundwater recharge are rainfall infiltration, river bed infiltration and irrigation return flows. Out of these three sources, the rainfall infiltration is the major source for groundwater recharge. The percentage of rainfall recharge is calculated and assigned based in the geological outcrop of the model area (Figure 2). Based on the geological outcrop and rain gauge station, 10 Theisson polygons were created defining groundwater

recharge zones (Figure 4). The groundwater recharge is higher in the alluvial formations than in the sandstone formation (Sivaraman and Thillaigovindaranjan 2012). A minimum 5% of average rainfall is infiltrating into the ground in the upper catchment part of study area (Muralidharan et al. 1988). The alluvial outcrops recharge a higher amount (20 % to 25%) of rainfall into ground (Anuthaman 2009). Irrigation return flow also forms a major part of the total recharge. Charalambous and Garratt (2009) states that almost 39% of irrigation water returns to the aquifer. The irrigation return flow was therefore estimated to be around 160 Mm<sup>3</sup>/a (39% of the abstraction used for irrigation).

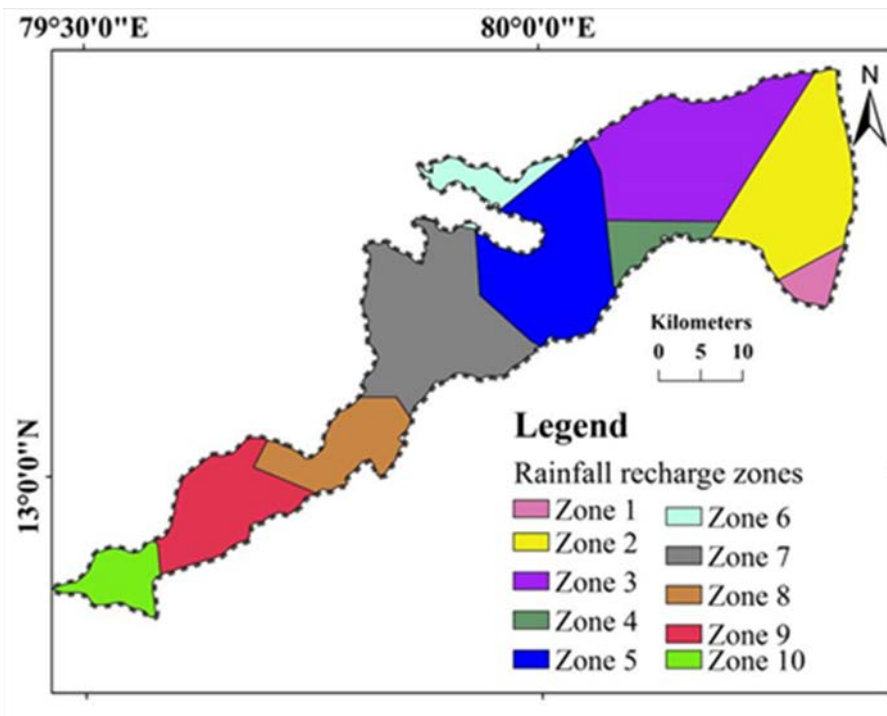


**Figure 4. Groundwater recharge zones**

### 3.8.2.3 Groundwater abstraction

Groundwater abstraction for irrigation was estimated from the crop water requirement. Landuse pattern of the area was prepared from satellite imagery of Linear Imaging Self Scanning Sensor (LISS – III) with a spatial resolution of 23.5 m (Figure 5). The landuse pattern is demarked by five categories such as crop area, built-up area, saltpan, aquaculture and non-agricultural area. The estimated groundwater abstraction in the A-K basin is around 480 Mm<sup>3</sup>/a. In addition to irrigation abstraction, groundwater is also continuously being pumped from the well fields for the Chennai municipal water supply. The pumping rate from the well field is collected from CMWSSB.

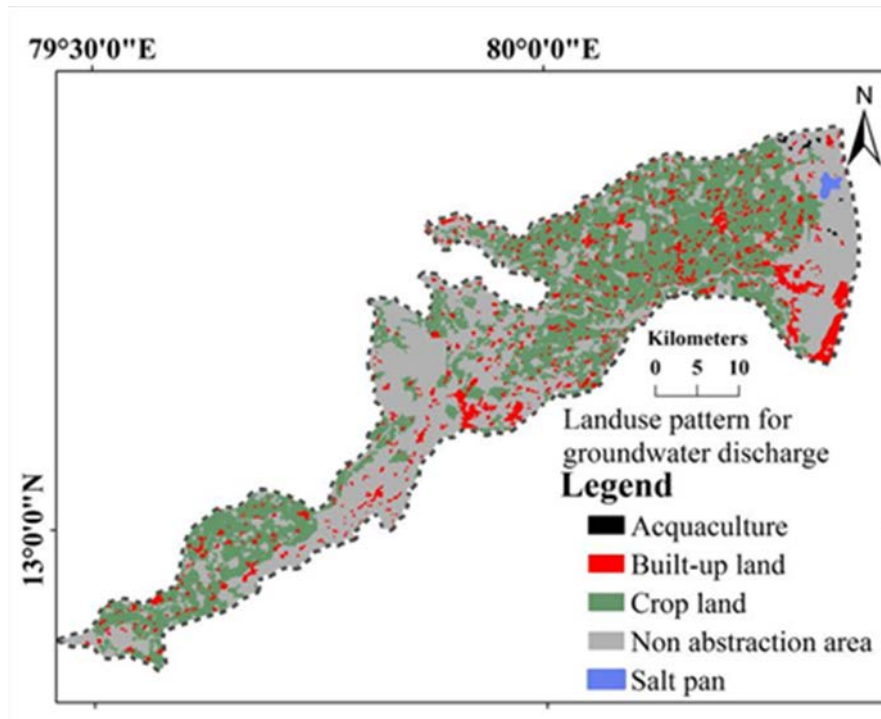


**Figure 5. Landuse pattern of the study area**

### 3.8.3 Coupling Concept

The interface module of IfmMIKE11 couples FEFLOW to MIKE 11 using the FEFLOW Interface Manager (IFM). In FEFLOW, rivers can be described by boundaries of the 1st kind (Dirichlet-type) or by boundaries of the 3rd kind (Cauchy-type). The Arani and Korttalayair rivers were defined by the latter boundary type, which is the only type supported by the coupling module IfmMIKE11. At the end of each FEFLOW time step the exchange rates to these FEFLOW boundary nodes are calculated by the module within FEFLOW. The time step of the groundwater model is controlled by FEFLOW. The spatial overlay of both meshes is automatically integrated within IfmMIKE11. The exchange discharges ( $Q$ ) between the ground- and surface water can be calculated within FEFLOW separately for each single boundary node of the 3rd kind. A successful attempt to couple ground- and surface models was made.

### 3.8.4 Density-Dependent modelling

A density-dependent component has been added to the uncoupled 3D-groundwater model, to account for freshwater-seawater interactions. The hydraulic head BC at the Bay of Bengal was transformed into a saltwater-head BC, to account for the difference in pressure between freshwater and seawater. Mass concentration boundary conditions was added at the same location as the existing hydraulic head BC, with a minimum concentration of 500 mg/l on the western and southwestern model areas and a maximum concentration of 35000 mg/l in the eastern boundary (coast). An initial mass-concentration distribution was defined, according to the range used in the boundary conditions.

To avoid numerical instabilities, the mesh was refined in the coastal region (high density gradient area), which increased the total number of elements from 1 to 1.5 million.

### 3.9 Results and discussion

#### 3.9.1 Surface water model

The NAM model parameters were calibrated and extended homogeneously over the entire A-K basin. Since the model was calibrated for an eight year time period, it covers a wide range of hydrologic and climate conditions, which builds confidence in the model's ability to predict stream flow conditions under a variety of scenarios. The model gives a satisfactory comparison with observed flow records with an R<sup>2</sup> value of 0.6. Main focus was given to achieve least volume and peak errors (Figure 6). The model over-predicts the total volume in eight years by 10.5%, and a peak error of almost 7% for a discharge greater than 300 m<sup>3</sup>/day. Furthermore, the model over predicts the volume of flow in case of a heavy rainfall year (Figure 7). In the water year 2005-06, the total annual rainfall was above 2000 mm, most likely one of the worst floods to have hit the city of Chennai. The flood occurred during the north-east monsoon season (November-December 2005) as a result of heavy rain. Tambaram, the southern suburb, received the maximum rainfall of 314 mm over a 24-hour period in the State (Achuthan, 2005). This flood produces a difference of almost 200 Mm<sup>3</sup> between observed and simulated discharge. In the subsequent years, the increment of accumulated discharge was found to be constant. Thus, it can be concluded that the model predicts the total volume very well in average and low rainfall years. The NAM model does not predict low flow accurately due to high surface and root zone storage coefficients. These coefficients define the water holding capacity of the soil, i.e. overland flow will occur once the rainfall is greater than the thresholds of these coefficients. In the observed discharge records, it was found that the response of a rainfall that results in runoff is relatively high and therefore in the model it was implemented accordingly.

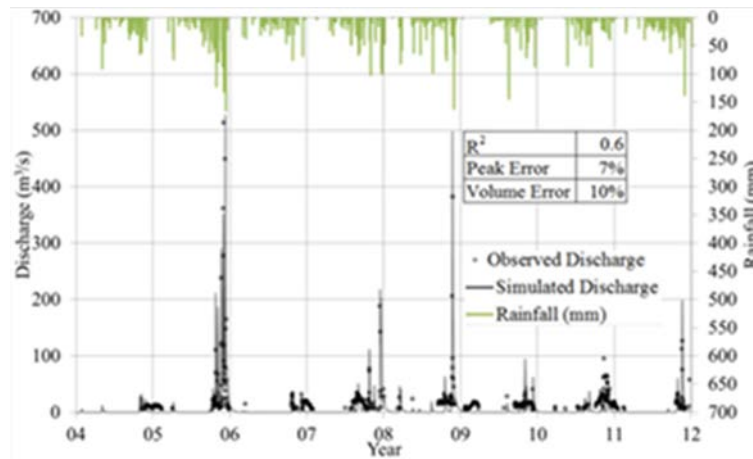


**Figure 6: Comparison of observed and simulated discharge from 2004 to 2012 at the inlet of Poondi reservoir.**

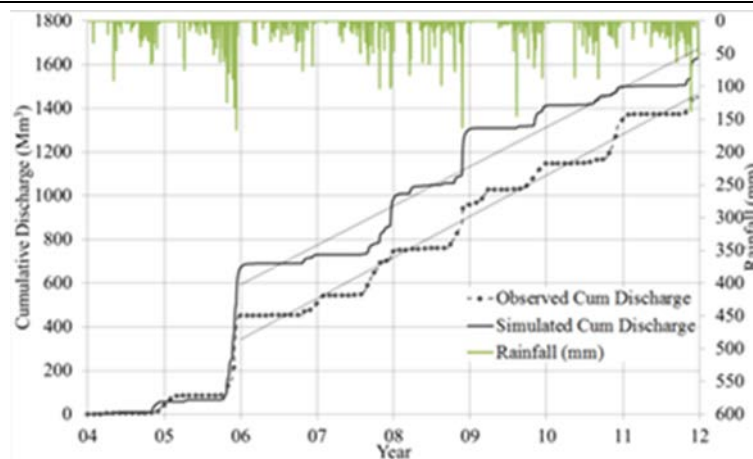


**Figure 7: Comparison of the observed and simulated cumulative discharge from 2004 to 2012 at the inlet of Poondi reservoir. The auxiliary lines show the slope of increment of cumulative discharge.**

The model results were used to create boundary conditions for the MIKE 11 HD model. The HD model was tested successfully for numerical stabilities and described all the basic functionalities, e.g. the effects of integrated structures, diversions and reservoirs in a realistic way. In a second stage, the HD model was extended to other tributaries west of the Poondi reservoir. All the streams greater than fourth order were implemented as network branches in the model in order to incorporate the upper reaches in the coupling framework.

### 3.9.2 Groundwater flow model

The model was calibrated in two stages: a steady state condition and a transient condition. The steady state calibration was carried out by varying the aquifer parameters within the allowable range in order to obtain a reasonable match between observed and simulated groundwater head. The steady state calibration was carried for the first of March 1996. Transient state calibration was carried out for a period of 14 years from

January 1996 to March 2010. Transient state calibration was conducted by trial and error method until best fit curve obtained for observed and simulated groundwater level. In the transient state calibration, the simulated groundwater level was matched with the observed groundwater level in most of the wells. The time series of the observed and simulated groundwater level for the well 7 (Figure 1) in the single aquifer is shown in Figure 8. Observed and simulated piezometric head fluctuation in the Minjur well filed well is shown in Figure 9.

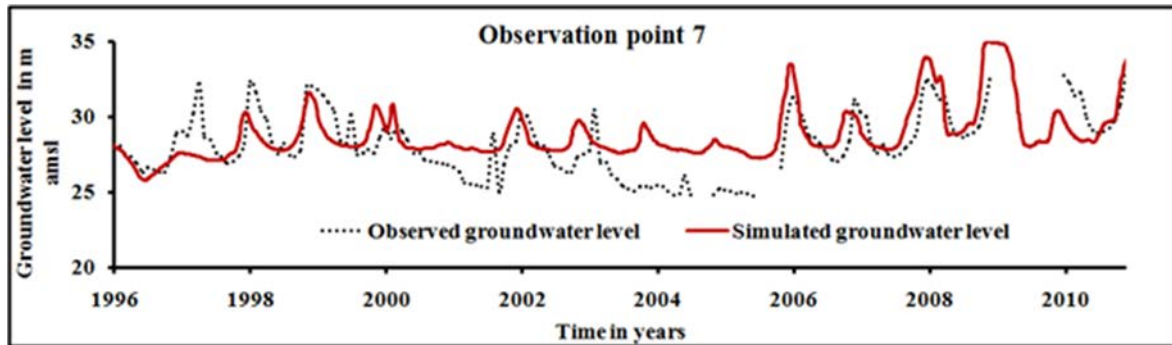


Figure 8. Observed vs. simulated groundwater level in single aquifer system

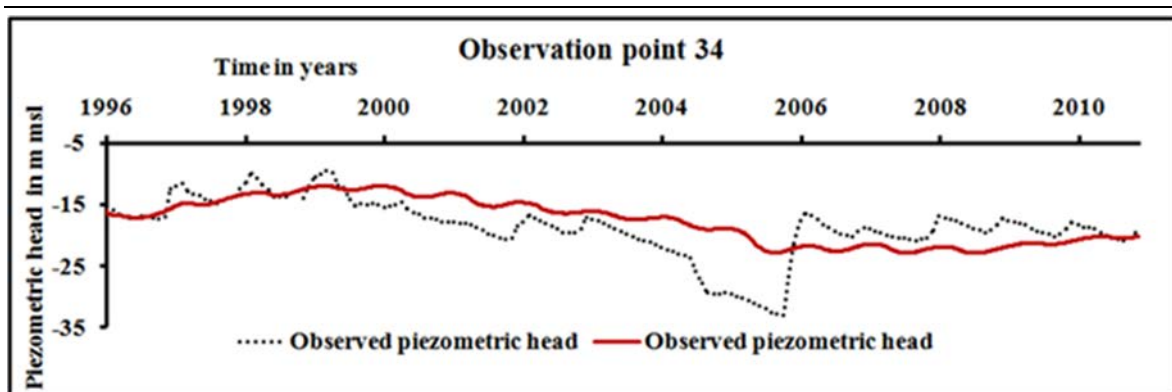


Figure 9. Observed vs. simulated piezometric head in bottom aquifer

### 3.9.3 Managed Aquifer Recharge

As a measure of MAR, check dams were implemented in the model to understand the groundwater level fluctuation. The aim was to increase the groundwater level when a higher number of check dams are implemented. Initially, the impact of check dams was computed and predicted, by using the uncoupled 3D groundwater model and representing the check dams in the 3<sup>rd</sup> Kind BC. There were a total of 10 check dams out of which 5 were in the Arani river and the remaining 5 were in the Koratalaiyar river which are constructed before the year 1996. Out of this 10 check dam, 9 check dam were considered for the simulation since one check dam in Arani river is located outside the model area. Groundwater level fluctuation in observation well 13 was simulated from the year 1996 to 2010 with respect to two scenarios (i.e.) with and without check dam and are shown in Figure 10. The justification to select observation well 13 as the reference well is that it is located near to the check dam which is suitable to explain the impact of check dam in groundwater. The red color dotted line shows the groundwater level fluctuation



with check dam and the black continuous line shows groundwater level fluctuation without the check dam. Groundwater level was increased to around 2 to 3 m with the presence of the check dam. Also, the volume of groundwater stored is increased by 0.638 Mm<sup>3</sup>/day with the construction of these check dams.

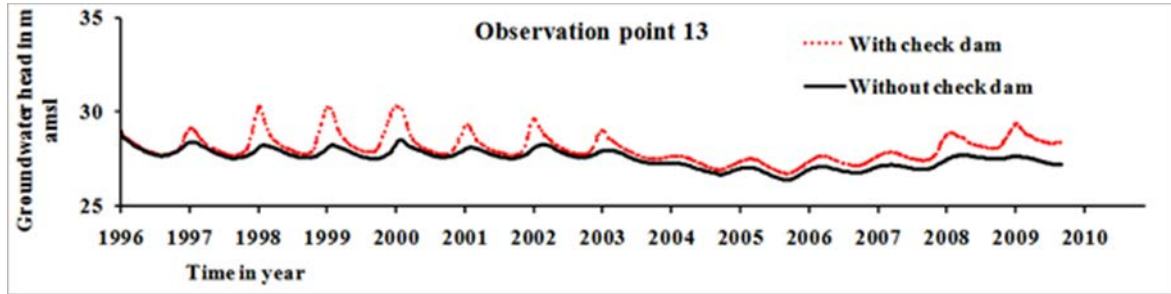


**Figure 10. Groundwater level fluctuation with and without check dam**

In a second stage, the groundwater model was coupled with the surface water model. The simulation was performed for the years 2004 to 2009. Two scenarios were simulated, scenario 1 considering most of the existing check dams until date (9 in total) and scenario 2 with three additional check dams (12 in total) and an increased dam crest of around 1 m at the remaining check dams.

The results indicate that there is an increase in the local groundwater levels, as can be seen at two exemplary locations, one in the Arani and the other at the Koratalaiyar River (Figure 11 to Figure 13). The resulting increase in groundwater levels at these locations is up to 2.5 m.

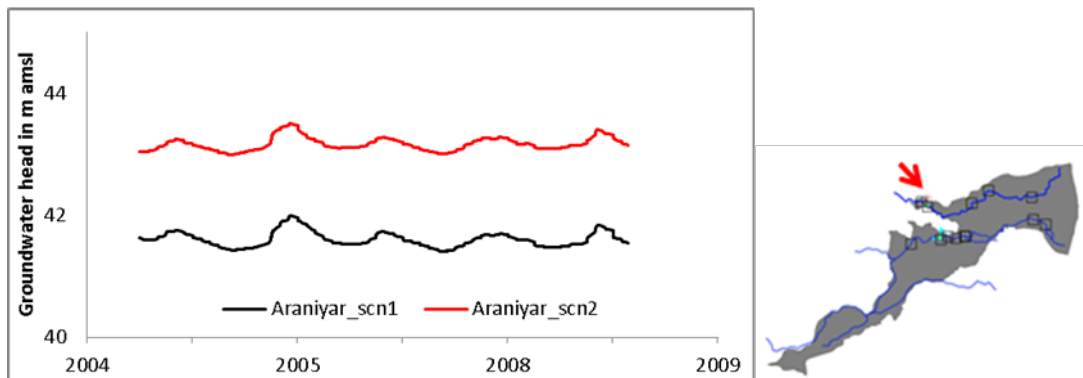


**Figure 11 – Comparison of groundwater levels for Scenario 1 and 2 at an exemplary location in the vicinity of an implemented check dam in the Araniyar River**

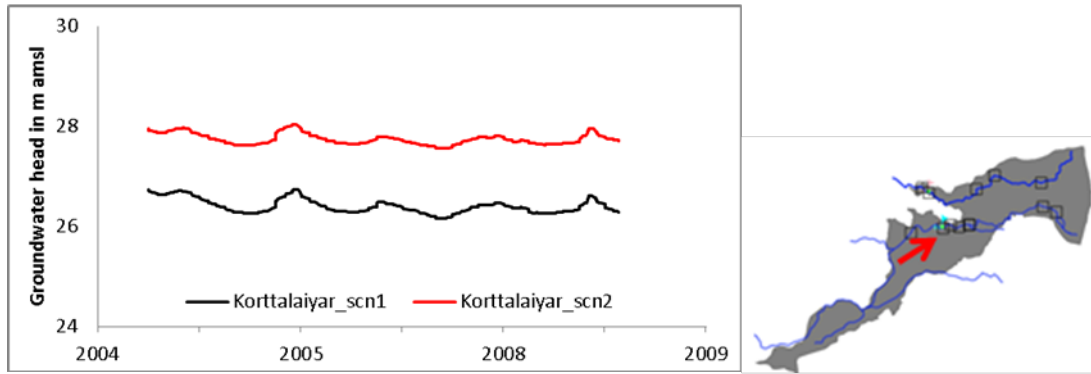


**Figure 12 – Comparison of groundwater levels for Scenario 1 and 2 at an exemplary location in the vicinity of an implemented check dam in the Korttalaiyar River**

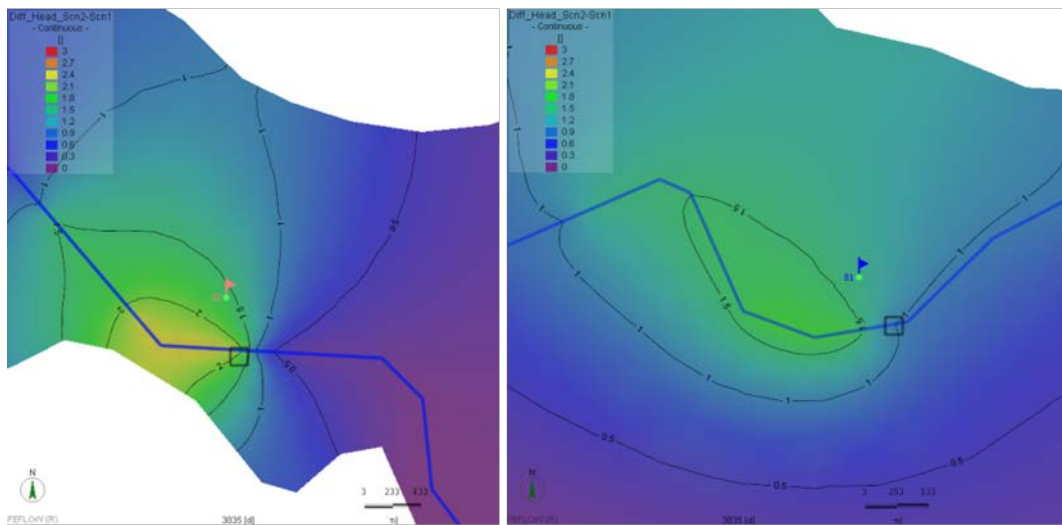


**Figure 13 – Comparison of groundwater levels for scenario 1 and scenario 2 in July 2006 at an exemplary location with implemented check dams in the Araniyar (left) and Korttalaiyar (right) Rivers**

#### 3.9.4 Density-Dependent model

The saltwater front was successfully represented using the uncoupled 3D groundwater model. Further numerical changes to improve the computational speed and reduce dispersivity are recommended. However, the current settings can be used to add the density component to the integrated surface and groundwater model.

An uncoupled density dependent seawater intrusion was simulated with the two scenarios i.e. with and without check dams. Figure 14 shows the spatial extent of simulated seawater intrusion with and without check dam. The extent of seawater intrusion distance is reduced to about 1 km with the construction of check dam during March 1988.

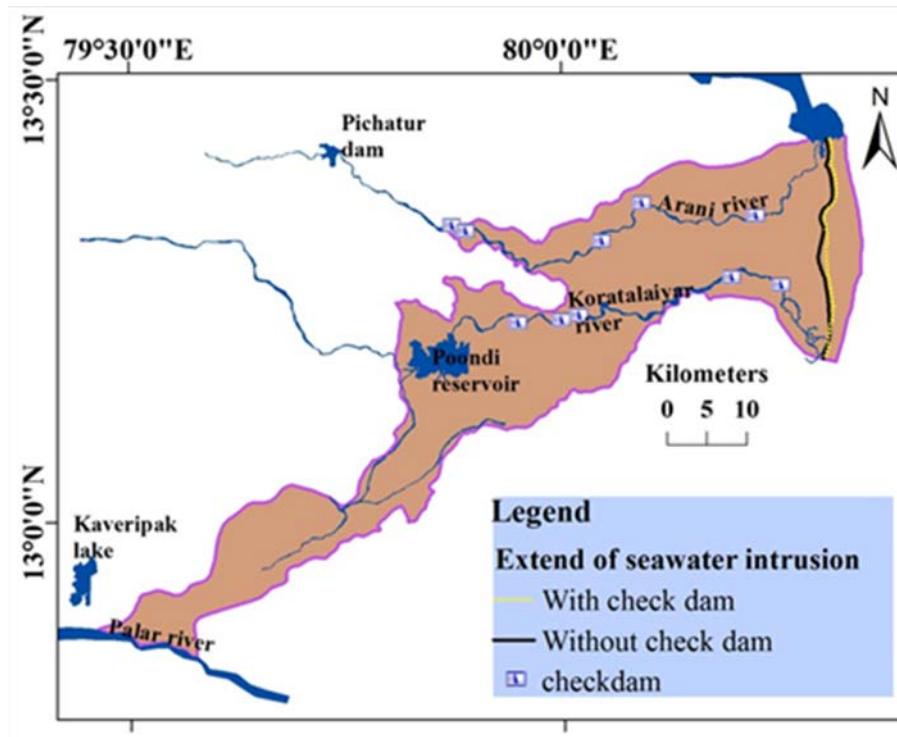


**Figure 14. Extent of seawater intrusion with two scenarios of with and without check dam during the month of March 1988**

### 3.10 Conclusion and future work

Based on the hydrogeological data, a multilayered aquifer system is identified in this study area. Two aquifer systems exist until 25 km from the coast line and a single aquifer is present beyond 25 km. The unconfined aquifer is identified in the upper 14 m and the semi-confined aquifer is recognized in the lower 35 m. The confining layer occurs between the unconfined and semi-confined aquifer, characterized by a mixture of clay and small amount of sand material. Hence, the lower aquifer is considered as a leaky aquifer. Field values of aquifer properties such as hydraulic conductivity and specific yield were achieved from the steady state simulation. Transient simulation results show good correlation between observed and simulated groundwater level. Rainfall recharge plays a major role compared to river infiltration since rivers are ephemeral and generally only carry water during 3 months in the rainy seasons. Over-exploitation of groundwater from well field caused great decline of groundwater for the year of 2004 and 2005. Due to this over exploitation, seawater has been intruding since the year 1981 to present.

The groundwater flow model has been coupled to a surface water model and serves as a tool to predict the groundwater flow dynamics under various recharge and discharge conditions. The effect of check dams has been analysed by running a scenario with additional check dams, as a measure of MAR. The results indicate that there is an increase in groundwater levels on a local scale, when additional check dams are implemented. Further an uncoupled density-dependent 3D groundwater model has been

set up, including a scenario with and without check dams. The implementation of several check dams showed a slight reduction on the extent of groundwater intrusion.

In future, the model can be used as a tool to predict groundwater level fluctuations and to determine the status of saltwater intrusion under various hydrological stress conditions.

### 3.11 Acknowledgements

Co-funding for the collaborative project 'Enhancement of natural water systems and treatment methods for safe and sustainable water supply in India – Saph Pani' ([www.saphpani.eu](http://www.saphpani.eu)) from the European Commission within the Seventh Framework Programme (grant agreement number 282911) is gratefully acknowledged. Department of Science and Technology, New Delhi, India (grant no: DST/WAR-W/SWI/05/2010) is kindly acknowledged. The Authors wish to acknowledge the Tamil Nadu Public Works Department, Chennai Metropolitan Water Supply and Sewerage Board, India, for providing the necessary groundwater level and bore hole data.

### 3.12 References

- Anuthaman, N.G. (2009) Groundwater augmentation by flood mitigation in Chennai region-A modelling based study, Ph.D Thesis, Anna University, Chennai, India.
- Ganesan, M., Thayumanavan, S. (2009) Management Strategies for a Seawater Intruded Aquifer System, *Journal of Sustainable development*, Vol. 2, No 1.
- Gnanasundar. D and Elango, L. (2000) Groundwater Flow modelling of a coastal aquifer near Chennai City, India, *Jou. of Indian Water Reso. Soc.*, Vol. 20, 4/162-171.
- Monnikhoff, B. 2011. Coupling the groundwater model FEFLOW and the surface water, *lfmMIKE11 2.0 User manual*. DHI-WASY Software.
- Rajaveni S.P, Indu S. Nair and Elango L. (2014) Application of remote sensing and GIS techniques for estimation of seasonal groundwater abstraction at Arani-Koratalaiyar river basin, Chennai, Tamil Nadu, India. *International journal of earth sciences and engineering*, Vol 07 (1), ISSN: 0974-5904
- Raudkivi A.J. and Callander R.A. (1976) *Analysis of ground water flow*. Edward Arnold (Publishers) Ltd, Old Woking, Surrey, London.
- Sivakumar C. and Elango, L. (2010) Application of solute transport modelling to study tsunami induced aquifer salinity in India. *Journal of Environmental Informatics*, 15(1), pp. 33-41.
- Sivakumar, C, Elango, L.and Gnanasundar, D (2006) Numerical modelling of groundwater flow in south Chennai coastal aquifer. In: *MODFLOW and More 2006 Managing groundwater systems*, Colorado School of Mines, USA, 21-24 May, pp 506-510.
- Sundaram, Dinesh, G, Ravikumar and Govindarajalu D. (2008), Vulnerability assessment of seawater intrusion and effect of artificial recharge in Pondicherry coastal region using GIS, *Indian Journal of Science and Technology*, Vol. 1, No. 7, 1-7.

UNDP (1987) Hydrogeological and artificial recharge studies, Madras. Technical report, United Nations Department of technical co-operation for development, New York, USA

## 4 Haridwar RBF system

*Title:* Use of travel time and flow path of groundwater to assess thermotolerant coliform breakthrough in riverbank filtration wells in Haridwar, India

*Authors* (HTWD + NIH): Cornelius Sandhu, Ulrike Feistel, Stefanie Fischer, Thomas Grischek, Narayan C. Ghosh

*Journal:* to be decided

*Status:* to be submitted

## 4.1 Abstract

The riverbank filtration (RBF) system by the Ganga River and Upper Ganga Canal (UGC) in Haridwar (Uttarakhand, India) has been sustainably meeting very dynamic drinking water demands in terms of quality and quantity for many years. Despite the fact that a substantial removal efficiency of TTC by the RBF system has been observed, the presence of bacteriological indicators (thermotolerant coliforms, TTC) has been detected in some wells abstracting a high portion of landside groundwater, thereby indicating the possibility of ambient groundwater being contaminated. In order to investigate this, a groundwater flow modelling study using Visual MODFLOW was conducted to determine the flow paths and travel time of the bank filtrate to the RBF wells and thus assess the risks to their well catchment zones from anthropogenic activities. Consequently the study has shown that the wells which abstract the highest portion of bank filtrate, have overall lower or at the most an equal magnitude (only in some cases) of TTC counts compared to RBF wells that abstract an equal or greater portion of ambient groundwater. On one hand the flow modelling study has helped to illustrate the effectiveness of the natural RBF system to remove pathogens, and on the other hand it illustrates the risk of contamination to unconfined aquifers from inhabited areas without appropriate collection, treatment and discharge of domestic sewage and wastewater. This highlights the need for the implementation of well-head and catchment protection zone measures, as well as continuous and robust disinfection of the water abstracted by the wells.

## 4.2 Introduction

Riverbank filtration (RBF) has been used since 1965 as a year-round natural treatment technology for the provision of drinking water to the population of >225,000 permanent residents (COI, 2011) of the city of Haridwar in the state of Uttarakhand in northern India and to the highly variable number of pilgrims who visit the city. It is reported that at least 50,000 pilgrims visit the city daily, whose number can increase up to 8.2 million on specific days when religious events such as the *Kumbh*, *Ardh Kumbh* and *Kanwar Mela* are held (Gangwar and Joshi, 2004). As of 2013 at least two-thirds, or 59,000 to 67,000 m<sup>3</sup>/day (Bartak et al., 2014), of the total raw water for drinking is abstracted from a total of 22 RBF wells with the remainder supplied by deep groundwater abstraction wells. The RBF wells are located on the west-bank of the Ganga river in the north, on Pant Dweep Island and on a narrow stretch of land between the Upper Ganga Canal (UGC) and the Ganga River in the southern part of the city (**Figure 4.1**).

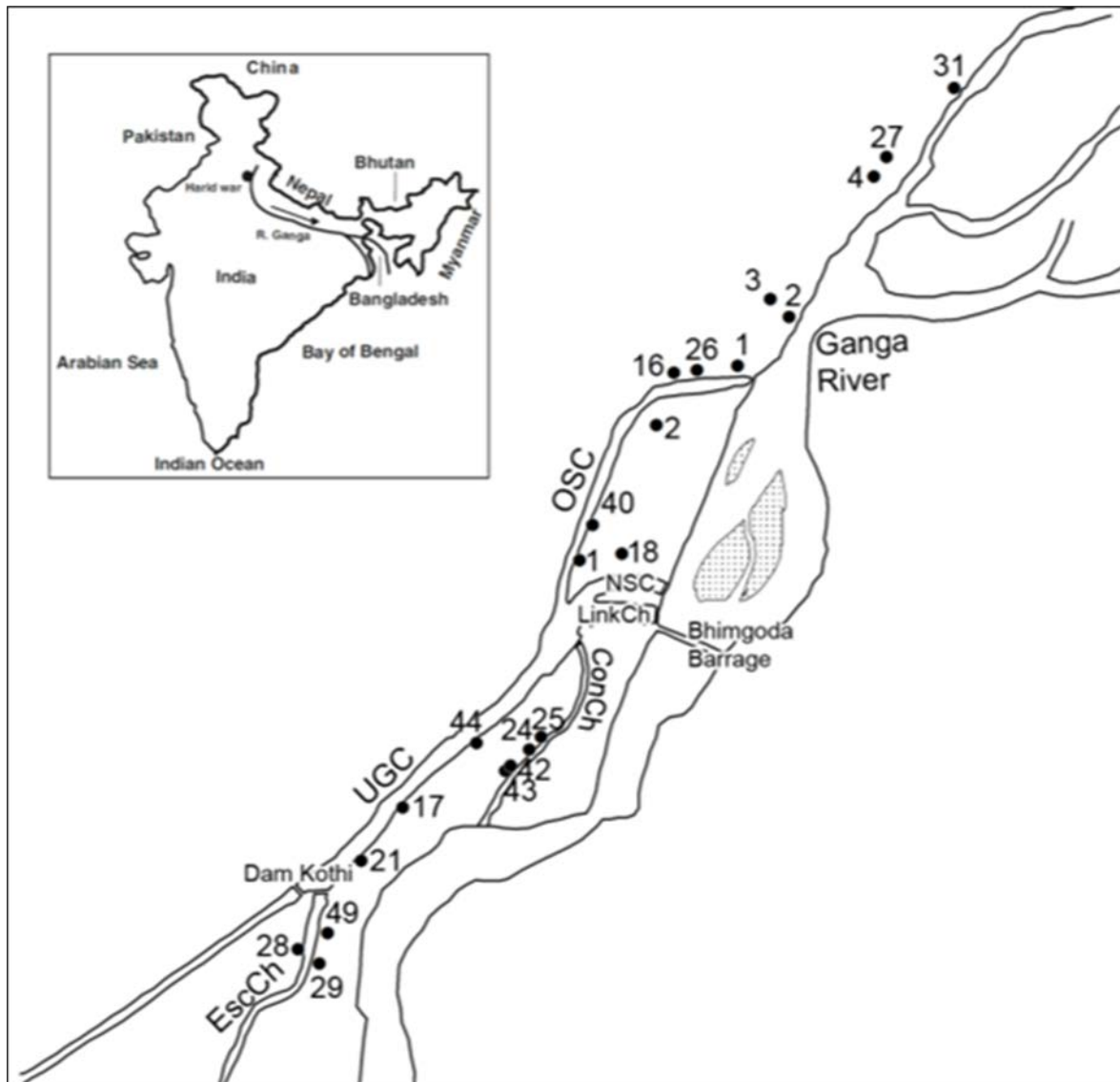


**Figure 4.1 Location of riverbank filtration wells in Haridwar**

Thus, by virtue of their proximity to the Ganga River and UGC that form natural recharge boundaries, the RBF wells abstract around 40 to 90 % bank filtrate (Bartak et al., 2014). The portion of bank filtrate abstracted by the wells located on Pant Dweep Island and further South is greater than those to the North. This is due to their location in an area influenced by the naturally occurring flow of bank filtrate between the UGC and Ganga River due to the difference in hydraulic gradient. The naturally pre-treated RBF water is abstracted from the upper unconfined alluvial aquifer, which is in hydraulic contact with the Ganga River and UGC. The aquifer comprises fluvial deposits of poorly graded sand (0.0075-4.75 mm) beneath which lies a lower layer of silty sand (Dash et al., 2010). After abstraction, the water is disinfected with sodium hypochlorite at the well prior to being distributed to the consumer. Although these wells are relatively shallow (7-10 m deep), they have a large storage capacity on account of their large diameter (~10 m). The abstraction from these wells is highly variable (790 to 7530 m<sup>3</sup>/day) and dependent on the season, with higher daily abstractions in monsoon as a result of longer operating hours



due to a greater water demand, but also due to an increase in groundwater levels due to greater recharge from the surface water bodies, compared to the non-monsoon period.

The discharge of partially treated sewage and untreated storm water run-off in to the Ganga River (and UGC in Haridwar) and its upstream tributaries, as well as large-scale ritualistic bathing, are a source of thermotolerant coliforms (TTC; *E. coli*) present in the surface water. In this context, mean TTC numbers measured in the 22 RBF wells, calculated from long term water quality data (2005 - 2013), were 18 TTC/100 ml during monsoon and 1 TTC/100 ml during non-monsoon compared with  $10^4 - 10^5$  TTC/100 mL in the Ganga, including UGC (Bartak et al., 2014). This highlights the significant removal efficiency of 3.5 to 4.4  $\log_{10}$  of TTC by RBF (Dash et al., 2010; Bartak et al., 2014).

### 4.3 Motivation

Despite the observed high TTC removal efficiency, TTC counts up to 93 MPN/100 ml were still observed in some RBF wells (Saph Pani D4.3, 2013; Bartak et al., 2014). In this context it has been observed that some RBF wells which are very close to the surface water body show the presence of coliforms, such as wells 40, 42, 17, 21 and 24 that are located at a distance of 6 - 36 m from the UGC and its escape channel.

However, it is also evident that RBF wells which are comparatively further away from the Ganga or UGC (48 - 190 m) and are located in the area where the Ganga enters Haridwar in the northern part of the city (thus low impact of upstream pollution), such as wells 3, 4, 26, 1 and 31, also have comparably high coliform counts of <2 - 93 MPN/100 ml (Bartak et al., 2014). Normally one would not expect wells to be contaminated at such a relatively far distance. But considering that the lack of well head protection zones, social land use practices such as public bathing/washing at the well heads, well head housing, cattle in and around the RBF wells and unsanitary defecation practices near/around the wells were identified as high risks for the Haridwar RBF system (Bartak et al., 2014), it is conceivable that the origin of coliforms in some RBF wells is not the bank filtrate from the Ganga River but rather ambient landside groundwater.

Thus, the objective of this study is to identify the flow paths of the bank filtrate to the RBF wells and the travel time in order to analyse the source of contamination of the wells in Haridwar. Additionally, an overall understanding of the hydrogeological system in response to dynamic hydrological regime of the Ganga River (high monsoon and low non-monsoon water levels) was to be achieved. The degree of confidence in the numerically simulated portion of bank filtrate abstracted by the RBF wells was to be ascertained through comparisons with analytical calculations from mean conductivity (EC; Bartak et al., 2014) and Oxygen-18 isotope values (Saph Pani D1.2, 2013).

## 4.4 Model set-up and Calibration

### 4.4.1 Data collection, water levels and RBF well abstraction rates

To describe and conceptualize the study area, data of different categories has been collected. Information about well and aquifer characteristics was collected from published and unpublished sources by the involved Saph Pani project partners (NIH, HTWD & UJS). Groundwater and river water levels were measured, and water quality samples were collected during field visits. In **Table 4.1** the collected information used for the preparation of a groundwater flow model for Haridwar is summarized.

**Table 4.1 Data used to prepare the groundwater flow model for Haridwar**

| Category           | Information about  |
|--------------------|--|
| Well data          | Location, diameter, depth, groundwater levels and discharge, running hours   |
| River data         | water levels, cross-sections, discharge (Ganga River)  |
| Water Quality data | Isotopes, major ions, iron, turbidity, coliforms   |
| Borehole-log data  | Large-diameter caisson well 18 (Pant Dweep), vertical filter well Bhupatwala, vertical filter well Mayapur                     |
| GIS data           | well, river and borehole-log locations, digital elevation model  |
| Literature data    | Range for hydraulic conductivity of the riverbed (Ganga River at Bhimgoda Barrage, UGC, NSC), monthly rainfall and temperature |

The groundwater level within each well was measured weekly during the monsoon season and monthly during non-monsoon season using a water-level tape. To determine the river water levels, five existing gauging stations (Central Water Commission, Old Supply Channel - OSC, Bhimgoda Barrage upstream and downstream, Link Channel and the Dam Kothi barrage on UGC) were read out in the mentioned time intervals. Additionally the surface-water levels at particular locations, especially downstream of Bhimgoda Barrage and at Pant Dweep Island, were measured at reference dates using a levelling instrument (autolevel and dumpy level). The actual abstraction rates and operating hours of the RBF wells were determined from ultra sonic flow meter measurements (**Table 4.2**). The abstraction rates for some wells were provided by UJS.

The actual hourly abstraction rates of the RBF wells for the monsoon and non-monsoon operating hours were normalised for a continuous operation (24 hour period) and assigned using the well boundary condition for the 22 RBF wells in the model at their respective locations

The caisson wells in the present case do not have a classical vertical filter screen. The water enters the well through the well-bottom. Such caisson wells have a significant storage capacity. Groundwater flowing from the aquifer into the well-storage can be extracted easily over the whole saturated depth of the well. Therefore, the required screen in Visual MODFLOW is defined from the top up to the well bottom.

**Table 4.2 Operation and abstraction rates of RBF wells in Haridwar (Sandhu, 2015)**

| Well No. | Location    | Mean discharge [m <sup>3</sup> /hour] | Monsoon (July – September)             |  | Pre- & post-monsoon (October – June)   |  |
|----------|-------------|---------------------------------------|--|--|--|--|
|          |             |                                       | Mean duration of operation [hours/day] | Mean daily discharge [m <sup>3</sup> /day] | Mean duration of operation [hours/day] | Mean daily discharge [m <sup>3</sup> /day] |
| 31       | Bhopatwala  | 229.9 <sup>b</sup>                    | 20                                     | 4598                                       | 10                                     | 2299                                       |
| 27       | Bhupatwala  | 118.8 <sup>b</sup>                    | 20                                     | 2375                                       | 14                                     | 1663                                       |
| 4        | Bhupatwala  | 100.8 <sup>b</sup>                    | 20                                     | 2016                                       | 20                                     | 2016                                       |
| 2        | Bhupatwala  | 213.0 <sup>c</sup>                    | 20                                     | 4259                                       | 10                                     | 2130                                       |
| 3        | Bhupatwala  | 170.1 <sup>c</sup>                    | 20                                     | 3401                                       | 20                                     | 3401                                       |
| 1        | Bhupatwala  | 176.3 <sup>c</sup>                    | 20                                     | 3526                                       | 20                                     | 3526                                       |
| 26       | Bhupatwala  | 102.0 <sup>a</sup>                    | 16                                     | 1632                                       | 16                                     | 1632                                       |
| 16       | Bhupatwala  | 108.0 <sup>d</sup>                    | 12                                     | 1296                                       | 12                                     | 1296                                       |
| 18       | Pantdweep   | 134.3 <sup>c</sup>                    | 10                                     | 1343                                       | 10                                     | 1343                                       |
| PD2      | Pantdweep   | 120.0 <sup>d</sup>                    | 10                                     | 1200                                       | 10                                     | 1200                                       |
| PD1      | Pantdweep   | 65.7 <sup>c</sup>                     | 12                                     | 789  | 12                                     | 789  |
| 40       | Pantdweep   | 109.6 <sup>c</sup>                    | 22                                     | 2412                                       | 22                                     | 2412                                       |
| 25       | R. Belwala  | 177.9 <sup>c</sup>                    | 22                                     | 3913                                       | 15                                     | 2668                                       |
| 24       | R. Belwala  | 202.6 <sup>c</sup>                    | 23                                     | 4660                                       | 15                                     | 3039                                       |
| 43       | R. Belwala  | 132.9 <sup>c</sup>                    | 22                                     | 2924                                       | 22                                     | 2924                                       |
| 42       | R. Belwala  | 110.7 <sup>b</sup>                    | 22                                     | 2435                                       | 22                                     | 2435                                       |
| 44       | Vishnu Ghat | 127.0 <sup>c</sup>                    | 24                                     | 3049                                       | 24                                     | 3049                                       |
| 17       | Lalta Rao   | 327.2 <sup>c</sup>                    | 23                                     | 7526                                       | 23                                     | 7526                                       |
| 21       | Alaknanda   | 108.0 <sup>c</sup>                    | 16                                     | 3344                                       | 16                                     | 3344                                       |
| 49       | B. Camp     | 108.0 <sup>a</sup>                    | 23                                     | 2484                                       | 23                                     | 2484                                       |
| 29       | B. Camp     | 149.7 <sup>c</sup>                    | 23                                     | 3443                                       | 23                                     | 3443                                       |
| 28       | M. Milan    | 209.4 <sup>c</sup>                    | 23                                     | 4815                                       | 23                                     | 4815                                       |

a: discharge provided by UJS in 2006; b, c: discharge measured using an ultrasonic flowmeter in 12/2012 and 10/2013 respectively; d: adapted from UJS (2006)

#### 4.4.2 Interpolation of undisturbed groundwater levels

As the RBF wells in Haridwar operate discontinuously for durations ranging from 10 to 24 hours (**Table 4.2**) it is difficult to ascertain undisturbed or rest groundwater levels. Consequently the undisturbed groundwater levels have been estimated by interpolating

between known surface water levels bounding the aquifer on both sides. Here, the surface water levels around the wells have been measured at particular points, to apply the interpolation method, which is visualized in **Figure 4.2**. The gradient  $I$  between the river water levels  $H_1$  and  $H_2$ , with a distance  $L_1$ , is calculated by equation (1). The undisturbed water level of the well  $H_{well}$  can be derived by (2), using the gradient  $I$  and the distance  $L$  between one of the rivers to the RBF well.

$$I = \frac{(H_1 - H_2)}{L_1} \quad (1)$$

$$H_{well} = H_1 - (I \cdot L_2) \quad (2)$$

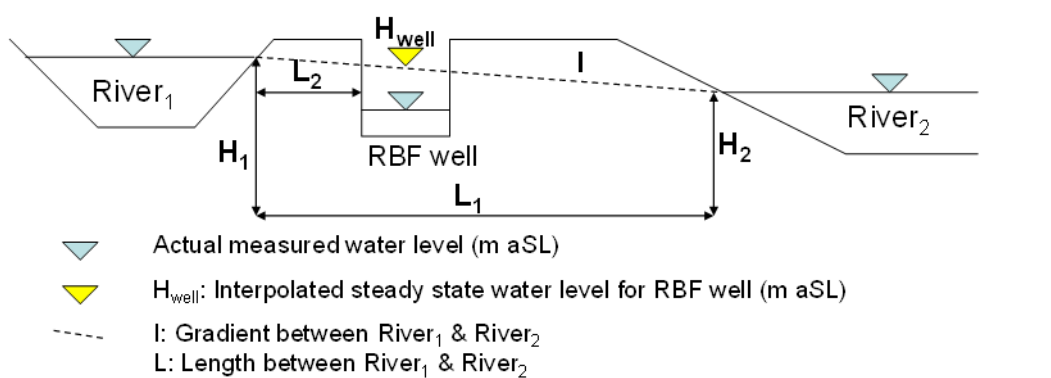


**Figure 4.2 Method to estimate the steady state (undisturbed) groundwater level for a RBF well by interpolation**

#### 4.4.3 Model set-up

A three dimensional finite element two layered numerical groundwater flow model was set up in Visual MODFLOW (version 2011.1). Using an ArcGIS-map of the well and river locations, the horizontal extent of the study area was determined to be 5000 m in X-direction and 6000 m in Y-direction. Hence, the horizontal model grid was divided into 50 columns and 60 rows to get a uniform cell size of 100 x 100 m. Additionally the model grid was refined for the well and river areas by adding rows and columns to allow a more detailed simulation, especially in those areas with steep hydraulic gradients (i.e. drawdowns around the wells). To avoid numerical instabilities, the size difference between adjacent cells did not exceed a factor of 2. Thus, the final spatial resolution of the horizontal model grid ranges between 12.5 and 100 m. According to the borehole-log results for Pant Dweep Island (Dash et al., 2010), the aquifer is assumed to have a uniform thickness of 21 m for the entire model area. To take into account the partial penetration of the large diameter bottom entry caisson wells and the predominantly two-layered aquifer comprising fluvial deposits of poorly graded sand (0.0075-4.75 mm) in the upper 12 m beneath which lies a layer of silty sand (Dash et al., 2010), the first layer ranges from the top of the surface to the bottom of the wells and is followed by the second layer, which extends to 21 m below the ground surface (**Figure 4.3**).

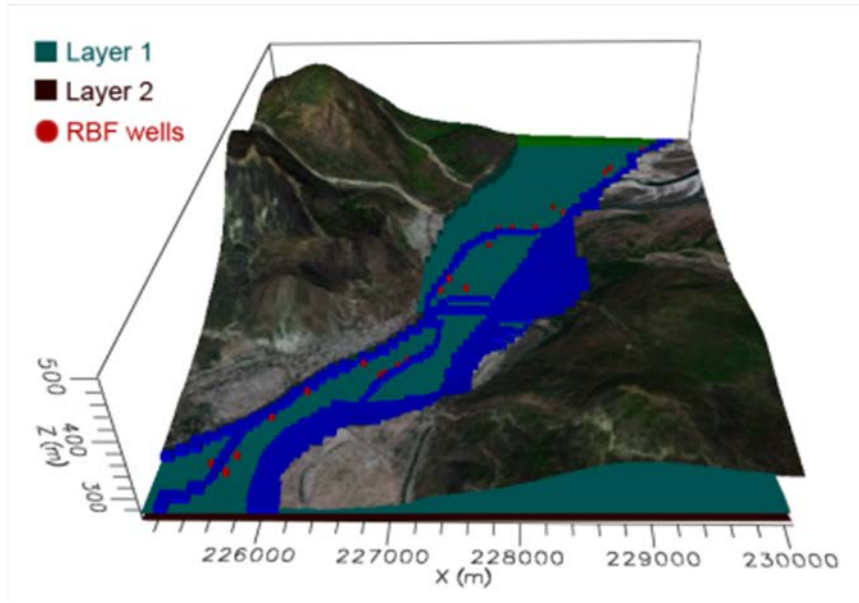


**Figure 4.3** Piedmont plain, the floodplain and vertical extent (2 layers) of the model area

#### 4.4.4 Model boundaries

The boundary condition in the north of the study area has been interpolated using the triangulation method for undisturbed groundwater levels and river water levels. Since well no. 31 is located close to the northern boundary of the model, a general head boundary was assigned instead of the more common used constant head (**Figure 4.4**). So the boundary head is not directly influencing the water level of IW 31. The Ganga River, UGC and its escape channel are represented by the river boundary condition. The hydraulic connection between the Ganga (and channels) and the aquifer is represented by the riverbed conductance factor, comprising the river cell dimensions, riverbed thickness and hydraulic conductivity of the riverbed. Consequently, the conductance value for each grid cell, which changes due to different cell sizes within the model, is calculated automatically. The river level is assigned at particular points where the stage has been measured. Riverbed elevation and width have been determined using cross-sections constructed from field measurements. Between those points, the required physical dimensions of the river are interpolated automatically by Visual MODFLOW. The hydraulic conductivity of the riverbed is finally set during the calibration. After Sandhu et al. (2010), the k-value of only the short stretch of the New Supply Channel (connecting the Bhimgoda Barrage to the UGC) located immediately to the South of Pant Dweep Island and the bed of the Ganga River only in the reservoir of the Bhimgoda Barrage along Pant Dweep's eastern boundary is  $0.2 \times 10^{-06}$  to  $9 \times 10^{-06}$  m/s, as determined by sieve analyses of riverbed material samples (after Hazen, 1893). This is representative of fine sediment material deposited by the barrage outflow as a result of the lower flow velocity ( $<1$  m/s) and gradient in the New Supply Channel (NSC). The high silt content of 40–70% deposited only on the bed of the NSC and the Ganga River within the Bhimgoda Barrage Reservoir (up to the northern

point of Pant Dweep Island where the UGC starts) is likely limits the hydraulic connection with the aquifer to a certain degree. Higher K-values of  $1.2 \times 10^{-4}$  to  $7.4 \times 10^{-3}$  m/s were assigned to the bed of the UGC (Sandhu et al., 2010).

Due to the fact that the area of interest is only the floodplain of Haridwar and to avoid unnecessary computational effort, the mountains in the western part and the cells next to the Ganga River in the eastern part of the model area have been assigned as inactive cells. **Figure 4.4** shows the model domain including pumping wells (dark red points), the observation well Kabir Ashram (pink point), inactive cells (turquoise), general head- (green cells) and river boundaries (dark blue cells).

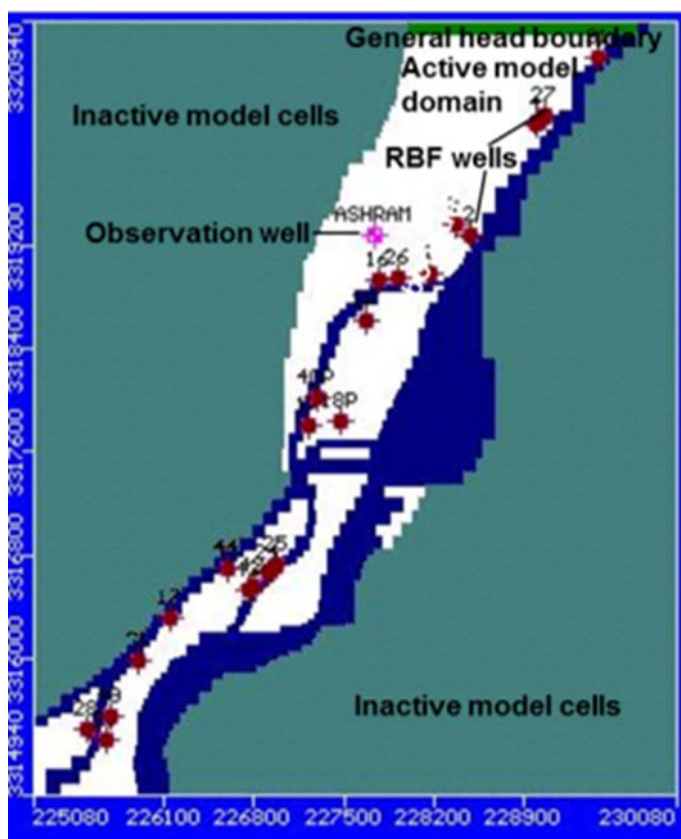


**Figure 4.4** Conceptualized model domain area of the 22 RBF wells in Haridwar

#### 4.4.5 Steady-state model calibration and particle tracking

The steady-state flow model was calibrated for a pre-monsoon condition (**Figure 4.5**, right; **Table 4.3**). Thereafter, the surface water levels and well discharges were applied to the model for the monsoon (August 2012) and post-monsoon (October) periods. A relatively good calibration was achieved for each of these conditions (**Figure 4.5**, left and centre; **Table 4.3**, left and centre).

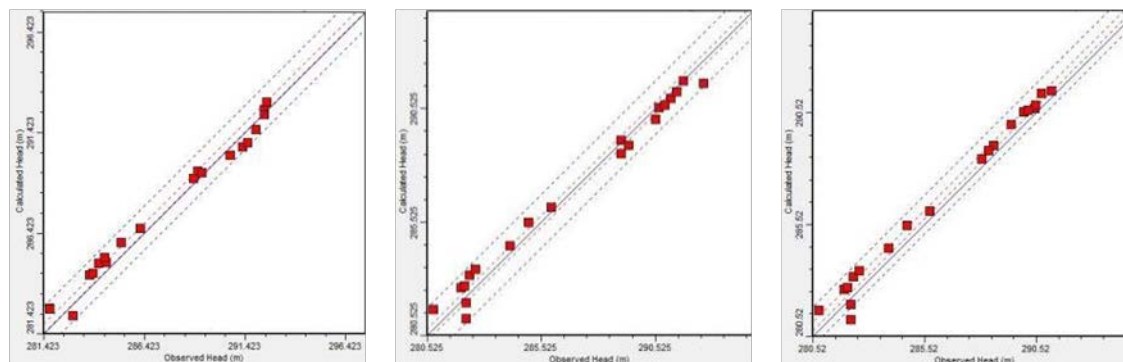


**Figure 4.5 Monsoon (August 2012 ; left), post-monsoon (October 2012 ; centre) and pre-monsoon (January 2013 ; right) steady-state calibration**

**Table 4.3 Summary of calibration parameters**

| Calibration parameter             | Monsoon<br>(August 2012) | Post-monsoon<br>(October 2012) | Pre-monsoon<br>(January 2013) |
|-----------------------------------|--------------------------|--------------------------------|-------------------------------|
| Standard error [m]                | 0.12                     | 0.13                           | 0.09                          |
| Root mean squared (RMS) error [m] | 0.57                     | 0.56                           | 0.61                          |
| Normalised RMS error [%]          | 5.3                      | 4.7                            | 5.8                           |
| Correlation Coefficient           | 0.994                    | 0.993                          | 0.994                         |
| Maximum residual head [m]         | 0.97                     | -1.01                          | -0.95                         |
| Minimum residual head [m]         | -0.01                    | 0.00                           | 0.26                          |
| Residual mean head [m]            | 0.27                     | 0.03                           | 0.45                          |
| Absolute residual mean [m]        | 0.52                     | 0.47                           | 0.57                          |

Subsequently the particle tracking tool was used in MODPATH to visualize the flow paths and travel times of water to the RBF wells. The zone budget method in MODFLOW was used to estimate the portion of bank filtrate abstracted by the RBF wells.

#### 4.5 Results

The simulated flow paths of the water to the RBF wells (**Figure 4.6**, left) corroborate to the portion of bank filtrate abstracted by them that have been calculated from long-term mean electric conductivity values (Bartak et al., 2014) and Oxygen-18 isotope values (Saph Pani D1.2, 2013). The flow of water to the wells in **Figure 4.6** (left) indicate that the RBF wells located in the northern part of Haridwar also receive a considerable portion of groundwater in addition to some bank filtrate. For the wells 3, 4, 26 and 1, the portion of ambient landside groundwater is between 40 - 60 % and consequently the remainder being bank filtrate, with a greater portion of bank filtrate abstracted in monsoon due to an increase in the Ganga River levels and thereby the water line of the river moving closer to

the bank and the wells. But as the area that lies in the groundwater catchment of the RBF wells is densely populated and substantially large, there is a greater risk of contamination from decentralised sewage disposal (septic tanks) and leaky wastewater drains. This would also explain the high TTC counts in in the RBF wells in relation to a relatively low portion of bank filtrate.

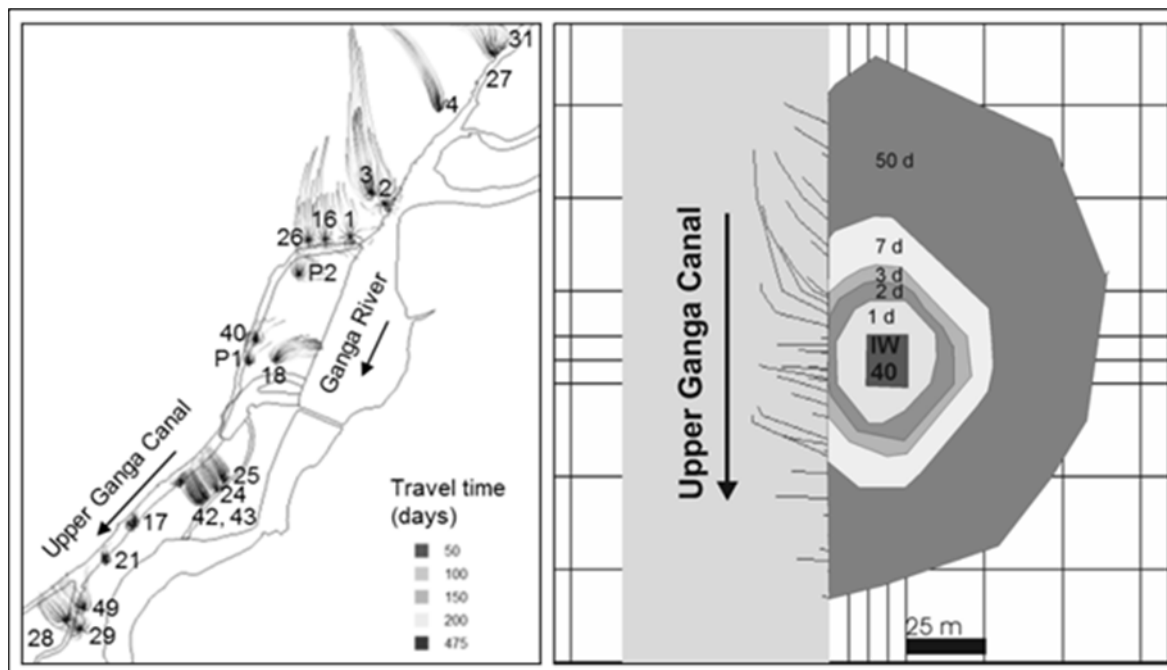


**Figure 4.6 Travel time and flow paths of bank filtrate for RBF system in Haridwar (left) and travel time of bank filtrate during monsoon for RBF well 40**

On Pant Dweep Island the shortest travel time of the bank filtrate to the wells 40 and P1, located only 15 m from the UGC, is around 3 days during the non-monsoon period that decreases to 2 days during monsoon (**Figure 4.6**, right). The mean portion of bank filtrate abstracted is 60 - 70 % and while the TTC counts in well 40 are <2 - 93 MPN/100 ml, they are <3 MPN/100 ml or below the detectable limit in well P1 (Bartak et al., 2014). Although both wells exhibit short travel times of bank filtrate, bathing and washing activities take place immediately next to well 40 by means of a tap attached to the main distribution pipe at the well. Thus the higher TTC count in well 40 and other wells located close to the UGC bank with similar short travel times, can be explained due to preferential flow of water in to the RBF wells from above ground and around the wells (not river / canal water) due to flooding, an intensive rainfall event or regular seepage / drainage of wastewater from bathing and washing activities (Saph Pani D1.2, 2013), which result in very short travel times (45 minutes to 4.5 hours) as demonstrated by a NaCl tracer experiment on well 40 by Sandhu et al. (2014). For RBF wells 18 and P2, located between 110 and 320 m from the UGC and Ganga River, the travel time of the bank filtrate is substantially longer (up to a year, **Figure 4.6**, left). Compared to well 40, the TTC count is lower with a maximum of only 15 MPN/100 ml. As the bank filtrate to these wells has considerably long travel times, the likely reason is above ground contamination from wide spread defecation on the vast



open spaces of the Pant Dweep Island that has an extremely large influx of pilgrims and tourists daily, especially during festivals like the *Kanwar Mela*. During longer festivals like the *Kumbh* and *Ardh Kumbh Melas*, pilgrims reside on the island for up to 4 months. Unlined pit-latrines are dug for such events that have been assessed as a risk to the wells (Bartak et al., 2014).

On the other hand, the remaining wells that are located at a distance of 15 m and more from the UGC in the southern part of Haridwar abstract the highest portion of bank filtrate of all RBF wells in Haridwar (80 - 90 %). The simulated portion of bank filtrate (using the zone budget tool in MODPATH) abstracted by these wells lies within a  $\pm 10\%$  confidence limit of the analytically calculated portions using EC and Oxygen-18 isotope data. The maximum TTC count observed in some wells was up to 15 MPN/100 ml while in the others it was below the detectable limit of  $<3$  MPN/100 ml, with the exception of one well having a maximum TTC count of 93 MPN/100 ml (Bartak et al., 2014). As the area between these wells and the UGC, its escape channels and Ganga River is not residential, the impact from domestic sewage (septic tanks, pit-latrines) is low. However, occasional high TTC counts can be attributed to washing and bathing activities and inappropriate drainage of water (wastewater, rainfall and/or storm water runoff) accumulated near/around the wells.

Most importantly, the comparatively overall low TTC counts highlights the high removal efficiency of the RBF system, because most of the public bathing takes place daily in this stretch of the UGC from which the bank filtrate to these wells originates. Furthermore, the annual monsoon and the location of the wells in an area result in a natural recharge to the RBF wells thereby ensuring sustainable operation during periods of peak water demand.

#### 4.6 Conclusions

The Haridwar RBF system is operating sustainably since 1965. The groundwater flow modelling study of the RBF system in Haridwar has identified the flow paths of bank filtrate and the groundwater catchment areas of the RBF wells. In conjunction with investigations on the risk of floods and health risk assessment to RBF wells using Haridwar as an example (Sandhu et al., 2014; Bartak et al., 2014), the groundwater flow modelling investigation has helped to identify potential sources of contamination to the wells. Consequently the study has shown that the wells which abstract the highest portion of bank filtrate, have overall lower or at the most an equal magnitude (only in some cases) of thermotolerant coliform counts compared to RBF wells that abstract an equal or greater portion of ambient groundwater. On one hand the flow modelling study has helped to signify the effectiveness of the natural RBF system to remove pathogens, and on the other hand it illustrates the risk of contamination to unconfined aquifers from inhabited areas without appropriate collection, treatment and discharge of domestic sewage and wastewater. This highlights the need for the implementation of well-head and catchment protection zone measures, as well as continuous and robust disinfection of the water abstracted by the wells. These measures have to be prioritised in lieu of the growing

pressure on land use and conflicting interests. The flow modelling study has also shown the benefit of locating RBF wells on islands and in areas where a natural flow between surface water bodies occurs to ensure sustainable abstraction. The groundwater flow model of the Haridwar RBF system is a useful tool to compliment the water quality and isotope investigations and can be integrated into a regional hydrogeological assessment of the Haridwar urban area.

#### 4.7 References

- Bartak R., Page D., Sandhu C., Grischek T., Saini B., Mehrotra I., Jain C. K. and Ghosh N. C. (2014). Application of risk-based assessment and management to riverbank filtration sites in India. *Journal of Water and Health*, doi:10.2166/wh.2014.075 (Available online 31 May 2014)
- Dash R. R., Bhanu Prakash E. V. P., Kumar P., Mehrotra I., Sandhu C. and Grischek T. (2010). River bank filtration in Haridwar, India: removal of turbidity, organics and bacteria. *Hydrogeology Journal*, 18(4), 973-983.
- Gangwar K. K. and Joshi B. D. (2004). A preliminary study on solid waste generation at Har Ki Pauri, Haridwar, around the Ardh-Kumbh period of sacred bathing in the river Ganga in 2004. *Environmentalist*, 28(3), 297-300.
- Hazen A. (1893). Some physical properties of sands and gravels. 24th annual report, Massachusetts State Board of Health, Boston, MA.
- Sandhu, C. (2015). Prospects and Limitations of Riverbank Filtration In India (provisional title). PhD thesis, in preparation, Dresden University of Technology, Institute of Waste Management and Contaminated Site Treatment, and Dresden University of Applied Sciences, Faculty of Civil Engineering/Architecture, Division of Water Sciences.
- Sandhu C., Grischek T., Ronghang M., Mehrotra I., Kumar P., Ghosh N. C., Rao Y. R. S., Chakraborty B., Patwal P. S. and Kimothi P. C. (2014) Overview of bank filtration in India and the need for flood-proof RBF systems. In: Wintgens T. and Nätörp A. (eds.) *Saph Pani – Enhancement of natural water systems and treatment methods for safe and sustainable water supply in India*. IWA Publishing, London, UK and Saph Pani D7.5 - Saph Pani Handbook. <http://www.saphpani.eu/downloads>
- Sandhu C., Schoenheinz D. and Grischek T. (2010). The impact of regulated river-flow on the travel-time and flow-path of bank filtrate in Haridwar, India. In: Zuber A., Kania J., Kmiecik E. (Eds.) *Extended Abstracts*, 38. IAH Congress, 12.-17.09.2010, Krakow, pages 2299-2305.
- Saph Pani D1.2 (2013). Guidelines for flood-risk management of bank filtration schemes during monsoon in India. Saph Pani Project Deliverable. <http://www.saphpani.eu/downloads> (accessed 19 August 2014)
- Saph Pani D4.3 (2013). Post-treatment Requirements of Different Natural Treatment Systems. <http://www.saphpani.eu/downloads> (accessed 19 July 2014)

## 5 New Delhi RBF system

*Title:* Transport of Ammonium in Porous Media – Column Experiments with Alluvial Sediments and Reactive Transport Modelling

*Authors (FUB, KWB):* Maike Groeschke, Theresa Frommen, Enrico Hamann, Gesche Grützmacher, Michael Schneider

*Journal:* probably Environmental Earth Sciences

*Status:* To be submitted

## 5.1 Abstract

In India's capital Delhi, the Yamuna River is highly influenced by sewage water and Ammonium concentrations up to 20 mg/L were measured in the river in 2012-13. Large production wells located in the alluvial aquifer along the river draw high shares of bank filtrate and after nearly forty years of operation ammonium concentrations reached 5-8 mg/L in the raw water of the production well closest to the river. In order to obtain input parameters for a field scale model, which is necessary for predicting the future development of ammonium concentrations, the transport of ammonium was studied in laboratory experiments. The aquifer consists of two lithological units, medium sand and gravel made up of calcareous nodules called kankar. Adsorption and desorption experiments were conducted with both materials in laboratory columns under suboxic and anoxic conditions with ammonium concentrations of 10 and 20 mg/L and negligible nitrite and nitrate concentrations in the feed water. Nitrogen mass balances reveal that all ammonium that is retained in the sediments during the adsorption experiments is desorbed again in the desorption experiments. Cation exchange is therefore the dominating transport mechanism. It took about ten flushed pore volumes until the 100% ammonium breakthrough occurred in the sand columns and 30 flushed pore volumes in the kankar material. To simulate the ammonium transport, 1D reactive transport models of the column experiments were developed with PHT3D. Transport parameters were obtained from pulse style tracer tests. Cation exchange was implemented in the model and the selectivity coefficients of the main cations and ammonium were adjusted according to calculated values derived from water and sediment analyses. The modelled curves fit the measured data well for both, the ammonium breakthrough and the other cation concentrations (Na, K, Ca, Mg).

*Key words* Alluvial aquifer, ammonium, cation exchange, column experiments, reactive transport modelling

## 5.2 Introduction

Natural treatment systems such as managed aquifer recharge (MAR), constructed wetlands and bank filtration (BF) are increasingly used worldwide as the benefits become widely recognized. Especially bank filtration, sometimes also called riverbank filtration (RBF), is increasingly used for drinking water production (Tufenkji et al. 2002, Doussan et al. 1997, Grünheid et al. 2005) as it has two main advantages: (1) Sufficient quantity of water can be produced independent of the usable groundwater capacity as BF is a form of artificial groundwater recharge (Bouwer 2002, Dillon 2005). (2) Low cost post treatment is often sufficient for the raw water as the process of bank filtration takes advantage of the natural filter capacity of the sediments during the soil passage (Kuehn and Mueller 2000). Usually, there is a significant increase in water quality for the bank filtrate compared to the

surface water regarding organic substances, color, coliform bacteria and fecal contaminants (Singh et al. 2010, Weiss et al. 2005). However, when bank filtration is applied at sewage contaminated surface waters, which is often the case in developing countries (Ray 2008) a range of problems can arise. When contaminated water infiltrates into the aquifer in large quantities, the capacity of the soil to filter the contaminants is often exceeded (Heberer 2002) - and one parameter of concern in this context is nitrogen, especially the reduced species ammonium (Hiscock and Grischek 2002).

A bank filtration site in central Delhi was studied where the infiltration of sewage contaminated surface water from Yamuna River caused a strong ammonium increase in the aquifer with peak concentrations up to 35 mg/L  $\text{NH}_4^+$  in the centre of the contamination plume and concentrations between 5-8 mg/L  $\text{NH}_4^+$  in the raw water of the first production well (Fig. 1). Besides hydrogeological conditions like flow velocity and mixing, several factors may control or influence the transport and fate of ammonium: reversible interactions with the aquifer matrix (sorption and ion exchange) and irreversible processes such as fixation (absorption in the interlayers of clay minerals) or degradation, which often plays a major role in the transport of redox-sensitive contaminants. The transport of ammonium is, therefore, strongly linked to site-specific conditions.

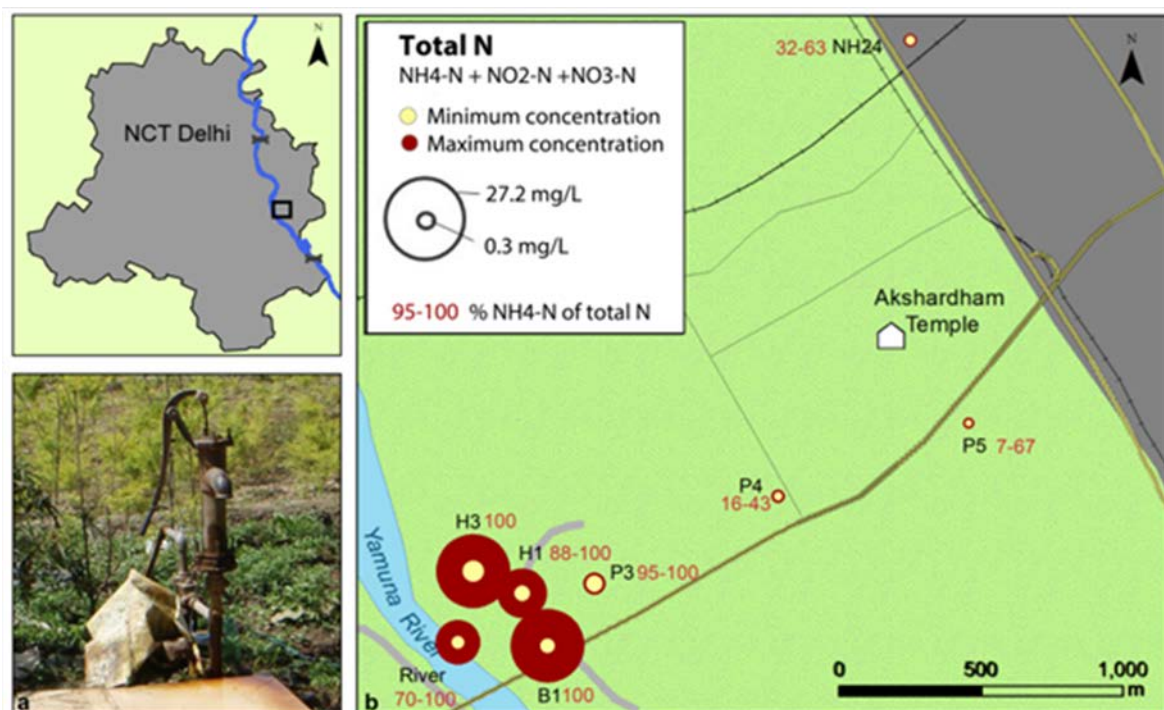


**Figure 1** Location of the study area and nitrogen concentrations at the field site. Close to the river, almost all nitrogen is present in form of ammonium. Note that concentrations are given as mg N/L.

Numerous studies have investigated ammonium contaminations in groundwater at different scales. Field investigations were mainly focusing on contaminations from point sources such as leachates from landfills (Buss et al. 2004, Lewin et al. 1995, Young 1995, Erskine 2000), chemical companies and industrial sites (Clark et al. 2008, Haerens 2004, Haerens *et al.* 2006), septic tank effluents (Hinkle et al. 2007, 2008), and former sewage farms (Hamann 2009); as well as on contamination through artificial recharge of treated sewage water (Cape Cod, Massachusetts - LeBlanc 1984, Ceazan et al. 1989, Böhlke et al. 2006, Repert et al. 2006) and treated septage water (DeSimone and Howes 1996, 1998). The infiltration of sewage influenced river water was studied in Glattfelden (Switzerland) by Schwarzenbach et al. (1983), and Jacobs et al. (1988), but elevated ammonium concentrations were only observed in the river and not in the aquifer. The authors conclude that complete nitrification takes place during infiltration. Doussan et al. (1997) and Doussan et al. (1998) studied the transport of nitrogen species at a BF site at the Seine (France), where the river was, at the time of the study, still heavily influenced by sewage treatment plant (STP) effluents and had high nitrate concentrations. Reducing conditions prevail in the aquifer owing to the decay of organic matter and the nitrate is reduced to ammonium during the soil passage while the mineralization of organic matter is an additional source of ammonium. On a laboratory scale, batch and desorption experiments have been conducted to determine Langmuir isotherms (DeSimone and Howes 1998) and distribution coefficients ( $k_d$ ) (Ceazan et al. 1989, Böhlke et al. 2006) for  $\text{NH}_4^+$  sorption on aquifer material. Column experiments to investigate transport of ammonium have been conducted with liner and filter materials (Thornton et al. 2001, Hinkle 2008) and with aquifer materials: Thornton et al. (2000 and 2005) studied the transport of landfill leachate with ammonium concentrations 1000 - 2000 mg/L in columns filled with disaggregated sandstone and Jellali et al. (2010) used synthetic wastewater with ammonium concentrations of 5 – 36 mg/L and sandy soil from a soil aquifer treatment (SAT) pilot plant. Furthermore, von Gunten and Zobrist (1993) used column experiments to investigate microbially mediated redox processes during infiltration of polluted water; however, behavior of ammonium was not the main focus in this study.

In this paper we investigate the transport of ammonium at low concentrations (10-20 mg/L) and naturally occurring flow rates in porous alluvial aquifer material from Yamuna River under suboxic and anoxic conditions by means of laboratory column tests. The  $\text{NH}_4^+$  degradation and attenuation were determined with adsorption and desorption experiments and reproduced in a 1D reactive transport model. The objectives of the study are (i) to determine the dominant processes for ammonium transport in an alluvial aquifer recharged by a sewage contaminated river, (ii) to quantify the retardation factor  $R$  to give indications on how fast the ammonium plume is spreading in the aquifer, and (iii) to determine optimum methodology for further research on RBF as natural treatment system. Results of this study provide input parameters for subsequent field scale modelling investigations.

## 5.3 Materials and Methods

### 5.3.1 Sediment sampling and analyses

The aquifer material investigated in this study was collected from the saturated zone of a shallow alluvial aquifer in central Delhi which is contaminated by infiltrating sewage influenced water from the Yamuna River (Groeschke 2013). Samples were collected by manual auger drilling operations at three locations 35 m, 250 m, and 500 m from the riverbank (Fig. 2). They include medium-grained sand samples taken at depths between 7.6 and 15.2 mbgl and kankar samples (Fig. 3) taken at depths of 13.7 mbgl. The term kankar (sometimes spelled kanker) refers, specifically for India and North Africa, to calcareous nodules, which consist mostly of sandy loam or clay loam (Singh and Singh 1972) and which are associated with cycles of evaporation and leaching (Salama 1983). Hydraulically the kankar can be viewed as a gravel, while the cation exchange properties are more similar to clays. After sampling, the material was packed airtight in plastic bags and stored in the dark at temperatures below 12°C until it was filled into the columns.

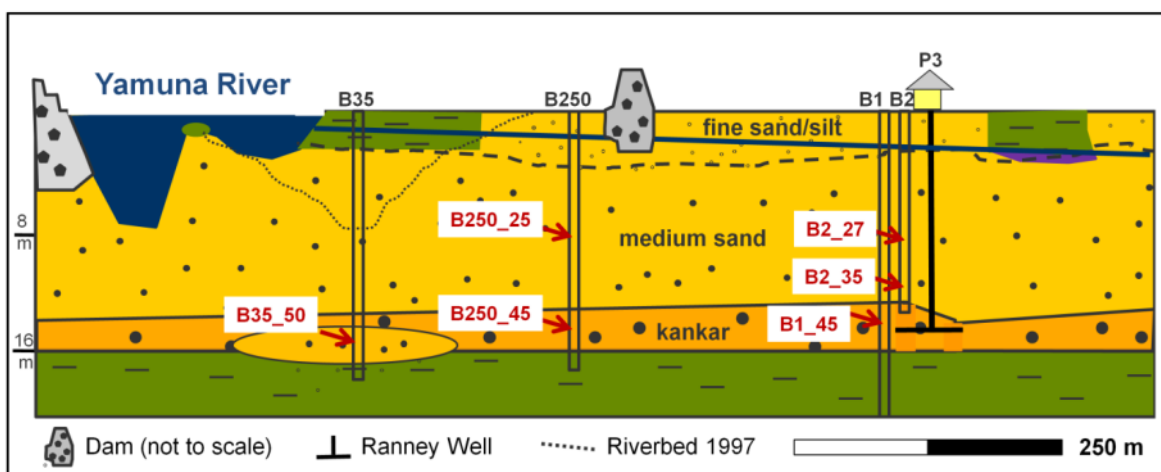


**Figure 2 Origin of sediment samples used for sediment analyses and column experiments. The first number in the sample name indicates the drilling location; the second number is the sampling depth in ft.**

For all samples, grain size distribution was analyzed by sieve test and sedimentation (DIN 18123), organic matter and carbonate content were measured by loss on ignition (DIN 18128).  $CEC_{sum}$  (Ross and Ketterings 2011) was analyzed by the percolating 0.1 M  $BaCl_2$  through 10g dried soil sample and measuring the extracted  $Na^+$ ,  $K^+$ ,  $Mg^{2+}$ ,  $Ca^{2+}$ , and  $Fe^{2+}$  by ICP-OES.  $NH_4^+$  was determined photometrically. In case of the kankar, all analyses were conducted with dried, unchanged material. Additionally the kankar was disaggregated by mixing with natriumpyrophosphate ( $Na_4P_2O_7$ ) and shaking for 24 hours. Total porosities were determined by measuring how much water could be added to small, tightly packed sediment columns until the sediment was water saturated. Furthermore

total porosities ( $n$ ) were calculated using the quartz density  $\rho=2.65 \text{ g/cm}^3$ , the volume of the columns  $V$  and the mass of the sediment in the column  $m$  (Vomocil 1965):

$$n = \frac{V - \left(\frac{m}{\rho}\right)}{V}$$

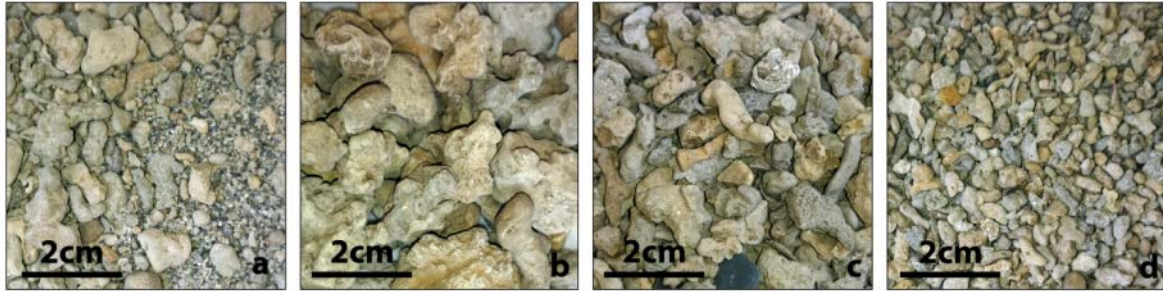


**Figure 3 a. Complete Kankar sample consisting of calcareous nodules of different sizes and sand b. Kankar fraction >8 mm c. Kankar fraction >4 mm d. Kankar fraction >2mm**

### 5.3.2 Experiments

#### Experimental Set-Up

Glass columns with an inner diameter of 45 mm and a sediment filled length of 145 mm were filled with aquifer material and were flushed with artificial groundwater (model water) in upflow direction. The concentrations and ratios of the main inorganic cations in the model water correspond approximately to the groundwater at the field site and are shown in Table 1. The flow was regulated using a peristaltic pump and was set to about 0.17 mL/min which corresponds to a pore velocity ( $u$ ) of roughly 0.9 m/d in the aquifer, which is in the range of the pore velocity published for the field site (Sprenger 2011 p.66). The column effluent was collected in glass vessels which, like the container of the artificial groundwater, were kept under an Ar gas atmosphere to prevent interactions with atmospheric nitrogen and the oxidation of reduced nitrogen species. Non-invasive oxygen sensors (Presens® Fibox mini) were attached to the artificial water reservoir, to the inlet of the columns, to two points inside the columns, to the outlet and in the sample collector vessels. ORP probes were installed at the outlet of the columns.



**Table 1 Model water composition during the adsorption and desorption experiments**

| Ion              | Unit                | Model water composition adsorption experiments |             | Model water composition desorption experiments |            |
|------------------|---------------------|--|-------------|--|------------|
|                  |                     | Start  | End         | Start  | End        |
| Na               | mgL <sup>-1</sup>   |  | 165.4 ± 9.1 |  |            |
| K                | mgL <sup>-1</sup>   |  | 16.5 ± 1.0  |  |            |
| Mg               | mgL <sup>-1</sup>   |  | 32.3 ± 1.6  |  |            |
| Ca               | mgL <sup>-1</sup>   | 17.3 ± 4.2                                     | 15.5 ± 1.7  | 25.1 ± 8.4                                     | 17.9 ± 5.5 |
| NH <sub>4</sub>  | mgL <sup>-1</sup>   | 20.2 ± 0.4                                     |             | 0.1 ± 0.1                                      |            |
| Cl               | mgL <sup>-1</sup>   | 303.1 ± 12.5                                   |             | 276.7 ± 9.1                                    |            |
| HCO <sub>3</sub> | mmolL <sup>-1</sup> |  | 3.8 ± 0.3   |  |            |
| EC               | µScm <sup>-1</sup>  | 1285 ± 33.8                                    |             | 1191.8 ± 26.2                                  |            |
| pH               |                     | 8.47 ± 0.02                                    |             | 8.52 ± 0.05                                    |            |

### Ammonium Experiments

With each sediment sample, experiments were conducted in two stages: adsorption experiments and desorption experiments. In the adsorption experiments, the columns were flushed with model water with ammonium concentrations of either 20 mg/L or 10 mg/L (prepared by adding NH<sub>4</sub>Cl to the model water) until the ammonium concentrations in the effluent were equal to the concentrations in the model water. During the following desorption experiments, the columns were again flushed with nitrogen-free artificial groundwater until nitrogen concentrations in the column effluent were sufficiently low. Before the first adsorption experiment, columns were flushed with nitrogen free model water. The experiments were conducted with duplet or triplet columns. To check for reproducibility, experiments were repeated one or two times. All adsorption and most desorption experiments were conducted under suboxic or anoxic conditions; desorption experiments for selected sediments were conducted with oxygen saturated water. The number of columns and experiments for each sediment and the redox conditions during the experiments are shown in Table 2.

**Table 2 Number and kind of experiments conducted with each sediment sample**

| Sedi-ment        | Sample ID | Depth [m] | Distance from River [m] | Number of columns | Number of adsorption experiments | NH <sub>4</sub> <sup>+</sup> in model water [mg/L] | Condi-tions        | Number of desorption experiments | Condi-tions        |
|------------------|-----------|-----------|-------------------------|-------------------|----------------------------------|--|--------------------|----------------------------------|--------------------|
| Sand             | B2_27     | 8.3       | 500                     | 2                 | 3                                | 20   | suboxic/<br>anoxic | 3                                | suboxic/<br>anoxic |
|                  | B2_35     | 10.7      | 500                     | 2                 | 3                                | 20   | suboxic/<br>anoxic | 3                                | suboxic/<br>anoxic |
|                  | B35_50    | 15.2      | 35                      | 1                 | 1                                | 20   | anoxic             | 1                                | oxic               |
| Sand with kankar | B250_25   | 7.6       | 250                     | 1                 | 1                                | 20   | anoxic             | 1                                | oxic               |
| Kankar           | B1_45     | 13.7      | 500                     | 2                 | 2                                | 10 and 20  | anoxic             | 2                                | anoxic             |
|                  | B250_50   | 13.7      | 250                     | 2                 | 1                                | 20   | anoxic             | 1                                | oxic               |

### Sampling and Analyses, Calculation of Mass Balances

Effluent samples were collected according to a fixed sampling scheme. To calculate nitrogen mass balances the complete column effluent was analyzed for ammonium, nitrite and nitrate concentrations. For precise nitrogen breakthrough curves, small sample volumes < 20 mL were collected twice a day for the measurement of nitrogen species. In addition, samples of the main ions (and nitrogen species) were taken once a day (sampling volume 40 - 60 mL) in which the pH and EC was measured in the first few minutes after sampling. The analyses and detection limits are summarized in Table 3.

**Table 3 Sediment samples and experiments conducted**

| Parameter  | Unit                | Method                    | Detection limit | Test number (Merck) | Measuring range | Error   | Sampling volume | Sampling frequency  |
|--|---------------------|---------------------------|-----------------|---------------------|-----------------|---------|-----------------|---|
| NH <sub>4</sub> <sup>+</sup> -N  | mgL <sup>-1</sup>   | Photometer                | 0.01            | 1.14752             | 0.010-0.500     | ±0.017  | < 20 mL         | Total effluent (3-4 samples per day and overnight sample) |
|  |                     |                           |                 | 1.14752             | 0.05-3.00       | ±0.08   |                 |   |
|  |                     |                           |                 | 1.00683             | 3.0-30.0        | ±0.3    |                 |   |
| NO <sub>2</sub> <sup>-</sup> -N  | mgL <sup>-1</sup>   | Photometer                | 0.001           | 1.14776             | 0.002-0.200     | ±0.005  |                 |   |
|  |                     |                           |                 | 1.14776             | 0.02-1.00       | ±0.03   |                 |   |
| NO <sub>3</sub> <sup>-</sup> -N  | mgL <sup>-1</sup>   | Photometer                | 0.1             | 1.14773             | 0.2-10.0        | ±0.3    |                 |   |
|  |                     |                           |                 | 1.09713             | 0.5-12.5        | ±0.12   |                 |   |
|  |                     |                           |                 | 1.09713             | 1-25            | ±0.6    |                 |   |
| Na <sup>+</sup> , K <sup>+</sup>   | mgL <sup>-1</sup>   | ICP-OES                   | 0.2             | ---                 | <10             | ±20-50% | 40-60 mL        | Once per day  |
| Mg <sup>2+</sup> , Ca <sup>2+</sup>  | mgL <sup>-1</sup>   | ICP-OES                   | 0.02            |                     | 10-30           | ±10%    |                 |   |
| Cl <sup>-</sup> , SO <sub>4</sub> <sup>2-</sup> , NO <sub>3</sub> <sup>-</sup> | mgL <sup>-1</sup>   | Ion chromatography        | 0.1             |                     | 30-100          | ±5%     |                 |   |
| HCO <sub>3</sub> <sup>-</sup>  | mmolL <sup>-1</sup> | Titrimetric determination | 0.2             | 1.11109             | 0.2-10.0        | ±0.2    |                 |   |

Nitrogen species were measured as  $\text{NO}_3\text{-N}$ ,  $\text{NO}_2\text{-N}$  and  $\text{NH}_4\text{-N}$ . Mass balances were calculated subtracting the total measured nitrogen output from the input. Error analyses were applied based on the specified accuracy of a measurement value given in the data sheet of the reagents as well as the accuracy derived from a number of own standard measurements. The  $\text{NH}_4^+$  sorption on the sediment was calculated with the total measured nitrogen. This assumption was made because >95% of the total measured nitrogen was in form of  $\text{NH}_4\text{-N}$ , and the low nitrate and nitrite concentrations which were measured could also have formed through oxidation during the sampling procedure; in the water samples taken at the field site from the center of the plume, 100% of the nitrogen occurs as  $\text{NH}_4\text{-N}$  (Fig. 1). The potentially sorbed ammonium was therefore calculated:

$$\text{NH}_4^+ \left( \frac{\text{meq}}{100\text{g}} \right) = \frac{\text{total desorbed N (meq)}}{\text{mass of sediment in column (g)}} * 100 * 1.286$$

### Tracer Tests

Pulse style conservative tracer tests were performed on the columns to determine effective porosities. 1 mL NaCl solution with a concentration of 10 g/L was injected at the inlet of the column. Electric conductivity (EC) was measured in 5 min intervals using an EC probe that was installed at the outlet of the column. Tracer concentrations were calculated:

$$C_{tracer} \left( \frac{\text{mg}}{\text{L}} \right) = \text{EC}_{\text{measured}} \left( \frac{\mu\text{S}}{\text{cm}} \right) - \text{EC}_{\text{background}} \left( \frac{\mu\text{S}}{\text{cm}} \right) * 0.53$$

Whereby the conversion factor 0.53 was determined through a laboratory test series, in which NaCl was added stepwise to the model water while measuring the changes in conductivity.

To ensure that no density stratification effects occur at those concentrations and injection volumes, an additional tracer test was conducted with 1 mL coloured NaCl solution (addition of 0.1 g Rhodamin B to 20 mL tracer solution) and one test was conducted with 1 mL coloured model water solution (addition of 0.1 g Rhodamin B to 20 mL model water).

### Determination of hydraulic conductivities

To determine the hydraulic conductivity (K) of the sediment, the hydraulic gradient was measured at the inlet and the outlet of the columns:  $K = Q / (A * I)$  with the flow rate Q, the area of the column A, and the hydraulic gradient I.

#### 5.3.3 Modelling

Models were developed using the interface ipht3d (Atteia 2014), for the USGS flow simulator MODFLOW 2000 (Harbaugh et al. 2000), the transport simulator MT3DMS

(Zheng 2010) and the reactive multicomponent transport model PHT3D (Prommer and Post 2010), which couples MODFLOW and MT3DMS with the geochemical modelling software PHREEQC-2 (Parkhurst and Appelo 1999). Tracer tests and adsorption experiments were modelled for all sediments; desorption experiments were only modelled in case they were conducted under anoxic or suboxic conditions.

### **Flow and nonreactive transport model - Tracer Tests**

A 2D flow and nonreactive transport model was developed to determine the effective porosities and the dispersivities. The flow simulations were carried out with MODFLOW and the advective-dispersive transport of the NaCl tracer was simulated with the transport simulator MT3DMS and additionally with PHT3D. The horizontal extent of the model domain was 0.25 m and included the sediment filled column length (0.145m) as well as the inlet and the outlet of the column. This takes into account the short lengths of the sediment filled columns and comparatively long flow paths in the inlet and the outlet, which might have an effect in pulse style experiments. The vertical extent of the model domain was 0.045 m; to reproduce the geometry of the columns (smaller diameter of the tubing compared to the column diameter) cells were set inactive at the inlet and the outlet. The resolution of the model grid was 0.002 m in the horizontal and 0.001 m in the vertical direction. The upstream boundary was defined by a constant flux, representing the actual inflow into the column, and the downstream boundary was defined by a constant head. The glass walls of the columns were represented by no-flow boundaries. Hydraulic conductivities were taken from laboratory measurements. The simulation time was one day. Tracer breakthrough curves were fitted by adjusting dispersivities and effective porosities, taking into account total porosities (Tab. 1) and literature values (Garling and Dittrich 1979, Davis & DeWiest 1966, Johnson 1967). To ensure that no numerical dispersion or oscillations occurred, the simulations were run with TVD and MMOC solver and selected models were furthermore rerun with smaller grid spacing (0.001 m and 0.0005 m in horizontal and vertical directions).

### **Flow and reactive transport model – Ammonium Experiments**

Using the transport parameters determined with the tracer model, a 1D flow and reactive transport model was developed with MODFLOW and PHT3D to simulate the adsorption and desorption experiments. Because these experiments were conducted in step mode (with a constant input concentration) the effect of the column design on the breakthrough curves is negligible and 1D modelling is applicable. The horizontal extent of the model domain was 0.15 m, representing the sediment filled length of the column, and was divided into a grid of 0.001 m cell lengths. As in the 2D model, the inflow boundary was defined by a constant flow and the outlet boundary by a constant head. The adsorption and corresponding desorption experiments were modelled in one simulation. The sediment was equilibrated with the water composition of the first sample taken during the adsorption experiment. The model water composition of the adsorption experiment was

used as the displacing solution for the duration of each adsorption experiment (3-8 days). The model water composition without ammonium was then used for the further 3 to 8 days simulation time as the displacing solution for the desorption experiment. The calcium concentrations decreased in the model water by 10 and 30% during the adsorption and desorption experiments (Tab. 1), most likely due to the precipitation of  $\text{CaCO}_3$  because the model water is oversaturated with calcite as calculations with PHREEQC show. Therefore, the model water composition measured at the beginning of the adsorption or desorption experiment was used for the first half of the adsorption or desorption simulation and the composition measured at the end of the experiment was used for the second half of the simulation. For the sediments where desorption experiments were conducted under oxic conditions, only the adsorption experiment was modeled. All water compositions were charge balanced using PHREEQC-3 (Parkhurst and Appelo 2013) before using them as input solutions.

### Implementation of cation exchange

Many investigations show that at contaminant sites, where the infiltrating water is strongly influenced by one contaminant, simple sorption isotherm models are insufficient to describe the ammonium behavior at field scale (Buss et al. 2004). Ion exchange models, which consider all species that compete for the exchange sites give better results (Hamann 2009). Therefore, reactive transport models were developed which consider ion exchange of/with and all main cations present. The reactive transport was computed with PHT3D (Prommer and Post 2010) using a slightly modified Amm.dat database provided with the software PHREEQC-2. The Amm.dat database decouples ammonium from the nitrogen system, which means that no oxidation of ammonium can occur in the model, which is in accordance with the experimental results showing no oxidation of ammonium to nitrite and nitrite at significant levels (see experimental result).

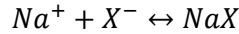
The cation exchange selectivity coefficient is the relative preference of an exchanger to adsorb different cations. It is not a thermodynamic constant, but varies with the exchanger composition (e.g. Jensen 1973 after Tournassat et al. 2007). For the exchanger phases of the three sediment types (sand, sand with kankar, kankar), equilibrium equations for Na/K, Na/Mg, Na/Ca, Na/ $\text{NH}_4$  were set up using the Gaines Thomas convention (Gaines and Thomas 1953) and measurements of the cation compositions on the exchanger as well as the corresponding activities in groundwater samples. Exchange selectivity coefficients with  $\text{Na}^+$  as the reference ion ( $K_{\text{Na} \setminus I}$ ) were then calculated using the Gaines-Thomas convention (Appelo and Postma 2007):

$$K_{\text{Na} \setminus I} = \frac{\beta_{\text{Na}} [I^{i+}]^{1/i}}{\beta_I^{1/i} [\text{Na}^+]}$$

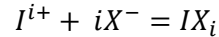
Log  $K_{\text{Na} \setminus I}$  values were calculated according to:

$$\log K_{Na\setminus I} = \log\left(\frac{1}{K_{Na\setminus I}^i}\right)$$

PHREEQC splits ion exchange reactions into half reactions and the reference reaction, which is in this case



is defined by  $\log K = 0$ .  $\log K_i$  for the half reaction of the ion  $I$



is therefore equal to  $\log K_{Na\setminus I}$ . The  $\log K$  values were then used to replace the default values in the Amm.dat database. The number of exchange sites was used to fit modelled ammonium breakthrough curves to measured data. The cation exchange capacity (CEC) is a measure for the number of exchange sites in sediments or soils and thus an important parameter for modelling cation exchange. Due to different factors (inhomogeneities in the sediment, pH dependency, uncertainties in the measurements) the exact determination of the number of exchange sites is difficult (Renault et al. 2009) and, therefore, it is the most uncertain factor in the system.

### Retardation factors

Retardation factors for ammonium were determined simulating a conservative tracer test by adding a non-reactive conservative tracer to the reactive transport model. The retardation factors of  $NH_4$  were then calculated from the modelled conservative tracer and  $NH_4$  breakthrough curves from the time required for the ammonium to reach a relative concentration ( $C/C_0$ ) of 0.5 at the outlet of the column compared to the time required for the tracer to reach  $C/C_0=0.5$  (Steefel et al. 2003) whereby the conservative tracer represents the velocity of the water (Appelo and Postma 2007 after Sillen 1951).

## 5.4 Results

### 5.4.1 Sediment analyses

The kankar and the sand have clearly distinct characteristics. Sieve curves are shown in Figure 4 and sediments characteristics are given in Table 4.

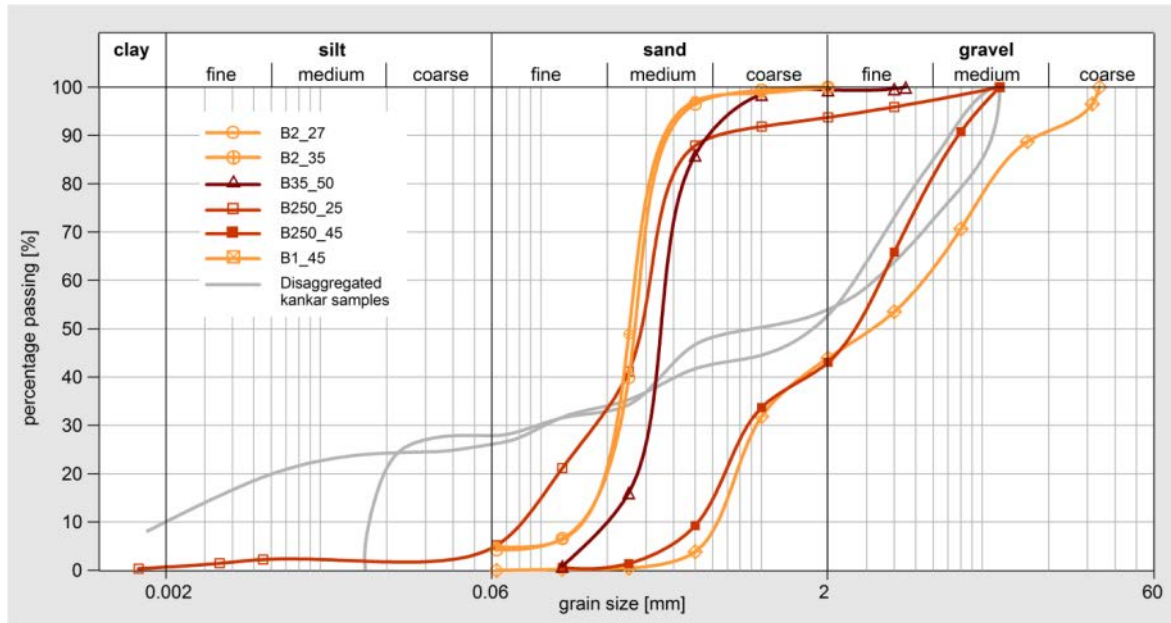


Figure 4 Grain size distribution curves

Table 4 Characteristics of the sediments used in the column experiments

|                         | Sample ID | Depth [m] | Distance from River [m] | Sediment type             | CEC <sub>sum</sub> [meq/100g] | Organic matter [%] | Carbonte [%] | n [measured] | n [calculated] | Dry weight in column [g] |
|-------------------------|-----------|-----------|-------------------------|---------------------------|-------------------------------|--------------------|--------------|--------------|----------------|--------------------------|
| <b>Sand</b>             | B2_27     | 8.3       | 500                     | poorly-graded medium SAND | 1.64                          | 0.7                | 1.6          | 0.36         | 0.38           | 375                      |
|                         | B2_35     | 10.7      | 500                     | poorly-graded medium SAND | 1.58                          | 0.6                | 2.5          | 0.35         | 0.39           | 370                      |
|                         | B35_50    | 15.2      | 35                      | poorly-graded medium SAND | 1.51                          | 1.2                | *            | 0.37         | 0.40           | 368                      |
| <b>Sand with kankar</b> | B250_25   | 7.6       | 250                     | well-graded gravelly SAND | 1.29                          | 1.3                | *            | 0.35         | 0.33           | 407                      |
| <b>Kankar</b>           | B1_45     | 13.7      | 500                     | coarse SAND-GRAVEL        | 2.16                          | 1.3                | 14.4         | 0.30         | 0.26           | 450                      |
|                         | B250_45   | 13.7      | 250                     | coarse SAND-GRAVEL        | 2.05                          | 1.3                | *            | **           | 0.29           | 430                      |

\* Adding HCl showed that carbonate was present

\*\* not measured

#### 5.4.2 Tracer Tests and Transport Parameters

The hydraulic conductivities of the sand samples range between  $1.9 \cdot 10^{-5}$  and  $6.7 \cdot 10^{-5} \text{ ms}^{-1}$ ; whereas the hydraulic conductivities of the two kankar samples are  $1.2 \cdot 10^{-4} \text{ ms}^{-1}$  ( $\pm$

$0.2 \cdot 10^{-4} \text{ ms}^{-1}$ ) and  $1.6 \cdot 10^{-4} \text{ ms}^{-1}$  ( $\pm 0.1 \cdot 10^{-4} \text{ ms}^{-1}$ ). The kankar and sand sample has a hydraulic conductivity of  $2.0 \cdot 10^{-5} \pm 0.1 \cdot 10^{-5} \text{ ms}^{-1}$ . Tracer breakthrough curves of the sand and kankar differ substantially. While the peaks in sand columns are narrow and high ( $C_{\text{max}}$  5 - 6.5 mmol/L) and occur after a flow of about 110 mL, the peaks in the kankar columns already occur after about 75 mL at a lower concentration (2 - 4 mmol/L). 2D models of the tracer tests reveal that the sand samples had effective porosities between 23 and 25 %, resulting in an effective pore volume of 53-58 mL. The kankar samples had a slightly lower effective porosity between 16.5 and 19%, resulting in effective pore volumes of 38-44 mL in the columns. Dispersivities of the sand were in the range of 1/100 while they were in the range of 1/10 for the kankar. The kankar and sand has a porosity and dispersivity in between the kankar and the sand. The measured and modeled tracer breakthrough curves for all the sediments of the saturated zone are shown in Figure 5. The transport parameters used in the ammonium transport models are summarized in Table 5. The measured variations in each group (sand and kankar) may be due to different packing of the columns or due to natural inhomogeneities in the sediments.

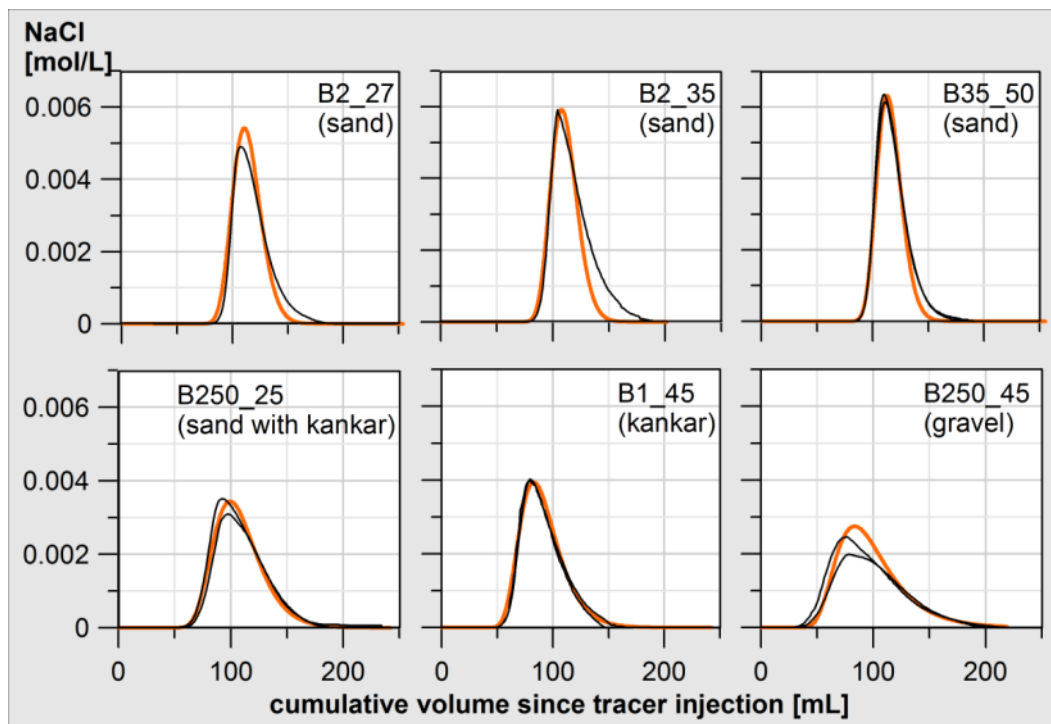


**Figure 5 Measured (black) and modelled (orange) tracer breakthrough curves**



**Table 5 Transport parameters obtained from the 2D solute transport models**

| Sediment         | Sample  | K [m/d] | $n_e$ | Dispersivity [m] |
|------------------|---------|---------|-------|------------------|
| Sand             | B2_27   | 3.4     | 0.24  | 0.0016           |
|                  | B2_35   | 1.7     | 0.23  | 0.0012           |
|                  | B35_50  | 5.8     | 0.25  | 0.0008           |
| Sand with kankar | B250_25 | 1.8     | 0.22  | 0.008            |
| Kankar           | B1_45   | 10      | 0.165 | 0.012            |
|                  | B250_45 | 14      | 0.19  | 0.024            |

### 5.4.3 Ammonium

#### Mass balances

All ammonium that was sorbed or exchanged during the adsorption experiments was desorbed again during the desorption experiments. At an ammonium concentration of 20 mg/L the sand samples had an average ammonium exchange capacity of  $0.11 \pm 0.01$  meq N/100 g sediment, corresponding to  $0.14$  meq  $\text{NH}_4^+$ /100 g sediment, while the kankar samples were able to exchange  $0.16 \pm 0.02$  meq N/100 g sediment. This corresponds to  $0.21$  meq  $\text{NH}_4^+$ /100 g sediment. The detailed results for all columns are given in Table 6. Almost all nitrogen was present as ammonium-N as is shown in Figure 6.

**Table 6 Nitrogen mass balances: Total N adsorbed and desorbed during the experiments in meq N/100 g sediment. Unless otherwise stated, all adsorption experiments were conducted with an ammonium concentration of 20 mg/L in the model water**

| Zone             | Sample ID | Set 1                              |      | Set 2                              |       |                                    |        | Set 3                              |      |                                    |      |                                    |      |
|------------------|-----------|------------------------------------|------|------------------------------------|-------|------------------------------------|--------|------------------------------------|------|------------------------------------|------|------------------------------------|------|
|                  |           | Total Nitrogen Adsorbed (meq/100g) |      | Total Nitrogen Desorbed (meq/100g) |       | Total Nitrogen Adsorbed (meq/100g) |        | Total Nitrogen Desorbed (meq/100g) |      | Total Nitrogen Adsorbed (meq/100g) |      | Total Nitrogen Desorbed (meq/100g) |      |
|                  |           | 1                                  | 2    | 1                                  | 2     | 1                                  | 2      | 1                                  | 2    | 1                                  | 2    | 1                                  | 2    |
| Sand             | B2_27     | 0.12                               | 0.11 | 0.12                               | 0.13  | 0.13                               | 0.13   | 0.12                               | 0.12 | 0.10                               | 0.12 | 0.10                               | 0.11 |
|                  | B2_35     | 0.10                               | 0.10 | 0.11                               | 0.11  | 0.11                               | 0.11   | 0.11                               | 0.11 | 0.10                               | 0.09 | 0.10                               | 0.10 |
|                  | B35_50    | 0.12                               |      | 0.13*                              |       |                                    |        |                                    |      |                                    |      |                                    |      |
| Sand with kankar | B250_25   | 0.14                               |      | 0.14*                              |       |                                    |        |                                    |      |                                    |      |                                    |      |
| Kankar           | B1_45     | 0.15                               | 0.15 | 0.15                               | 0.14  | 0.09**                             | 0.09** | 0.08                               | 0.08 |                                    |      |                                    |      |
|                  | B250_45   | 0.18                               | 0.18 | 0.17*                              | 0.18* |                                    |        |                                    |      |                                    |      |                                    |      |

\* Desorption experiment conducted with oxygen saturated artificial groundwater and not modelled

\*\* Experiment conducted with 10 mg/L  $\text{NH}_4^+$  in the artificial groundwater

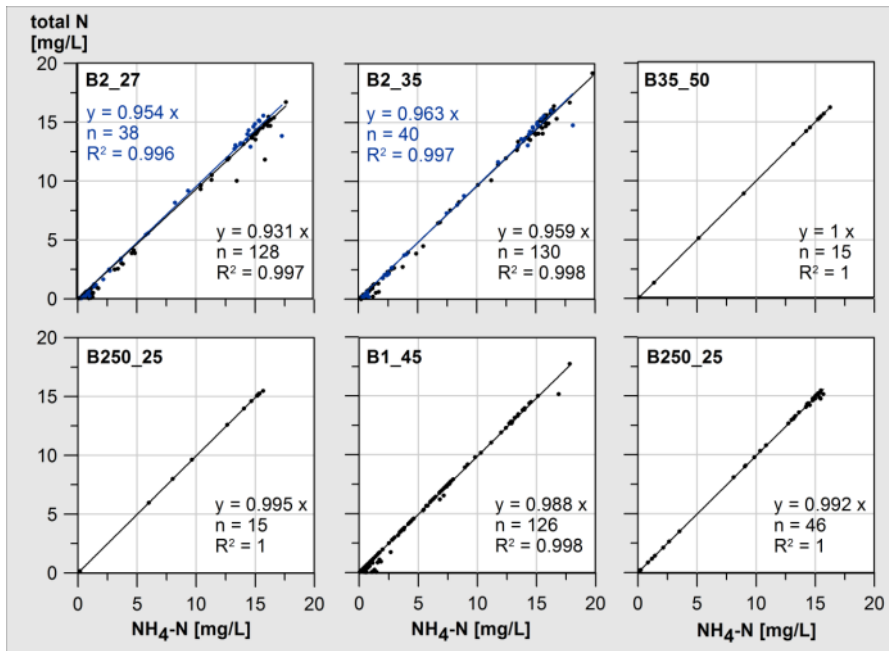


**Figure 6 NH<sub>4</sub>-N vs. Total N in the effluent samples of the column experiments. Three sets of experiments were conducted with B2\_27 and B2\_35 of which the first two (black symbols) were conducted under suboxic conditions and the last one under anoxic conditions (blue symbols)**

### Error Analyses of Mass Balances

For the nitrogen mass balances of the adsorption experiment, the total errors were in the range of 9-15% for the experiments conducted with 20 mg/L ammonium in the model water. For the mass balances of the desorption experiments, the total errors were in the range of 5-8%. Errors were larger for the adsorption experiments because of the higher error ( $\pm 0.3$  mg/L) for high ammonium concentrations as opposed to an error of  $\pm 0.017$  or  $\pm$  detection limit (0.01) for low ammonium concentrations (see Table 3). A summary of the errors of the second adsorption and desorption experiment of sediment B2\_27 is given in Table 7.

**Table 7 One example of an error analyses (Sediment B2\_27, second experiment)**

| B2_27ft                                    | Unit | Adsorption experiment |             |             |             | Desorption experiment |             |              |             |
|--|------|-----------------------|-------------|-------------|-------------|-----------------------|-------------|--------------|-------------|
|  |      | Column 1              |             | Column 2    |             | Column1               |             | Column 2     |             |
|  |      | Value                 | Error       | Value       | Error       | Value                 | Error       | Value        | Error       |
| <b>Input</b>                               |      |                       |             |             |             |                       |             |              |             |
| NO3-N                                      | mg   | 0.042                 | 0.091       | 0.041       | 0.091       | 0                     | 0.081       | 0            | 0.080       |
| NO2-N                                      | mg   | 0.005                 | 0.004       | 0.005       | 0.004       | 0                     | 0.001       | 0            | 0.001       |
| NH4-N                                      | mg   | 13.499                | 0.258       | 13.461      | 0.257       | 0.089                 | 0.014       | 0.088        | 0.014       |
| Sum N <sub>in</sub>                        | mg   | 13.545                | 0.353       | 13.508      | 0.352       | 0.089                 | 0.096       | 0.088        | 0.094       |
| <b>Output</b>                              |      |                       |             |             |             |                       |             |              |             |
| NO3-N                                      | mg   | 0.205                 | 0.098       | 0.269       | 0.099       | 0.316                 | 0.097       | 0.289        | 0.096       |
| NO2-N                                      | mg   | 0.434                 | 0.023       | 0.457       | 0.034       | 0.273                 | 0.018       | 0.307        | 0.018       |
| NH4-N                                      | mg   | 6.202                 | 0.155       | 6.155       | 0.156       | 5.827                 | 0.168       | 5.823        | 0.164       |
| Sum N <sub>out</sub>                       | mg   | 6.841                 | 0.267       | 6.881       | 0.290       | 6.416                 | 0.283       | 6.419        | 0.278       |
| N <sub>in</sub> – N <sub>out</sub>         | mg   | <b>6.70</b>           |             | <b>6.63</b> |             | <b>-6.33</b>          |             | <b>-6.33</b> |             |
| Error <sub>in</sub> + error <sub>out</sub> | mg   |                       | <b>0.63</b> |             | <b>0.64</b> |                       | <b>0.38</b> |              | <b>0.37</b> |
| Error                                      | %    |                       | <b>9.4</b>  |             | <b>9.7</b>  |                       | <b>6.0</b>  |              | <b>5.9</b>  |

### Ammonium Breakthrough

During the adsorption experiments, the nitrogen breakthrough in the sand columns starts after about five flushed pore volumes. Nitrogen concentrations in the column effluent then rapidly increase until the input concentration of 20 mg/L NH<sub>4</sub> (15.55 mg/L N) is reached after 10-12 flushed pore volumes. The sand samples taken at a distance of 500 m and 35 m from the river show the same behaviour, while in the sand and kankar sample B250\_25, the input concentration is only reached after about 20 flushes. In the kankar, the ammonium breakthrough is slower than in the sand columns and the input concentration is reached after 30-35 flushed pore volumes for both, ammonium concentrations of 10 mg/L and 20 mg/L in the model water. In the desorption experiments it took about 15 and 40 pore volumes to flush the ammonium out of the sand and kankar columns respectively (Fig. 7).

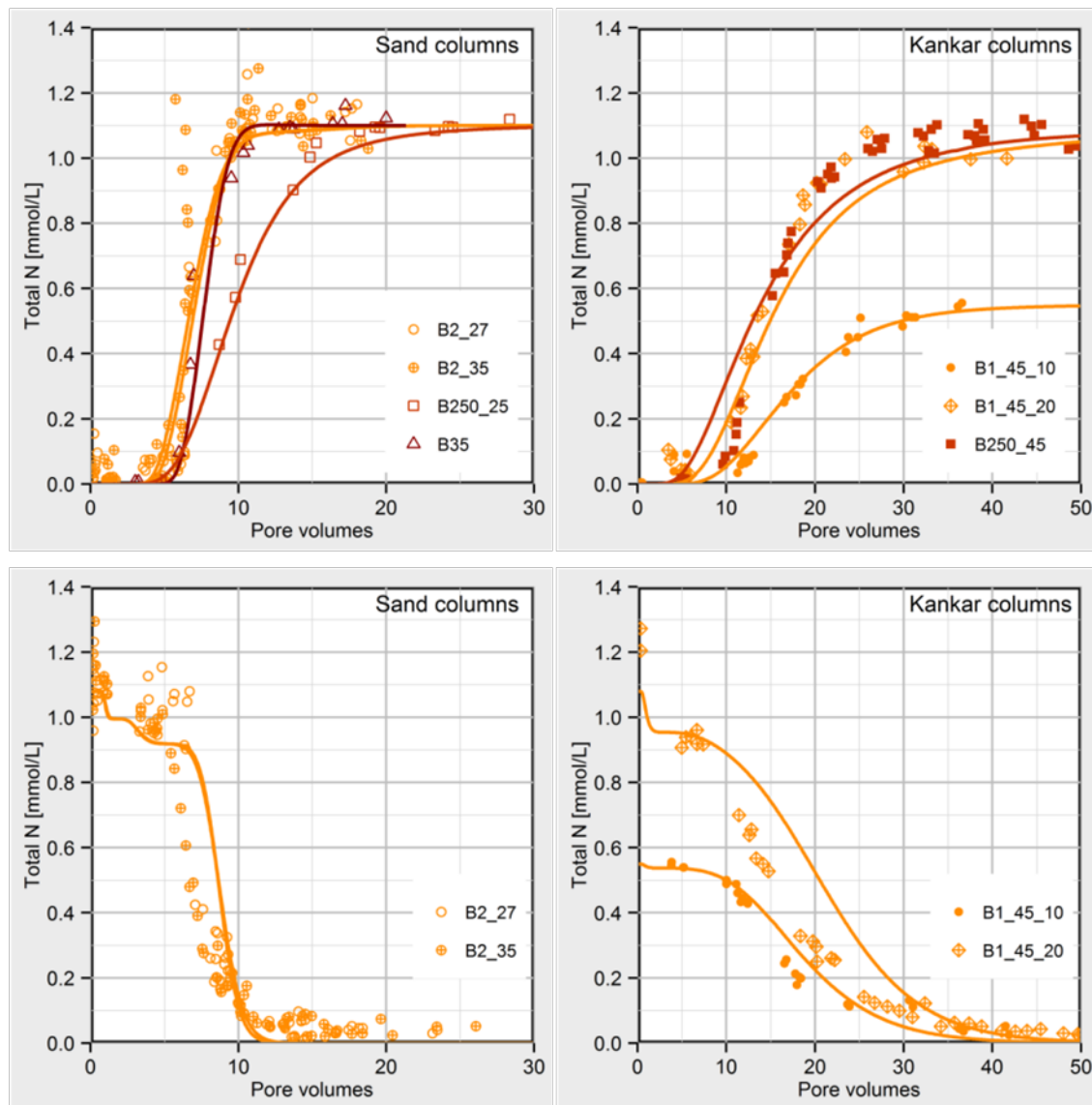


**Figure 7 Measured data (different shapes) and modelled breakthrough curves (lines) for the adsorption (above) and desorption experiments (below). Note the different scales on the x-axes.**

### Reactive Transport Modelling and Sorption Coefficients

The ammonium breakthrough was successfully modelled using adjusted selectivity coefficients for cation exchange. The modelled breakthrough curves and the measured data are shown in Figure 7. The default selectivity coefficients used in PHT3D and the adjusted coefficients for each sediment type are shown in Table 8. With the adjusted selectivity coefficients it was possible to reproduce the concentrations of the other cations (Na, K, Mg, Ca) within a good enough range (Fig. 8).

**Table 8 Selectivity coefficients compared to the default values of the Amm.dat database and adjusted cation exchange capacities**

|                   | Log_k <sub>Na/K</sub> | Log_k <sub>Na/Mg</sub> | Log_k <sub>Na/Ca</sub> | Log_k <sub>Na/NH<sub>4</sub></sub> | Sediment | CEC 1L sand | CEC adjusted |
|-------------------|-----------------------|------------------------|------------------------|------------------------------------|----------|-------------|--------------|
| Amm.dat (default) | 0.7                   | 0.6                    | 0.8                    | 0.6                                |          |             |              |
| Sand              |                       |                        |                        |                                    | B2_27    | 0.026       | 0.013        |
|                   |                       |                        |                        |                                    | B2_35    | 0.025       | 0.013        |
|                   | 0.98                  | -0.09                  | 0.18                   | 0.81                               | B35_50   | 0.024       | 0.016        |
| Sand with kankar  | 0.75                  | -0.48                  | 0.07                   | 0.76                               | B250_25  | 0.023       | 0.0155       |
| Kankar            |                       |                        |                        |                                    | B1_45    | 0.042       | 0.038        |
|                   | 0.67                  | -0.28                  | 0.10                   | 0.55                               | B250_45  | 0.038       | 0.038        |

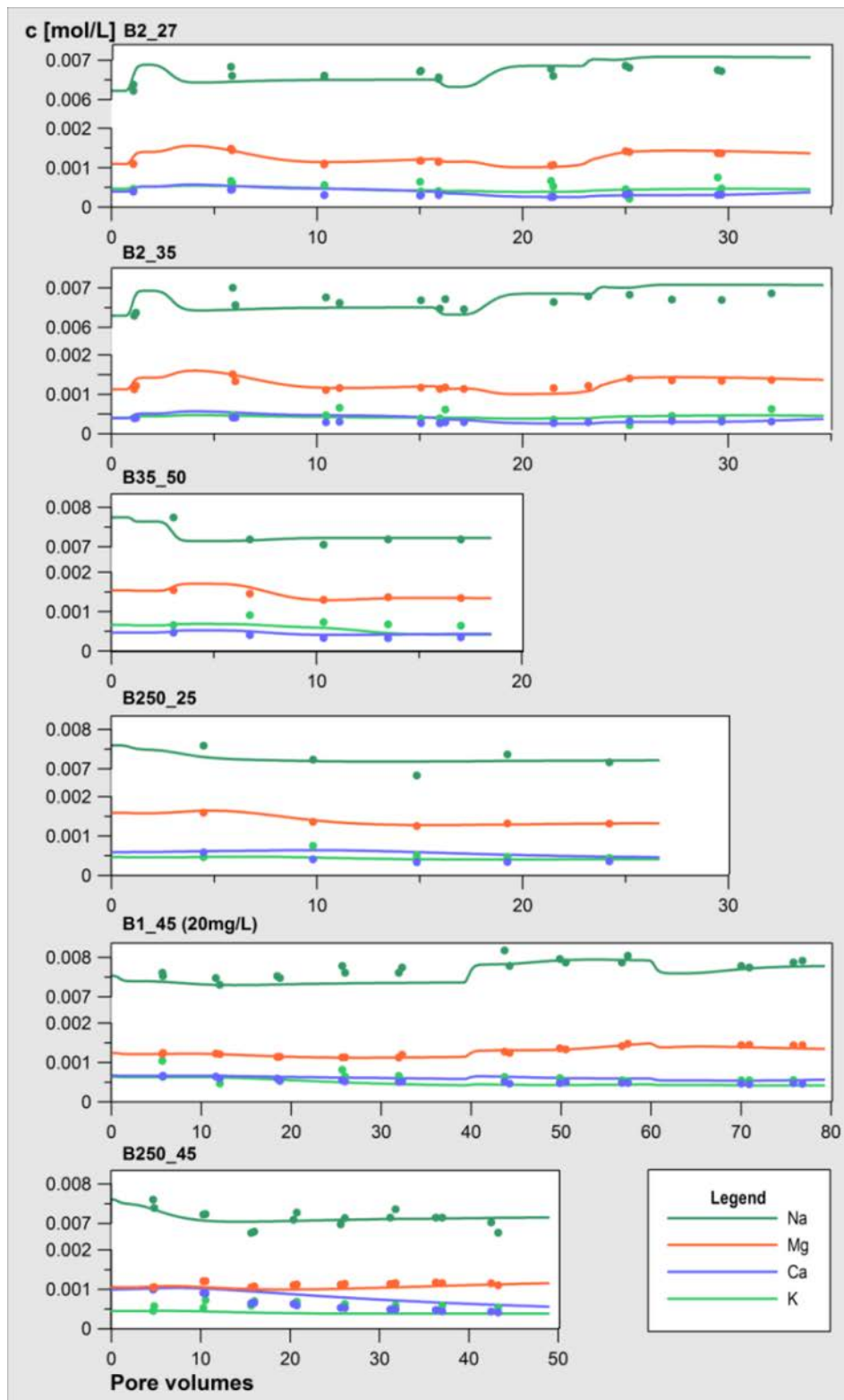
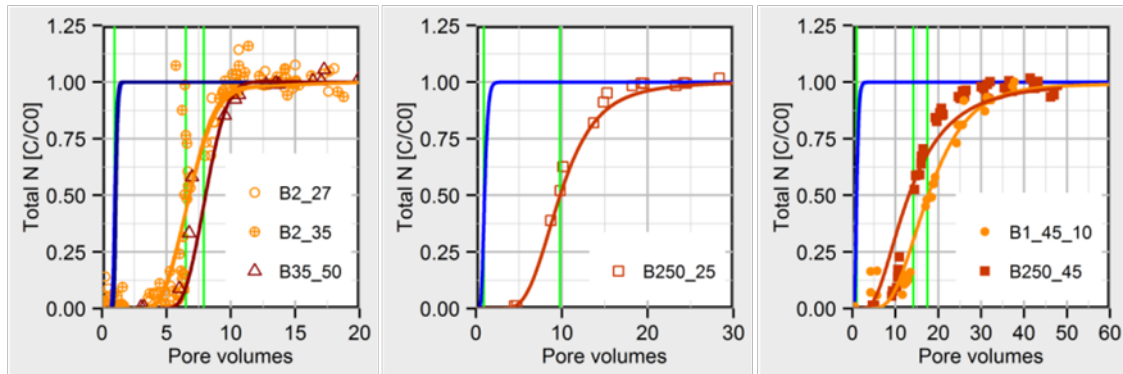


Figure 8 Measured (symbols) and modelled (lines) cation concentrations

### Retardation factors

Retardation factors ( $R_f$ ) between 6.7 and 7.4 were determined for the sand; a factor of 10.0 was determined for the sand and kankar. The retardation factor varied between 16.0 and 19.8 for the kankar. Conservative tracer breakthrough curves in comparison with nitrogen breakthrough curves are shown in Figure 9.



**Figure 9 Ammonium retardation factors were determined by comparing the 50% ammonium breakthrough to the 50% Si breakthrough. Si breakthrough curves are kept in blue, the 50% breakthrough is marked by the green lines**

## 5.5 Discussion

### 5.5.1 Sediment Characteristics

In the saturated zone at the field site, three sediments were encountered: well sorted medium sand, unsorted sand with kankar and kankar with high shares of sand and fine grain. The medium sand and the kankar of B1\_45 can be viewed as endmembers. Transitions between the lithological units are gradual (data not shown) and thus any mixture with different sand and kankar proportions can occur. The sand and the kankar have substantially different characteristics. The analytical results of the kankar and sand samples were mostly found to be between the results of the endmembers. Due to the completely different sediment properties, it is advised to at least differentiate between sand and kankar layers when developing a transport model on field scale. Depending on the resolution of the model and the required degree of detail, a kankar sand transition layer might also be incorporated.

### Hydraulic and Transport Properties

Hydraulic conductivities have been determined from hydraulic head differences in the columns and transport parameters were determined by 2D modelling of pulse style conservative tracer tests in the columns. The kankar hydraulically acts like gravel and has hydraulic conductivities in the range of  $10^{-4} \text{ ms}^{-1}$  as opposed to  $10^{-5} \text{ ms}^{-1}$  in the sand. Due to the poor sorting, the effective porosities are slightly lower in the kankar (0.165-0.19) than in the sand (0.23-0.25). The values are in good agreement with literature values for

sandy gravel and sand (e.g. Krapp 1983). The dispersivities in the kankar samples are in the range of 1/10 of the column lengths while the dispersivities in the sand samples were in the range of 1/100 of the column lengths. This is also the range given as a general rule of rough estimation for porous media. The comparably high dispersivities in the kankar can be explained by the poor sorting and the more diverse flow paths.

### **Physico-Chemical Properties**

Clay content, organic matter, carbonate and  $CEC_{sum}$  were analyzed using standard laboratory methods. In the sand, clay contents were below 1% and the organic matter content varied between 0.6 and 1.2% leading to a measured cation exchange capacity  $CEC_{sum}$  of about 1.6 meq/100 g sediment. In unchanged kankar samples, organic matter contents of 1.3% were measured and no clay was found. However, in the disaggregated kankar clay contents increased up to 10% of the total weight.  $CEC_{sum}$  of about 2 meq/100g sediment was measured in the unchanged kankar. Although the difference between 1.6 and 2.0 meq/100 g sediment does not seem very large, taking into account the total porosity and the effective porosity leads to a much higher proportion of exchange site per kg water in the kankar than in the sand. In order to fit the measured data, the number of exchange sites was adjusted in the ammonium transport models. The adjusted number of sites in the sand was only about half of the measured value (0.013 mol/1L sediment as opposed to the measured value of about 0.025 mol/1L sediment). A reason for this gap might be the large errors of ICP-OES measurements at low concentrations (see Table 3). In the CEC measurements of the kankar, the measured concentrations were significantly higher thus making measurements more reliable. Regarding the adjusted values, the kankar has three times more exchange sites in 1 L sediment. Therefore, the kankar layer has a great importance for the transport of ammonium at the field site and cannot be neglected in transport models at field scale.

#### 5.5.2 Ammonium Transport

### **Column Experiments**

Column experiments under anoxic conditions are an appropriate method to study transport of ammonium in a medium allowing for cation exchange. According to mass balances derived from adsorption/desorption experiments, degradation or fixation of ammonium does not occur in significant quantities. Duplicate columns and the repetition of experiments show that results are reproducible; the total error in the mass balances fall in the range between 5 and 15%. The differences between the sand and the kankar columns are above variations due to analytical errors. Due to the absence of electron acceptors – oxygen for the nitrification process or nitrate and nitrite for anaerobic ammonium oxidation – no oxidation of ammonium takes place in the columns.

### **Ammonium Modelling**

The transport of ammonium was modelled using cation exchange; exchange selectivity coefficients were adapted for each sediment type using Gaines and Thomas selectivity coefficients calculated from CEC measurements and groundwater samples. Overall,



modeled curves fit the measured data well (Figure 7). All three sand samples, B2\_27, B2\_35 and B35 were modelled using the same selectivity coefficients and it was possible to reproduce the steep ammonium breakthrough curves that were measured. Similar results were achieved for the sand and kankar and the kankar. However, for the kankar, especially for sediment B250\_45, the model overestimates ammonium concentrations at the beginning of the breakthrough curve. This might be caused by inaccurate selectivity coefficients due to the high measuring error in the  $CEC_{sum}$  determination. More precise measurements or a parameter optimization with PEST might increase the accuracy of the fits. Nevertheless, measured values cannot be reproduced using the default values of the Amm.dat database and ammonium breakthrough in the kankar can also not be modelled using the sand selectivity coefficients (data not shown).

It is furthermore possible that different clay minerals are present with different selectivity coefficients for ammonium. Although this effect should also occur in the sand and the sand with kankar, the effect must be most pronounced in the kankar as it has the most sorption sites. A multi-site approach as proposed by Vulava et al. (2000) would probably increase the model fit in all sediments, and especially that of the kankar. In their publication the authors show that their data was reproduced reasonably by the Gaines-Thomas model, but that none of the one site models provided a perfect fit of the data, which is what can also be observed with our data.

In the desorption experiments, the ammonium concentrations in the column effluents of the sand columns (B2\_27 and B2\_35) decrease more rapidly than the models suggest (5 flushed pore volumes vs. 7 pore volumes). However, in both the experiments and the models, the ammonium is washed out after about 12 flushes (14 flushes in the experiments). The same phenomenon was observed in the kankar sample B1\_45 in the experiment conducted with 20 mg/L ammonium. It might be an indication for a slight degradation or fixation of ammonium in the columns, in a range below the accuracy of our measurements and mass balances. However, 56 out of 60 samples of the B1\_45\_20 desorption experiment have a proportion of above 95%  $NH_4-N$  of the total measured nitrogen, which is a strong indication that no significant degradation takes place.

### **Selectivity Coefficients**

The number of exchange sites was used to fit the modelled curves to the measured data. Before adjusting the exchange sites, the modelled ammonium breakthrough curves were identical in the slope and form but shifted to the right on the x-axis. This is a strong indication that the calculated selectivity coefficients were appropriate to describe the cation exchange, but the CEC was assumed to be too high (see section physico-chemical properties). Decreasing the number of exchange sites not only improved the ammonium fits, but also improved the modelled concentrations of the other cations, especially Mg.

Overall, the approach to model the transport of ammonium using adapted selectivity coefficients gives reasonable good fits of the measured data. The crucial point with this method is the accurate determination of CEC and selectivity coefficients. However, if this

is done with the needed accuracy, the models are a good tool to predict the transport behaviour of ammonium in natural sediments.

### **Retardation Factors**

To be able to compare the transport of ammonium at the Delhi field site, retardation factors were determined for each sediment. A non-reactive conservative tracer was added in the model runs and the ammonium breakthrough (at a relative concentration  $C/C_0 = 0.5$ ) was compared to the conservative tracer breakthrough (The resulting retardation factors (6.7 – 7.4 in the sand, 10.0 in the sand and kankar and 16.0-19.8 in the kankar) are higher than the retardation factor reported by Ceazan et al. 1989 ( $R_f=3.5$ ) for a shallow sand and gravel aquifer with a clay content less than 1.0%. They are still higher than the retardation factors (between 4.0 and 6.4) Boehlke et al. 2006 report for the same site but determined by another method. This shows the importance of evaluating each field site carefully concerning the transport of ammonium as it strongly depends on the sediments and the solute composition. However, retardation factors are not best suited for making predictions for ammonium transport and should only be used for making first estimations; reactive transport model give more precise results.

## 5.6 Summary and Conclusion

The transport of ammonium in aquifer material from an alluvial sand and kankar aquifer was studied to gain a better understanding of the development of an ammonium plume originating from infiltrating sewage water at an RBF site in central Delhi. Laboratory column experiments show that the transport of ammonium is strongly dependant on the sediment characteristics. It is therefore necessary to incorporate the different lithological units – the sand and the kankar - as different layers in field scale models. The column experiments were conducted in conditions similar to those found in the ammonium plume at the field site and sorption was found to be the dominating/only transport process in both lithological units of the saturated zone.

Retardation factors ( $R_f$ ) vary between 6.7 and 7.4 in the sand and between 16.0 and 19.8 in the kankar. Although reactive transport models give more precise results, the retardation factors reflect the fact that ammonium transport in the kankar layer takes about three times longer than in the sand. However, for field application one has to take into account that pore water velocity is likely to be much higher in the kankar layer due to higher hydraulic conductivities. Reactive transport models have been set up incorporating cation exchange with adjusted selectivity coefficients for each lithological unit. With this approach, both the measured ammonium concentrations as well as the main cation concentrations could be reproduced within a good range. With a more precise measurement of the cation exchange capacity, it will most likely be possible to improve the modelled curves to measured data.

At RBF sites located at sewage contaminated surface waters under conditions met at the field site, ammonium is adsorbed onto the aquifer material during the underground passage. Due to the high retardation this problem is often not detected until production

wells are affected when ammonium breakthrough occurs. Desorption experiments reveal, that all of the ammonium that was sorbed onto the sediment particle surfaces can be desorbed again when infiltrating water is ammonium-free. The desorption approximately takes an equal time span as the ammonium breakthrough and therefore elevated ammonium concentrations will prevail for a long time (in case of the field site several decades) in the raw water of the production wells. Fingering effects are most likely to occur at the plume front and the groundwater sampled is mixed water from differently affected sediment layers. Therefore the ammonium concentration in the groundwater sample is probably not the concentration of the water which is in equilibrium with the analysed sediment sample. In order to achieve a correct determination of selectivity coefficients it is important to take water and sediment samples from the centre of the plume.

### **Acknowledgements**

This research was conducted in the framework of the Saph Pani project and co-financed by the European Commission within the Seventh Framework Programme Grant agreement No. 282911. We thank Andreas Winkler, Olivier Atteia, Janek Greskowiak and Marie Pettenati for the helpful discussions about the modelling. Laura Krömer conducted some of the ammonium experiments and Mario Eybing conducted sediment analyses with some of the sediment samples. We thank Dietrich Lange for constructing the laboratory columns.

### 5.7 References

- Appelo, C.A.J. and Postma, D. 2007. *Geochemistry, groundwater and pollution*. 2<sup>nd</sup> edition, 3<sup>rd</sup> printing. A.A. Balkema Publishers, Leiden, The Netherlands.
- Atteia, O., 2014. *ipht3d Manual Version 2-e 28/05/2014*. 23 p. <http://oatteia.usr.ensegid.fr/iPht3d/>.
- Böhlke, J.K., Smith, R.L. and Miller, D.N., 2006. Ammonium transport and reaction in contaminated groundwater: Application of isotope tracers and isotope fractionation studies. *Water Resources Research*, 42(5): W05411.
- Bouwer, H., 2002. Artificial recharge of groundwater: hydrogeology and engineering. *Hydrogeology Journal*, 10(1): 121-142.
- Buss, S.R., Herbert, A.W., Morgan, P., Thornton, S.F. and Smith, J.W.N., 2004. A review of ammonium attenuation in soil and groundwater. *Quarterly Journal of Engineering Geology and Hydrogeology*, 37(4): 347-359.
- Ceazan, M.L., Thurman, E.M. and Smith, R.L., 1989. Retardation of ammonium and potassium transport through a contaminated sand and gravel aquifer: the role of cation exchange. *Environmental Science & Technology*, 23(11): 1402-1408.
- Clark, I., Timlin, R., Bourbonnais, A., Jones, K., Lafleur, D. and Wickens, K., 2008. Origin and Fate of Industrial Ammonium in Anoxic Ground Water—15N Evidence for

- Anaerobic Oxidation (Anammox). *Ground Water Monitoring & Remediation*, 28(3): 73-82.
- Davis S. and De Wiest R. (1966). *Hydrogeology*. John Wiley & Sons, Inc., New York, 463 p. [Porosities and specific yield for alluvial sediments]
- DeSimone, L.A. and Howes, B.L., 1996. Denitrification and Nitrogen Transport in a Coastal Aquifer Receiving Wastewater Discharge. *Environmental Science & Technology*, 30(4): 1152-1162.
- DeSimone, L.A. and Howes, B.L., 1998. Nitrogen transport and transformations in a shallow aquifer receiving wastewater discharge: A mass balance approach. *Water Resources Research*, 34(2): 271-285.
- Dillon, P., 2005. Future management of aquifer recharge. *Hydrogeology Journal*, 13(1): 313-316.
- DIN 18123, 2011-04. Baugrund, Untersuchung von Bodenproben – Bestimmung der Korngrößenverteilung. Deutsches Institut für Normung, Beuth Verlag.
- DIN 18128, 2002-12. Baugrund - Untersuchung von Bodenproben – Bestimmung des Glühverlustes. Deutsches Institut fuer Normung, Beuth Verlag.
- Doussan, C., Poitevin, G., Ledoux, E. and Delay, M., 1997. River bank filtration: Modelling of the changes in water chemistry with emphasis on nitrogen species. *Journal of Contaminant Hydrology*, 25(1-2): 129-156.
- Doussan, C., Ledoux, E. and Detay, M., 1998. River-Groundwater Exchanges, Bank Filtration, and Groundwater Quality: Ammonium Behavior. *J. Environ. Qual.*, 27(6): 1418-1427.
- Erskine, A.D., 2000. Transport of ammonium in aquifers: retardation and degradation. *Quarterly Journal of Engineering Geology and Hydrogeology*, 33(2): 161-170.
- Garling F. and Dittrich J. (1979 ) *Gesteinsbemusterung*. Dt. Verlag für Grundstoffindustrie, 54 pp.
- Gaines, G.L. and Thomas, H.C., 1953. Adsorption Studies on Clay Minerals. II. A Formulation of the Thermodynamics of Exchange Adsorption. *The Journal of Chemical Physics*, 21(4): 714-718.
- Gunten, U.v. and Zobrist, J., 1993. Biogeochemical changes in the groundwater-infiltration systems: Column studies. *Geochimica et Cosmochimica Acta*, 57(16): 3895-3906.
- Groeschke, M. 2013 Challenges to riverbank filtration in Delhi (India): Elevated ammonium concentrations in the groundwater of an alluvial aquifer. *Zbl. Geol. Paläont. Teil I*, 2010, 1/2, pp. 1-9.
- Grünheid, S., Amy, G. and Jekel, M., 2005. Removal of bulk dissolved organic carbon (DOC) and trace organic compounds by bank filtration and artificial recharge. *Water Research*, 39(14): 3219-3228.
- Hamann, E., 2009. Reaktive Stofftransportmodellierung einer urbanen Grundwasserkontamination aus einem ehemaligen Rieselfeld. Dissertation Thesis, Humboldt Universität zu Berlin, Berlin, 159 pp.

- Haerens, B., 2004. Reactive Transport Modelling of a Groundwater Contamination from a Former Coking Plant, Dissertation. Katholieke Universiteit Leuven, 258 pp.
- Haerens, B., Prommer, H., Lerner, D.N. and Dassargues, A., 2006. Reactive transport modelling of a groundwater contamination by ammoniacal liquor. MODFLOW and More 2006: Managing Ground-Water Systems. (Proc. International Ground Water Modelling Conference, Golden, Colorado USA, 22-24 May 2006).
- Harbaugh, A.W., Banta, E.R., Hill, M.C. and McDonald, M.G., 2000. MODFLOW-2000, the U.S. Geological Survey Modular Ground-Water Model - User Guide to Modularization Concepts and the Ground-Water Flow Process. U.S. Geological Survey, Open-File Report 00-92: pp. 121.
- Heberer, T., 2002. Tracking persistent pharmaceutical residues from municipal sewage to drinking water. *Journal of Hydrology*, 266(3–4): 175-189.
- Hinkle, S.R., Böhlke, J.K., Duff, J.H., Morgan, D.S. and Weick, R.J., 2007. Aquifer-scale controls on the distribution of nitrate and ammonium in ground water near La Pine, Oregon, USA. *Journal of Hydrology*, 333(2–4): 486-503.
- Hinkle, S.R., Böhlke, J.K. and Fisher, L.H., 2008. Mass balance and isotope effects during nitrogen transport through septic tank systems with packed-bed (sand) filters. *Science of The Total Environment*, 407(1): 324-332.
- Hiscock, K.M. and Grischek, T., 2002. Attenuation of groundwater pollution by bank filtration. *Journal of Hydrology*, 266(3–4): 139-144.
- Jacobs, L.A., von Gunten, H.R., Keil, R. and Kuslys, M., 1988. Geochemical changes along a river-groundwater infiltration flow path: Glattfelden, Switzerland. *Geochimica et Cosmochimica Acta*, 52(11): 2693-2706.
- Jellali, S., Diamantopoulos, E., Kallali, H., Bennaceur, S., Anane, M. and Jedidi, N., 2010. Dynamic sorption of ammonium by sandy soil in fixed bed columns: Evaluation of equilibrium and non-equilibrium transport processes. *Journal of Environmental Management*, 91(4): 897-905.
- Jensen, H.E. 1973. Potassium–calcium exchange equilibria on a montmorillonite and a kaolinite clay. *Agrochimica*, 17 (1973), pp. 181–190.
- Johnson, A.I., 1967. Specific Yield - Compilation of Specific Yields for Various Materials. U.S. Geological Survey, Geological Survey Water-Supply Paper 1662, 74 p.
- Kuehn, W. and Mueller, U.W.E., 2000. riverbank filtration an overview. *Journal (American Water Works Association)*, 92(12): 60-69.
- Krapp, L., 1983. Determination of regional rock-mass permeabilities. *Bulletin of the International Association of Engineering Geology - Bulletin de l'Association Internationale de Géologie de l'Ingénieur*, 26-27(1): 443-447.
- Lewin, K., 1995. Landfill monitoring investigations at Burntstump Landfill, Sherwood Sandstone, Nottingham, 1978-1993 (ENV 9003) : final report. CWM/035/94. DoE.
- Leblanc, D.R., 1984. Sewage Plume in a Sand and Gravel Aquifer, Cape Cod, Massachusetts, United States Geological Survey Water-Supply Paper 2218.

- Parkhurst, D.L. and Appelo, C.A.J., 1999. User's guide to PHREEQC (Version 2) : a computer program for speciation, batch-reaction, one-dimensional transport, and inverse geochemical calculations.
- Parkhurst, D.L., and Appelo, C.A.J., 2013, Description of input and examples for PHREEQC version 3 — A computer program for speciation, batch-reaction, one-dimensional transport, and inverse geochemical calculations: U.S. Geological Survey Techniques and Methods, book 6, chap. A43, 497 p., <http://www.hydrochemistry.eu/ph3/index.html>
- Prommer, H. and Post, V., 2010. PHT3D: A Reactive Multicomponent Transport Model for Saturated Porous Media - User's Manual v2.10. 200 p. <http://www.pht3d.org>.
- Ray, C., 2008. Worldwide potential of riverbank filtration. *Clean Technologies and Environmental Policy*, 10(3): 223-225.
- Renault, P., Cazevielle, P., Verdier, J., Lahlah, J., Clara, C. and Favre, F., 2009. Variations in the cation exchange capacity of a ferralsol supplied with vinasse, under changing aeration conditions: Comparison between CEC measuring methods. *Geoderma*, 154(1–2): 101-110.
- Repert, D.A., Barber, L.B., Hess, K.M., Keefe, S.H., Kent, D.B., Leblanc, D.R. and Smith, R.L., 2006. Long Term Natural Attenuation of Carbon and Nitrogen within a Groundwater Plume after Removal of the Treated Wastewater Source. *Environmental Science and Technology*, 40: 1154-1162.
- Ross, D.S. and Ketterings, Q., 2011. Recommended Methods for Determining Soil Cation Exchange Capacity, Recommended Soil Testing Procedures for the Northeastern United States. Cooperative Bulletin No. 493.
- Vomocil, J.A., 1965. Porosity. In: C.A. Black (Editor), *Methods of Soil Analysis. Part 1. Physical and Mineralogical Properties, Including Statistics of Measurement and Sampling*. Agronomy Monograph. American Society of Agronomy, Soil Science Society of America, pp. 299-314.
- Vulava, V.M., Kretzschmar, R., Rusch, U., Grolimund, D., Westall, J.C. and Borkovec, M., 2000. Cation Competition in a Natural Subsurface Material: Modelling of Sorption Equilibria. *Environmental Science & Technology*, 34(11): 2149-2155.
- Salama, R.B., 1987. The evolution of the River Nile. The buried saline rift lakes in Sudan—I. Bahr El Arab Rift, the Sudd buried saline lake. *Journal of African Earth Sciences* (1983), 6(6): 899-913.
- Schwarzenbach, R.P., Giger, W., Hoehn, E. and Schneider, J.K., 1983. Behavior of organic compounds during infiltration of river water to groundwater. Field studies. *Environmental Science & Technology*, 17(8): 472-479.
- Sillén, L.G., 1951. On filtration through a sorbent layer. IV. The  $\psi$ -condition, a simple approach to the theory of sorption columns. *Ark. Kemi*, 2: 477-498.

- Singh, P., Kumar, P., Mehrotra, I. and Grischek, T., 2010. Impact of riverbank filtration on treatment of polluted river water. *Journal of Environmental Management*, 91(5): 1055-1062.
- Singh, L. and Singh, S., 1972. Chemical and morphological composition of Kankar nodules in soils of the Vindhyan region of Mirzapur, India. *Geoderma*, 7(3-4): 269-276.
- Sprenger, C., 2011. Surface- / groundwater interactions associated with river bank filtration in Delhi (India) – Investigation and modelling of hydraulic and hydrochemical processes, Dissertation, Freie Universität Berlin, Berlin, 154 pp.
- Thornton, S.F., Tellam, J.H. and Lerner, D.N., 2000. Attenuation of landfill leachate by UK Triassic sandstone aquifer materials: 1. Fate of inorganic pollutants in laboratory columns. *Journal of Contaminant Hydrology*, 43(3-4): 327-354.
- Thornton, S.F., Lerner, D.N. and Tellam, J.H., 2001. Attenuation of landfill leachate by clay liner materials in laboratory columns: 2. Behaviour of inorganic contaminants. *Waste Management & Research*, 19(1): 70-88.
- Thornton, S., Tellam, J. and Lerner, D., 2005. Experimental and Modelling Approaches for the Assessment of Chemical Impacts of Leachate Migration from Landfills: A Case Study of a Site on the Triassic Sandstone Aquifer in the UK East Midlands. *Geotechnical & Geological Engineering*, 23(6): 811-829.
- Steeffel, C.I., Carroll, S., Zhao, P. and Roberts, S., 2003. Cesium migration in Hanford sediment: a multisite cation exchange model based on laboratory transport experiments. *Journal of Contaminant Hydrology*, 67(1-4): 219-246.
- Tournassat, C., Gailhanou, H., Cruzet, C., Braibant, G., Gautier, A., Lassin, A., Blanc, P. and Gaucher, E.C., 2007. Two cation exchange models for direct and inverse modelling of solution major cation composition in equilibrium with illite surfaces. *Geochimica et Cosmochimica Acta*, 71(5): 1098-1114.
- Tufenkji, N., Ryan, J.N. and Elimelech, M., 2002. Peer Reviewed: The Promise of Bank Filtration. *Environmental Science & Technology*, 36(21): 422A-428A.
- Weiss, W.J., Bouwer, E.J., Aboytes, R., LeChevallier, M.W., O'Melia, C.R., Le, B.T. and Schwab, K.J., 2005. Riverbank filtration for control of microorganisms: Results from field monitoring. *Water Research*, 39(10): 1990-2001.
- Young, C.P., 1995. Landfill monitoring investigations at Gorsethorpe Landfill, Sherwood Sandstone, Nottinghamshire 1978-1992 : report. CWM 034/94. DoE.
- Zheng, C., 2010. MT3DMS v5.3 - A modular three-dimensional multispecies transport model for simulation of advection, dispersion and chemical reactions of contaminants in groundwater systems. Supplemental User's Guide. . Technical Report to the U.S. Army Engineer Research and Development Center, Department of Geological Sciences, University of Alabama, 51 p. <http://hydro.geo.ua.edu/mt3d>.

## 6 Musi River CWL system

*Title:* Water balance study of the Musi riverine-agriculture wetland system, Hyderabad: An Application of distributed hydrologic model -MIKE SHE

*Authors (DHI, IWMI, CSIR-NGRI):* Mohammad Fahimuddin (DHI), Mahesh Jampani (IWMI), Priyanie Amarshinghe (IWMI), Sahebrao Sonkamble (CSIR-NGRI), Sarah Sarah (CSIR-NGRI) Shakeel Ahmed, (CSIR-NGRI)

*Journal:* Environmental Modelling and Software

*Status:* to be submitted



## 6.1 Abstract

The paper presents a study on integrated catchment modelling (MIKE SHE) and water balance analysis that was aimed at understanding the soil aquifer treatment processes in an area where wastewater irrigation has been practiced for over 30 years. The overarching goal of the study was to study the impact of long-term wastewater irrigation on the groundwater through water balance analysis with the help of a numerical model. A distributed hydrologic flow model, MIKE SHE, was set up to analyze different flow components like, runoff, unsaturated flow, saturated flow and exchange with channels through a water balance study. Pilot scale short term monitoring supplemented by previous research reports provided the necessary input, calibration and validation data. The model calibration was done with groundwater depth below the surface and the model results were found to be consistent with the observed data in the area. The results show that the groundwater level in the area has risen significantly over the years, due to irrigation, canal seepage and the presence of small reservoirs created by the weirs on the Musi River, converted the watershed and riparian zone into a wetland. The model quantified the exchange of water flux among the various zones. The water balance results show that net groundwater recharge is in the order of 20% and the total evapotranspiration loss from canopy, saturated zone, overland, soil matrix accounted for about 50-60 %. The base flow discharge to the river was about 4-5 %. The simulated irrigation demand showed that the current irrigation practice by the farmers is to allow maximum deficit of 50-60 % before applying water. Overall, the existing hydrodynamic condition appears to be in equilibrium. More rainfall or irrigation will result in more surface and sub-surface return flows. Results also showed that the groundwater gradient reversed when the pumping rates increased in the northern region of the catchment, away from the riparian zone, which in turn can have an impact on the groundwater quality regime. The integrated modelling and its results illustrate the applicability of MIKE SHE as a distributed hydrologic model to a complex watershed (wetland) influenced by open channels, weirs, pumping, and irrigation in understanding the movement of water through surface and sub-surface levels. While water fluxes across the surface and sub-surfaces are well illustrated, the model can also shed light on the movement of pollutants and the overall capacity of the wetland to improve the water quality in the watershed. The science based evidence will be utilized to develop recommendations for good farming practices within the locality.

## 6.2 Introduction

*“Wetlands are areas where water is the primary factor controlling the environment and the associated plant and animal life. They occur where the water table is at or near the surface of the land, or where the land is covered by shallow water”* (Ramsar, 2013).

The Ramsar convention, 2013 further elaborated the definition of wetland as defined a wetland as *“areas of marsh, fen, peatland or water, whether natural or artificial, permanent*

*or temporary, with water that is static or flowing, fresh, brackish or salt, including areas of marine water the depth of which at low tide does not exceed six metres” (Ramsar 2013).*

The Ramsar convention classified all types of wetland into three major groups: Marine and Coastal Wetlands, Inland Wetlands, and Human-made Wetlands. Human made wetlands include fish and shrimp ponds, farm ponds, irrigated agricultural land, salt pans, reservoirs, gravel pits, sewage farms and canals etc. The wetland ecosystems (including lakes, rivers, marshes, and coastal regions to a depth of 6 meters at low tide) cover more than 1,280 million hectares globally (WRI, 2005). Wetlands play an important role in providing ecosystem services for livelihood enhancement and poverty alleviation. Therefore, it is important to understand wetland functions and how they can be influenced by anthropogenic activities.

Wetlands, whether human made, (i.e., constructed) or purely natural, are also considered to be a cheaper and low-cost alternative technology for wastewater natural treatment. A constructed wetland system is one that was purposefully designed and constructed artificially for water quality improvement is popularly known as a ‘Constructed Wetland Treatment System’ (CWTS). The constructed wetlands are of broadly two types, free water surface wetland in which water surface is exposed to atmosphere and sub-surface flow wetland water level in the wetland is maintained below the top of the surface (Crites et.al. 2006). In constructed wetlands, the major components like soil profile, vegetation, water flow rate, dry-wetting schedules are pre-planned, designed and most of the material parameters and boundary conditions of these components are known and correct. In some cases, a natural land is modified and converted into a wetland by creating an artificial hydraulic boundaries vegetation and water flow. These constructed wetlands are used to treat low volumes of wastewater with degradable organic matter for small populations in urban areas, established mostly by municipalities and industries.

### 6.2.1 Hydrodynamic characteristics of a wetland

Natural wetlands are generally found on flat areas or shallow slopes where there is perennial water lies at or near the land surface, or in low lying areas such as in topographic depressions, along flood plains (Rasmussen, T, 2008). Seepage wetlands form where ground water discharges on slopes, behind levees, pond, reservoirs, and also in irrigation command areas due to canal seepage loss and excessive flooded cultivation like in rice cultivation etc. Also, perched wetlands form above low-permeability substrates where infiltration is restricted. Wetland formation, their sizes, functions and persistence are controlled by hydrologic processes. Distribution and differences in type of wetlands are caused by topography, soil, drainage, vegetation, geology, climate, land use, as well as infrastructures like canal, controlled and impounded natural drainage, or human-induced disturbance. In turn, the wetland soils and vegetation alter water velocities, flow paths, and chemistry. The roles wetlands play in changing the quantity or quality of water moving through them are related to the wetland's physical setting and attributes (Rasmussen, T, 2008).

Hydrologic processes occurring in wetlands are same to hydrologic cycle. Major components of the hydrologic cycle are precipitation, surface or overland flow, sub surface flow, vertical infiltration, and evapotranspiration. Wetlands and uplands continually receive or lose water through exchange with the atmosphere, streams, and ground water. Favorable geologic settings, an adequate and continuous supply of water are necessary for the existence and sustainability of wetlands. Water table depth and its temporal variability, movement of water from one level to another through the wetland are the key parameters in characterizing the types and behavior of a wetland. Some wetland systems exchange water quickly, with water remaining within the wetland for only a short duration of time, while water may travel very slowly through other wetland systems. The residence time is the ratio of the volume of water within the wetland to the rate of flow through the wetland (Rasmussen, T, 2008).

An important feature of a wetland is its condition of oxygen deficiency. Anaerobic conditions develop more quickly in saturated soils than in unsaturated soils due to low oxygen solubility in water, slow rates of water advection, and slow diffusion rates of oxygen through water. Anaerobic conditions in wetland soils affect vegetation by creating adverse conditions for root survival and growth. Thus, the presence of water substantially affects soil oxygen concentrations, which affects plant growth and survival (Rasmussen, T, 2008).

#### 6.2.2 Waste water irrigation and natural treatment

In most developing countries, the disposal of untreated urban sewage to open water bodies and in rivers is common, and rapid. As a result of urbanization and the growing cities the large amounts of sewage are being generated and discharged into the cities' rivers, streams, water bodies converting them into perennial rivers and ponds. Therefore, there is a renewed interest to use wastewater for various purposes in the recent years Urban wastewater use for irrigation is informal, unsupervised and uncontrolled. The waste water irrigation practice especially in peri urban areas is an old and worldwide adopted practice. In 1800`s and early 1900`s, there existed sewage farms throughout Europe, Australia, Latin America and the USA. At the time, the main objective for the use of wastewater for irrigation was to keep the rivers free from faecal contamination. However, as the treatment technologies improved and awareness on water borne diseases also increased with time the practice was discouraged. But within in last 50-60 years, with increasing water demand and cities producing vast amounts of wastewater, the discussion on the waste water use for irrigation and other uses is gaining interest. In the developing world, wastewater use in peri-urban agriculture is still informal and continues to grow, because farmers like the nutrient rich water which allows less input with ready markets for its produce. The main factors which influence the wastewater use are competing demand, nutrient value, and ready markets for the produce. However, some negative externalities like health risks to farmers and consumers are often disregarded. The developments which encourage waste water for irrigation purpose are water scarcity, high cost of artificial fertilizers and advanced treatment plants, socio cultural acceptance of the

practice and also the awareness and demonstration that health risks and soil damage could be minimized if necessary precautions are taken.

### 6.2.3 The concept of soil aquifer treatment (SAT)

Soil-aquifer treatment is a natural method of recharging aquifers, where the soil/organisms act as a medium for removing contaminants. It is a low cost technology, and has high potential of recharging aquifers. A high degree of upgrading the water quality can be achieved by disposing partially-treated sewage effluent over land to infiltrate into the soil and move down to the groundwater. The unsaturated zone acts as a natural filter and can remove almost all suspended solids, biodegradable materials, bacteria, viruses, and other micro-organisms. Significant reductions in nitrogen, phosphorus, and heavy metals concentrations can also be achieved. Once the sewage is applied on the land/ infiltration basin or agriculture field, it gets natural treatment while passing through the unsaturated zone and finally joins the groundwater which further is allowed to flow some distance through the aquifer before it joins nearby streams. This additional movement through the aquifer provides further purification (removal of micro-organisms, precipitation of phosphates, adsorption of synthetic organics, etc.) of the sewage. Since in this process, utilizes soil and aquifer as treatment medium, it is called soil-aquifer treatment system or SAT system.

Sewage water should travel a sufficient distance through the soil and aquifer so that its residence time (travel time) in the SAT system is long enough, to produce naturally treated water of the desired quality. The degree of improvement in water quality while passing through soil and aquifer system depends on the quality of sewage effluent infiltrating into the ground, the soil type in the unsaturated zone and aquifer, the depth to groundwater, vegetation and climate etc.

### 6.2.1 The Musi wetland: A case of wastewater impacted riverine agriculture wetland

The Musi River, a major tributary of Krishna River, starts in the hill of Anathgiri near Vikrabad, North West of Hyderabad in Rangareddy district of Andhra Pradesh, India and flows down in the South east direction passing through the Hyderabad city and joins Aluveru River near Dharmaram .east of Hyderabad. The Musi River has been tapped by two major reservoirs, Himayat sagar and Osman sagar, upstream of the City. Below these two reservoirs, the Musi River receives only Hyderabad city's waste water and storm water. It receives water from its upper catchment only when excess flood is released from these reservoirs.

The Musi River downstream of the reservoirs, flows through the city (20 km), and enters a long stretch that is damed by small diversion structures (weirs), that diverts water into canals for agriculture. The river receives wastewater (both domestic and industrial) from the city which is either partially treated or untreated. The water is either lifted from canals or fed by gravity flows, some even after storage in sedimentation tanks. The wastewater flow in the river has made it a perennial river which became a significant resource in this

semi-arid peri-urban environment where the cultivation of fodder grass, paddy and vegetables has provided economic benefits to many peri urban inhabitants. Year round cultivation, irrigation canal, overflowing diversion structures (weirs), storage ponds etc has converted the riparian zone along the river into a constructed wetland in a natural setting. Since in the wetland, waste water is applied on the surface as irrigation water and exposed to atmosphere as well as waste water is getting infiltrated (from canal and river) into aquifer directly, the Musi wetland includes both types of constructed wetlands (surface and sub- surface ) defined by Crites, et. al. 2006.

Any development in the watershed changes the surface and sub-surface hydrologic and hydrodynamic regime. The irrigation infrastructures, series of weirs and irrigation canal networks which run almost parallel along the river on both sides' banks seems prima facie, to have changed the pristine natural flow regime significantly. The raised ponding level in the river due to over flowing weir has reduced the sub surface and groundwater flow slope resulting in decrease in the outflow rate. Similarly, return flow, excess recharge due to irrigation water application, and canal seepage have also significantly raised water table over the years. Therefore, the combined effect of weirs, canal and irrigation has converted the riverine agriculture area into a wetland type where groundwater table has risen, interacting with overland. Further, salinization of land due to waste water irrigation is quite understood; however, salinization also increases where the groundwater table comes near the surface due to reasons like irrigation, canal seepage and reduction in groundwater gradient near river due to weirs across natural drainage creating waterlogged and wetland type conditions where and groundwater starts exchanging water with overland followed by evaporation directly from the saturated zone.

Hyderabad, one of India's largest cities, disposes large amounts of its wastewater untreated into the Musi River. In water short semi-arid river basins with a fast growing mega city like Hyderabad, reuse of wastewater appears to be an increasingly important and complex issue and as well as an alternative option in absence of fresh water before the peri urban habitant to meet their water demand for agriculture purpose. As the city grows, waste water generation will also increase and more water will be available in the river and irrigation system which may increase the area of agriculture irrigated with waste water. Therefore, the urban growth will lead to considerable changes in irrigated agriculture in the future, in terms of its wastewater irrigated area and water resource availability for existing irrigated systems (Daan et. al., 2005). The waste water use for agriculture has added advantages like the supply is perennial, reliable, cheap, and high nutrient loaded. High nutrient wastewater has another advantage that is reduces the further application of fertilizers. Furthermore, due to its diversion to agriculture field, the flow in the main channel (river) reduces, therefore, the downstream length of the river and riparian zones under the impact of wastewater is contained and limited to move far downstream and vulnerability to contamination to downstream river and aquifer system is reduced. The downsides of waste water diversion for agriculture use are increasing soil salinity, contamination of ambient groundwater reserve, farmer's health, ecology and environment risks.

In last 10 years, a number of research projects have been carried out by different organizations and researchers on the different issues of waste water irrigation in the study area. A number of studies have been done on the Musi peri urban waste water agriculture on different perspectives such as: waste water use (Devi,et al, 2008), water balance of Hyderabad (Van Roojan et al., 2005), the impact waste water agriculture on farmers health (Hofstedt, 2005; ), economy (Brian et al.,2009), sewage dispose and water quality of the Musi river (Ensink et.al.,2009), river and soil salinity (McCartney et al, 2008, Biggs and Jiang,2008),water balance at agriculture field level (Hytteborn, 2005), agronomic risks and benefit (Amerasinghe et al., 2009). However, a fully distributed physics based hydrological numerical model has not been carried out including all the hydrologic process zones to characterize the hydrodynamic behavior of the wetland area and understand the interaction of groundwater and surface water through water movement and water balance analysis.

In this present study, physics based distributed hydrological model MIKE SHE has been applied to the study area to analyze interactions between overland, unsaturated, saturated, river, and canal through water balance and to assess the water quality of the system through mass transport. A similar type of modelling using MIKE SHE was carried out in Vietnam for a waste water irrigation field (Jensen, 2005). The water management, environment and health issues related to waste water reuse for agriculture in Vietnam case are studied and documented (IWMI, 2001)

### 6.3 Study area

The study area lies between coordinates 17° 15' N, 17° 30.'N and 78° 30'E, 78° 45.0'E near Peerzadaguda, Kachwani Singram and Mutialguda villages in eastern side outskirts of Hyderabad city on the northern side left bank of the Musi River, Figure 1. The study area falls in Rangareddy district. The climate of the district is hot summer and is generally dry except during the southwest monsoon season. The district has a normal rainfall of 781.5 mm and is in semi-arid region.

The Musi River downstream of Osman Sagar reservoir passes through the center of the old Hyderabad city and receives a number of sewers discharging waste water into it. The Musi river, after 35km downstream of Osman Sagar, has about 14-15 number of weirs across it in a stretch of about 65 km and water is diverted into irrigation channels taking off at these weirs on both sides of the river, the area has an extensive network of irrigation canals and drainage channels. These canals are interconnected with small reservoirs, locally known as tanks, forming a complex artificial flow and storage network. The A large part of area on both sides the Musi River is affected by a high water table in the irrigated area and near the Musi River. The waste water irrigation in the area started 30-40 years back when the water table depth was about 9 m. It appears the water table has risen because of waste water irrigation, canal seepage and reduced drainage due to the artificial reservoirs created by placing a number of weirs across the river drainage. Also, these weirs on the river are supposed to have created waste stabilization ponds (WSP)

and aided the river's self-purifying ability and could thus provide irrigation water safe for use in agriculture (Ensink, 2009).

The left bank canal taking off from the first weir near village Peerzadiguda passes through the study area running parallel to the Musi river at a distance of about 150-200m only. The first two weirs fall in the present study area river reach. Near village Kachiwani Singram, there exists a first order stream of catchment area about 2.25 km<sup>2</sup>, which outfalls into the reservoir of the second weir. In the study area, the Musi River appears to be gaining stream (Effluent River) receiving water from groundwater-saturated zone; precipitation runoff and irrigation return flow.

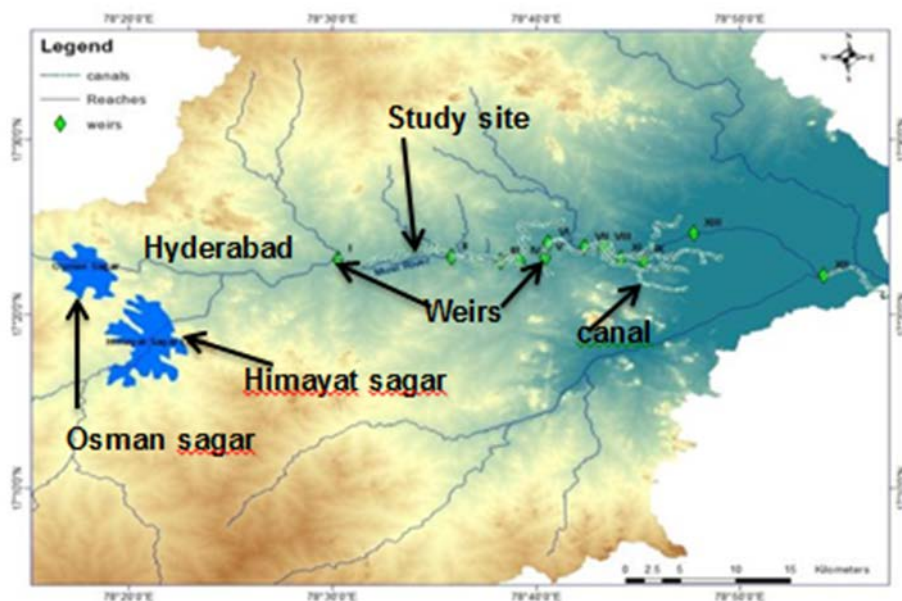


**Figure 1 Study area near Hyderabad, India**

### 6.3.1 Objective

The main objectives of this study were to assess the impact of waste water irrigation on local groundwater quality; determine the interactions between Musi River water and groundwater, groundwater budgeting in the area and evaluate the impact of future water-use scenarios on the groundwater system.

The distributed hydrologic model development was considered to be an important part in the hydrodynamic characterization of a wastewater impacted wetland. The assessment of the impact on local groundwater resources, soil as well as water quality improvement capacity of sub soil and irrigation practice as a natural soil aquifer treatment system is attempted. . This paper describes the development and application of an distributed hydrologic model using MIKE SHE for the Musi River waste water agriculture field, with an aim to analyze the water movement and water balance as a first step to understand the groundwater surface water interactions followed by water quality modelling in the next step to assess the performance of the system as a natural treatment system.

## 6.4 Distributed hydrologic modelling: Application of MIKE SHE

### 6.4.1 MIKE SHE model

MIKE SHE is a physics based distributed hydrologic modelling with flexible framework. It has two main modules: Water Movement (WM) and Water Quality (WQ). The Water Movement module has a modular structure which includes six process-oriented components of the hydrological cycle that are interception/evapotranspiration, overland/channel flow, unsaturated zone, saturated zone, snow melt and the exchange between aquifers and rivers (Figure 2) (DHI, 2014) . Each of these processes can be included in the model at different levels of spatial distribution and complexity as per objectives of the modelling study, the availability of data, as well as computer's capacity and the modeler's choices as well. MIKE SHE uses MIKE 11 to simulate channel flow and interact with surface water. MIKE 11 includes comprehensive facilities for modelling complex channel networks, lakes and reservoirs, and river structures, such as gates, sluices, and weirs. MIKE SHE 's strength lies in its features to provide a simulation of coupled unsaturated-saturated zone, interaction between evaporation and shallow water table, better evapotranspiration module with root zone exchange apart from efficient coupling with open channel. In view of the overall objective of the modelling, all the above hydrological processes considered necessary to be included in the proposed model and therefore, the MIKE SHE was selected for the modelling. Pertaining to the current modelling, the most important features of MIKE SHE, i.e., coupling unsaturated-saturated zone and groundwater-surface water (MIKE SHE-MIKE 11) are briefly discussed below.

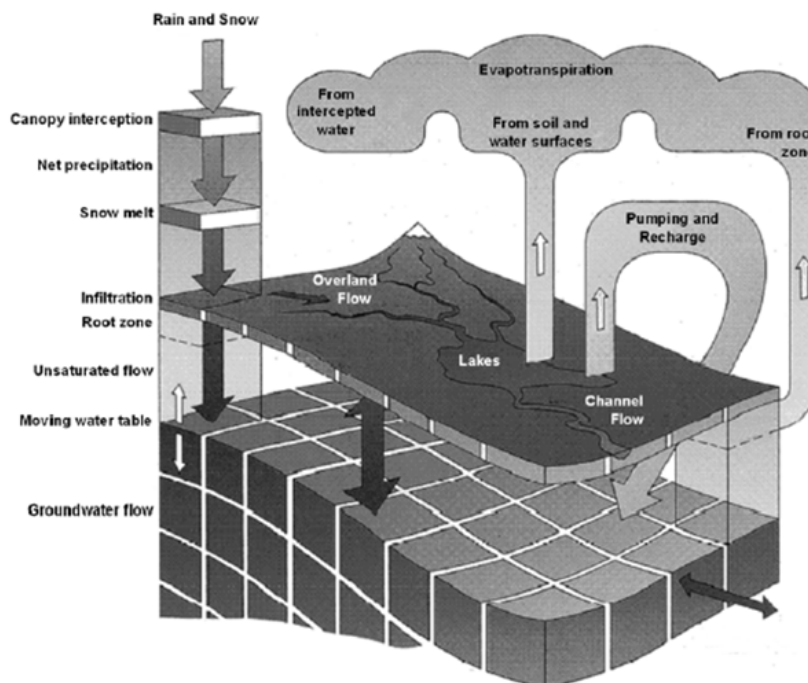


Figure 2 Hydrological processes and their interaction in MIKE SHE (DHI, 2014)



### **Coupling the Unsaturated Zone to the Saturated Zone**

The key feature of MIKE SHE is its ability to simulate coupled unsaturated–saturated flow. The unsaturated zone is dynamics characterized by cyclic fluctuations in the soil moisture which is replenished by rainfall or irrigation application and removed by evapotranspiration and balance join to the groundwater table. Unsaturated flow is considered predominantly vertical since gravitational force plays the major role in infiltration. Therefore, in MIKE SHE also the unsaturated zone is calculated vertically in one-dimension. MIKE SHE uses an iterative technique to couple unsaturated zone and the saturated zone and compute the correct soil moisture and water table dynamics in the lower part of the soil profile. There are three options in MIKE SHE for calculating vertical flow in the unsaturated zone: (i) Using Richards equation, (ii) a simplified gravity flow procedure, which assumes a uniform vertical gradient and ignores capillary forces, and (iii) a simple two-layer water balance method for shallow water tables. The Richards's equation being highly nonlinear and computation intensive takes long simulation time although it is accurate. The simplified gravity flow procedure provides a suitable solution when the primary aim is to estimate the time varying recharge to the groundwater table based on actual precipitation and evapotranspiration and not the dynamics in the unsaturated zone. The simplest two-layer water balance method is suitable when the water table is shallow and groundwater recharge is primarily influenced by evapotranspiration in the root zone.

A correct description of the recharge process is difficult because when water enters the saturated zone from the unsaturated zone the water table rises which further affects flow conditions in the upper unsaturated zone. The unsaturated and the saturated zones are coupled applying an iterative technique. The main issue in coupling the two zones arises from the fact that the two components (modules) are explicitly coupled (i.e., run in parallel) and are not solved in a single matrix with an implicit flux coupling of the UZ and SZ differential equations. The explicit coupling of the two zones is used in MIKE SHE to optimize the time steps used and also allows use of time steps that are representative of the unsaturated zone (minutes to hours) and the saturated zone (hours to days) regimes.

In coupling unsaturated zone and saturated zone, there could be three conditions: (i) If the unsaturated zone model is within the top layer of the saturated zone and the water table goes up in the unsaturated zone then the lower boundary becomes a normal pressure boundary, (ii) If the water table falls below the bottom of the unsaturated zone then an error is generated and the simulation is stopped, and (iii) If the unsaturated model extends below the top saturated zone layer and the top saturated zone dries out, then the unsaturated zone model treats the bottom boundary as either a pressure boundary with the pressure equal to the elevation of the bottom of the uppermost SZ layer, or a zero-flux boundary if there is an upward gradient at the lower boundary. The above three possible conditions are shown in Figure 3 below. The most important limitation of the coupling of the two zones is that the unsaturated zone exchanges water only with the top node of the saturated zone.

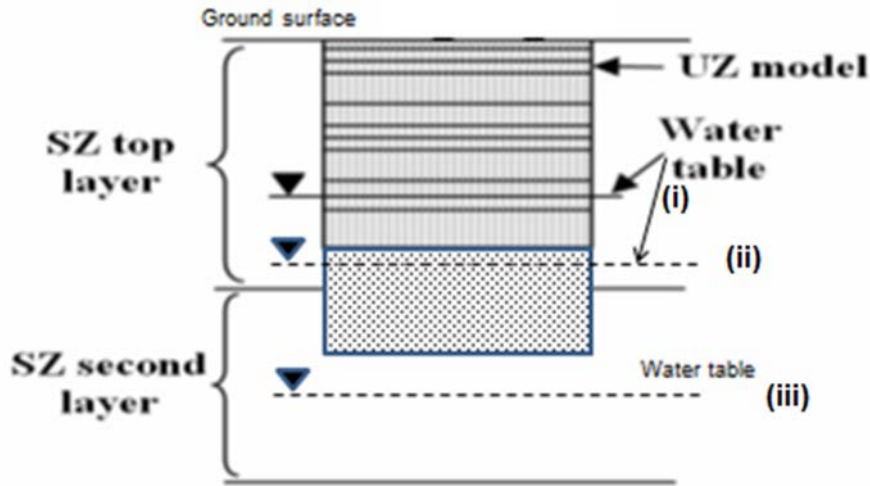


Figure 3 Coupling between unsaturated-saturated zones

**Coupling between MIKE SHE and MIKE 11**

The coupling between MIKE 11 and MIKE SHE is made via river links, which are located on the edges of two separate adjacent grid cells. Figure (a) shows part of a MIKE SHE model grid with the MIKE SHE river links, the corresponding MIKE 11 coupling reaches, MIKE SHE exchanges water with the coupling reaches only, however, the entire river could be included in the hydraulic model.

The MIKE 11(HD) hydraulic model uses the precise cross-sections whereas the exchange of water between MIKE 11 and MIKE SHE is calculated based the river-link cross section Figure (b). The river-link cross section is a simplified, triangular cross-section interpolated (distance weighted) from the two nearest MIKE 11 cross-sections. The top width is equal to the distance between the cross-section’s left (marker 1) and right bank levels (marker 3). The elevation of the bottom of the triangle equals the lowest depth (marker 2) of the MIKE 11 cross-section.

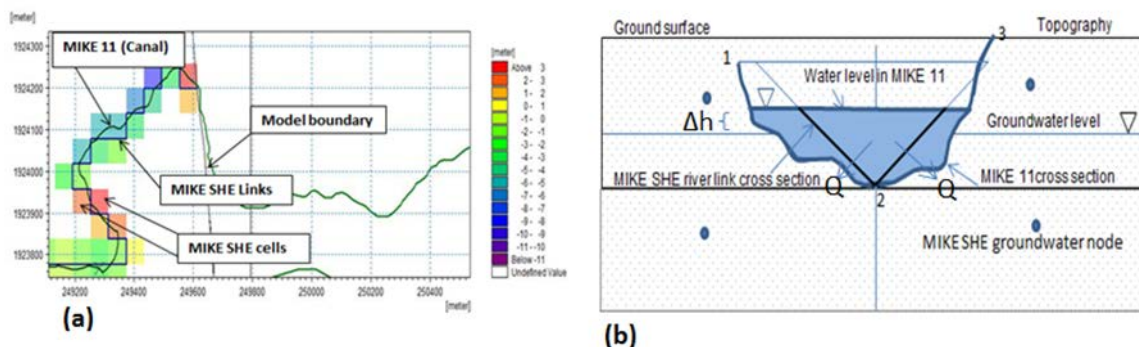


Figure 4 Coupling MIKE 11 and MIKE SHE

In case, MIKE 11 cross-section is wider than the MIKE SHE cell size, the river-link cross-section is reduced to the cell width. This is an important limitation as it embodies the assumption that the river is narrower than the MIKE SHE cell width. If the river is wider

than a cell width, this situation is addressed with the concept of flooding using two options: Flooding using Flood Codes or the Direct Overbank Spilling to and from MIKE 11. In case it is not required to simulate flooding, the reduction of the river link width to the cell width does not cause any problem, because MIKE SHE assumes that the primary exchange between the river and the aquifer takes place through the river banks (DHI, 2014)

The exchange of water (Q) between groundwater and channel is calculated as a conductance (C) multiplied by the head difference ( $\Delta h$ ) between groundwater level (grid cell) and channel level as:

$$Q = C \cdot \Delta h$$

The exchange Q is calculated twice, i.e., for both sides linked cells of the river link, Figure , to account for different flow on either side of the river if there is groundwater head gradient across the river or if the aquifer properties are different. The conductance C is calculated based on three possible situations as below.

The exchange between river and aquifer is estimated in three possible situations for the coupling reaches: (i) Aquifer only, when the river is assumed to be hydraulically connected fully with aquifer and assumed that there is no head loss due to river bed clogging / low permeable lining. This is a typical condition assumed for a gaining reach, (ii) River bed only, when there is a low permeable river bed and there is head loss across the bed. This type of condition exists when the bed material is thick and very fine and the aquifer material is coarse, and (iii) Aquifer + Bed, when there is a low conductivity river bed lining, then there will be a head loss across the lining. In this case, the exchange is a function of both the aquifer conductivity and the total conductivity of the river and the adjacent groundwater can be calculated as a serial connection of the individual conductance (DHI, 2014).

### **Time step control**

The different components have their different response time to perturbation, for example the response time of overland flow is less than the response time of unsaturated flow and saturated zone has the largest response time. Coupling of processes having different response time is one of the critical aspects of the distributed /integrated model. In MIKE SHE, the simulation time step is dynamic, however, the maximum allowed time step for every process needs to be specified as the model automatically adjusts its time step within the provided maximum allowed time step.

### **Results output: water balance**

The hydrologic cycle is all about water exchange and the analysis of this exchange is the water balance. Issues related with the water sustainability and environmental impacts are directly related to the water balance study which is an important tool for characterizing the behavior of a watershed. There are basically three types of water inflows and outflows components such as: (i) atmospheric components rainfall, snow, evaporation, and transpiration, (ii) subsurface inflows and outflows and (ii) interaction with surface water, including overland flow, as well as from rivers and streams. The relative importance of each component in maintaining wetlands varies both spatially and temporally, but all these

components interact to create the hydrology of an individual wetland. Since MIKE SHE includes all of the processes in the hydrologic cycle, it includes a sophisticated water budgeting tool (\*.wbl) for summarizing, mapping and plotting the exchange of water between all of the hydrologic processes. One important limitation with the current water balance tool is that it does not give branch wise exchange of water between MIKE SHE (groundwater) and Surface water (MIKE 11). The water balance tool gives exchange of water with MIKE 11 but does not give water balance within MIKE 11 itself. Once water enters MIKE 11 it no longer part remains part of the MIKE SHE water balance (DHI, 2014) MIKE 11 output like discharge is instantaneous at a location whereas MIKE SHE gives average flow into a cell in one time step. The water balance tool gives total exchange of water from all branches collectively. Therefore, when there are number of branches (canal and river networks) in a domain it is difficult to assess which branch (or the stretch of the branch) is in losing or gaining conditions and how much water is being exchanged between groundwater and surface water. However, exchange of quantity can be assessed from MIKE 11 results where outputs are instantaneous. In MIKE SHE water balance, outputs are accumulated in a step.

A large number of projects and researches have been carried out using MIKE SHE with different scopes and objectives (Thompson et. al., 2004; Singh et.al., 1999; Demetriu et.al., 1999; Dai et.al., 2010, Wijesekara, et. al., 2014). Refsgaard et al (1995) discussed various features of MIKE SHE with issues and challenges in its development and also cited a number of research projects carried out with the application of MIKE SHE. MIKE SHE has also been in a project for the assessment of impact waste water irrigation at Nam Dinh, red river delta, Vietnam (Jensen and Raunso, 2005) similar to the present study.

#### 6.4.2 Musi model conceptualization

The main objective of the study was to assess the impact of wastewater irrigation on the groundwater and soil in the area. Therefore, based on the study area features and the objectives, an integrated catchment modelling was needed which can include all the hydrologic processes in simulation like flow through unsaturated zone, overland flow, evapotranspiration, exchange of water between surface water system like river, canal, ponds, pumping wells etc. Since the primary aim of the modelling is to assess the waste water irrigation practice as natural soil aquifer treatment system, the role of unsaturated zone becomes very important, and the frequency of application of irrigation water over the land, which is subjected to drying and wetting at intervals becomes another important aspect which needed to be examined in the modelling.

A distributed hydrologic model should represent all the important natural processes and should also be able to include the relevant human interventions on the system. Some of the important human developments in any watershed which alter the pristine hydrologic regime are; irrigation infrastructures weirs and canal, groundwater pumping, artificial ponds, vegetation, built-up area. In the Musi wetland, all the kinds of human interventions as mentioned above are present. In the area, the canal and the river both are carrying

polluted waste water which is being used for irrigation in the catchment and make the entire system even more complex one.

The very first step in any model development is to define the model area. On large catchment or regional scale, the model boundary is defined typically along topographic divide, a groundwater divide or a combination of the two. However, on a local small-scale level or in very flat terrain, defining boundary for groundwater zone is difficult because groundwater boundary is dynamic, and depends on pumping rates as well. Modelling a micro watershed is somewhat difficult because its topographical boundary may be not be the groundwater boundary. This is the case in the present study and it appeared that the model domain needed to be up scaled suitably to have a realistic groundwater boundary. For this reason, the model catchment was up-scaled to 12.68 km<sup>2</sup> towards the upland area towards the north up to Narapalli village (Figure 5). The topography in the model domain includes upland area away from the river having steep slope as well as low lying area near the Musi River

The northern part of the watershed comprised of red soils while close to the river it was black. The simulation of the unsaturated zone was done using simple Gravity Flow option considering the extensive simulation time taken by Richard Equation option. The unsaturated zones of both the soil profile be vertically discretized suitably going from finer layer depth at the top to coarser at the bottom. In the current model, only one layer of SZ has been included, therefore, the depth of the UZ was sufficiently extended considering that in no case water table should fall below the bottom of the UZ. Extending sufficiently has no impact on the estimation of exchange because water exchanges with the top node of the SZ. The saturated zone could be considered as an unconfined aquifer with just one layer of 60 m depth below the ground surface. The overland flow can be simulated using finite difference method option considering objectives.

Both, the canal and the Musi River with weirs could be integrated in the model by coupling MIKE SHE with MIKE 11. First of all a stand-alone MIKE 11 was simulated successfully and then MIKE 11 simulation file is included as an input into MIKE SHE. The coupling of the canal was difficult as in the study reach; the canal is running parallel to the Musi River. Ideally a canal is supposed not to receive overland flow as its bank is always above the ground level. However, in the present case, if canal bank is raised above the ground it obstructs the overland flow to the river. To handle this problem, the canal was assumed to intercept the overland flow in such a way that it receives overland flow from upstream side and spills over towards the Musi side. In this case, it was tackled by considering the canal with spillover option available in the MIKE SHE. The canal should be considered to exchange (seepage) water through bed only. The Musi was considered as exchanging water with MIKE SHE through aquifer only.

Different vegetation could be included and simulated using typical values of LAI and RD. No pumping was considered from 15 Jun to 15 Oct every year. In absence of time varying data of irrigation applied for different crops, in different period, therefore, we can simulate crop water demand applying Crop Stress factor or Maximum Allowable Deficit (MAD)

options available in the irrigation module of MIKE SHE in order to generate wetting and drying period and to compare the total simulated demand with the total water irrigation being done as estimated from field survey.

In the current model the key processes, overland (OL), unsaturated zone (UZ), evapotranspiration (ET), saturated (SZ), rivers and lakes, were included in the simulations and detailed water balance study was performed for various scenario.

#### 6.4.3 Model setup and parameterization

In this study, coupled MIKE SHE-MIKE 11 was used to simulated the full hydrological cycle of the of the watershed including evapotranspiration (ET), unsaturated zone (UZ), saturated zone (SZ), overland flow (OL) and channel flow that is the Musi river and canal system with weirs. The main input parameters for model setup include data such as: topography, soils, land use and land cover, natural and canal drainage network, locations of weirs and their hydraulic parameters, well numbers and locations, agriculture and irrigation data, rainfall, potential evapotranspiration, aquifer parameters etc.

The model domain was divided into 60mx60 m cells. The vegetation and soil type were spatially distributed according to use and land cover data. The overland flow was simulated with a finite difference method, unsaturated zone using gravity flow and saturated zone using finite difference.

Two types of soils were included in the model, Red soil type was considered in the upland area where as black soil was for the area near the Musi River in lower part under cultivation area. The vertical discretization of the soil profile was done through small cells near the ground surface and increasing cell thickness with depth. The distribution of land use and land cover with well locations is shown in Figure 6 and the area distribution of land use and land cover as well as source of water for irrigation is presented in Table 1 below

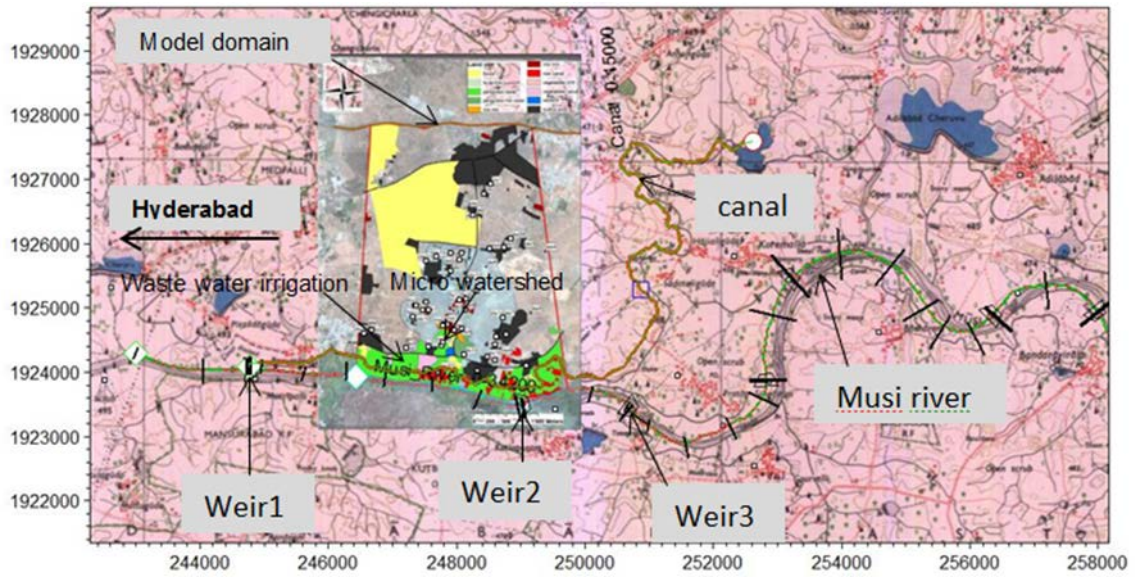


Figure 5 The model domain, Musi river, canal, weirs and pilot study area

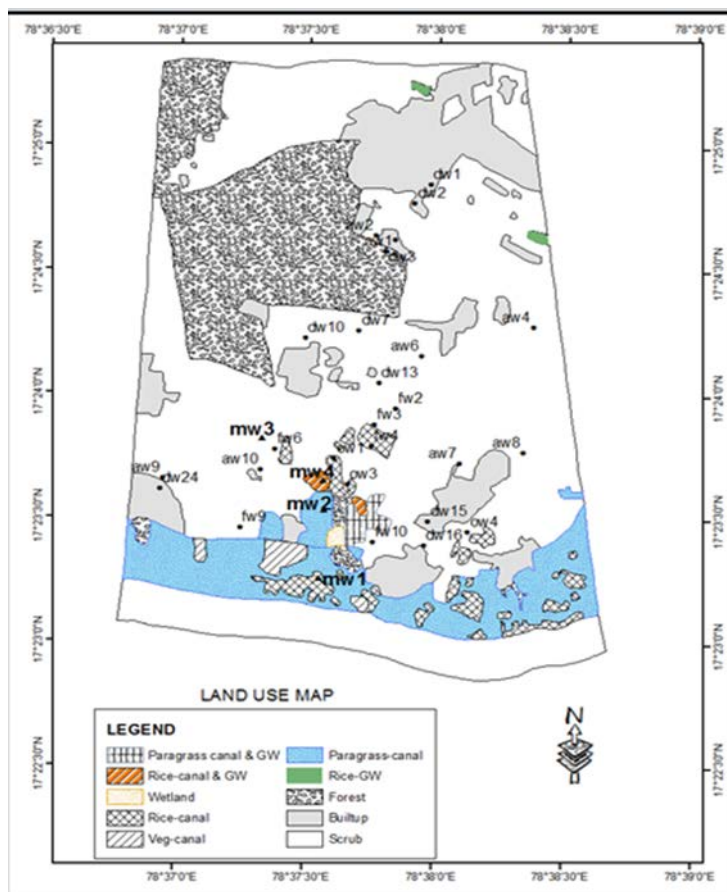


Figure 6 Land use, well locations

**Table 1 Land use area distribution (12.6828Km2)**

| Land use  | Irrigation water source     | Area, Km2 | % of Model domain |
|-----------|-----------------------------|-----------|-------------------|
| Forest    |                             | 2.1384    | 16.86             |
| Paragrass | wastewater                  | 1.1772    | 9.28              |
| Paragrass | Waste water and groundwater | 0.0720    | 0.57              |
| Rice      | Waste water and groundwater | 0.0360    | 0.28              |
| Rice      | wastewater I                | 0.3348    | 2.64              |
| Vegetable | wastewater I                | 0.0828    | 0.65              |
| Wetland   |                             | 0.0180    | 0.14              |
| Builtup   |                             | 1.6488    | 13.00             |
| Scrub     |                             | 7.1460    | 56.34             |
| Rice      | Groundwater                 | 0.0288    | 0.23              |
| Total     |                             | 12.6828   | 100.00            |

All geospatial data like land use, model domain, well locations, river, canal, weir locations soil types, etc. other were digitized and geo referenced on Arc GIS and shape files were used as MIKE SHE Inputs. Other data which were used in the model setup are presented in Table

**Table 2 Data types and sources**

| Data   | Sources   |
|--|---|
| MIKE SHE setup   |   |
| Topography (DEM)   | 30 m Aster Digital Elevation Model (DEM)              |
| Rainfall   | Daily, National Geophysical Research Institute (NGRI) |
| Potential evapotranspiration                                     | FAO Climwat   |
| Soil, Land use, Geological and aquifer data, Irrigation Practice | (Perrin, 2010)  |
| Crop/vegetation parameters                                       | MIKE SHE vegetation templates                         |
| Soil type  | (Schmitt, 2010)                                       |
| Pumping, Irrigation  | (Schmitt, 2010),                                      |
| Groundwater level observed data                                  | Pilot scale monitoring and Perrin, 2010               |
| MIKE 11 setup  |   |
| Musi river cross section   | Generated from 30 M Aster DEM                         |
| Canal cross section  | Field measurement                                     |
| Weirs locations, length, height                                  | (Ensink, 2009), Google earth imagery                  |



digitization, weir height was kept about 5m from the lowest bed

Canal and Musi river flow

Ensink et al 2009. Field measurements

.

#### *Simulation specification*

In the Musi model, the initial time step was kept 4 hours and the maximum allowed time steps for OL, UZ and SZ zones were kept as 6,12 and 24 hours.

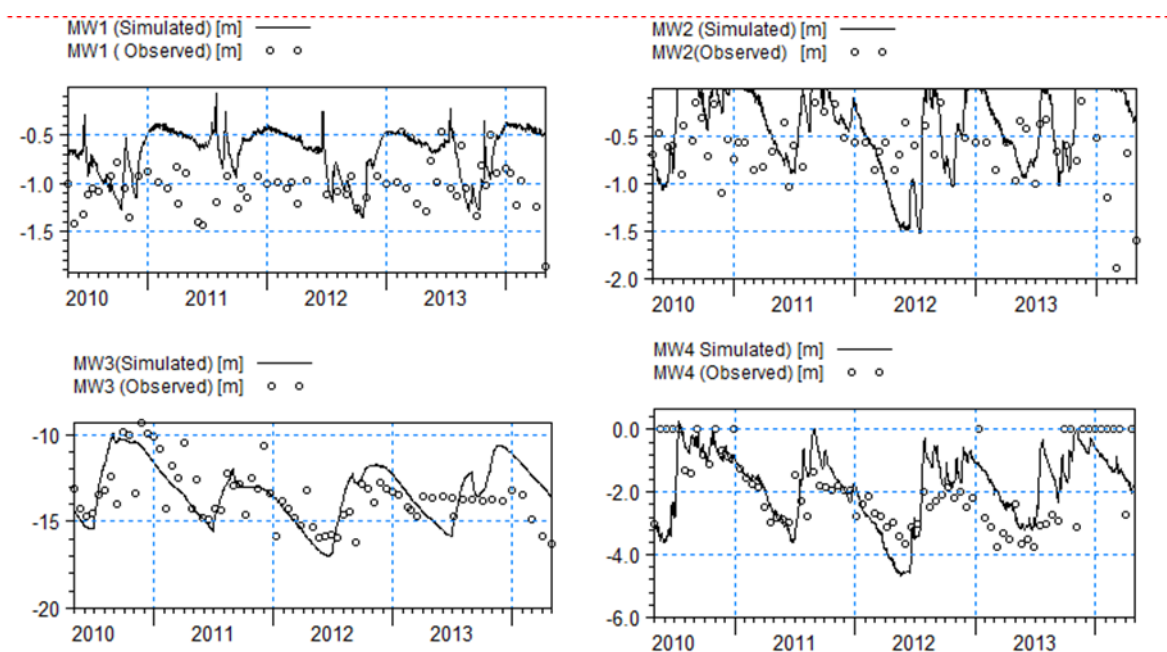
#### 6.4.4 Model calibration and validation

Ideally, an integrated surface water-groundwater model should be calibrated with river discharge as well as groundwater depth. In the present model, the study area is very small and densely covered by vegetation and in the catchment there is no stream or ditch of significant size which carries significant surface runoff during dry periods or even during rainfall, hence, the observed discharge was not available for the calibration. However, measured groundwater table data at sizable locations were available; therefore, the model was calibrated with the measured depth of groundwater table below surface only. The main emphasis of the calibration process was to provide good temporal and spatial agreements between simulated and observed groundwater levels throughout the catchment. The calibration was performed for monitoring wells (MW1, MW2, MW3, MW4), Figure 7, looking at Mean Error (ME) and Root Mean Square Error (RMSE) values which were tried to be minimized. The calibration results in terms of ME, MAE and RMSE are presented in Table 3. The table shows that apart from the monitoring wells, for which observed data were available for years, 2010-2014), other abandoned wells (aw), pumping wells (dw and fw) and other well (ow) for which we had just one year observed data (2010) have also shown good consistency with the observed and simulated water table below ground surface. In a small catchment of about 12.68 km<sup>2</sup> area, at 11 locations the simulated water table is quite near to the observed values. These observation wells are also located in different parts of the catchment, i.e., in the lower part near the river as well as in the upland area.

Since the calibration has been done for observed vs. simulated depth of water below ground level (bgl), some locations do not show good match, and this may be attributed to topography difference between actual location elevation and corresponding model cell elevation. Also, the observed data, except for MW3 and MW4, were not available continuously for the entire calibration period. While calibrating, after every simulation, water balance results were also reviewed to analyze the water movement from one zone to another and return flow, total evapotranspiration, and groundwater recharge were evaluated to see the results consistency and model performance. The comparisons of observed and simulated groundwater depth below surface at monitoring well locations are shown in Figure 7. The calibration could be considered as satisfactory.

**Table 3 Statistical parameters of errors between observed and simulated water table (SCN3)**

| Locations | ME    | MAE  | RMSE | Period          |
|-----------|-------|------|------|-----------------|
| MW1       | -0.32 | 0.40 | 0.47 | 2010 to<br>2014 |
| MW2       | -0.18 | 0.45 | 0.56 |                 |
| MW3       | -0.02 | 1.10 | 1.50 |                 |
| MW4       | -0.31 | 0.87 | 1.13 |                 |
| dw13      | -0.36 | 0.36 | 0.40 | 2010            |
| dw24      | -2.10 | 2.10 | 2.15 |                 |
| dw16      | -1.40 | 1.80 | 1.99 |                 |
| fw6       | 1.00  | 1.01 | 1.23 |                 |
| ow1       | 1.97  | 1.97 | 2.12 |                 |
| fw2       | 0.61  | 1.80 | 2.26 |                 |
| fw3       | 1.51  | 1.51 | 1.51 |                 |

**Figure 7 Simulated and observed groundwater depth below surface at Monitoring wells (MW1, MW2, MW3 and MW4)**

The model was initially calibrated for parameters specific yield, soil moisture, drainage time constant and manning number for overland flow for the period 2010-2014. Later on, the model was fine-tuned for with specific yield and drainage time constant. The observed groundwater depths from surface at 31 locations distributed in different parts of the domain (Figure 6) have given general idea of depth of groundwater table which helped in

the overall evaluation of the parameters. The final input parameters are presented in Table 4

**Table 4 Final input parameters**

| Parameters                     | Values      | Distribution/Remarks      |
|--------------------------------|-------------|---------------------------|
| Sp yield                       | 0.004       | Global                    |
| Horizontal conductivity(m/s)   | 3.40E-05    | Global                    |
| Vertical conductivity (m/s)    | 3.40E-06    | Global                    |
| Saturated moisture content     | 0.38        | Red soil upland area      |
| Residual moisture content      | 0.068       |                           |
| Alpha and n                    | 0.008, 1.09 |                           |
| Saturated moisture content     | 0.41        | Black soil near river     |
| Residual moisture content      | 0.095       |                           |
| Alpha and n                    | 0.019, 1.31 |                           |
| Overland Manning number(M=1/n) | 30          | agriculture area          |
|                                | 50          | scrub and upland          |
| Overland Detention (mm)        | 2           | Global                    |
| Depth (m)                      | -0.5        | from Surface              |
| Drainage time constant, TC     | 2.00E-07    | Global                    |
| Musi river                     |             | Aquifer exchange,         |
| Waste water canal              |             | River bed only            |
| Canal leakage coefficient      | 1e-8        |                           |
| Crop parameters                |             |                           |
| LAI                            | 2-6         | Vegetation based          |
| Root depth (mm)                | 200-1000    | Vegetation based          |
| Irrigation demand              | 0.5         | Maximum Allowable Deficit |

## 6.5 Results and Discussion

After calibration and freezing of the parameters, five scenarios (Table 5) with different objectives were developed to assess the response of the system. The results were analyzed for the water table, water balance, return flow, irrigation demand and other important parameters that explain the hydrodynamic behavior of the watershed.

**Table 5 Scenarios and their objectives**

| Scenario code | Description                         | Objective   |
|---------------|-------------------------------------|---|
| SCN1          | Baseline                            | Current hydrodynamic behaviour and water balance with user specified irrigation demand based on field survey (Perrin, 2010) with no irrigation during Aug-Sep |
| SCN2          | Without irrigation, weirs and canal | Impact of irrigation infrastructure on the pristine hydrologic regime   |

|      |                                   |   |
|------|-----------------------------------|---|
| SCN3 | Irrigation application at MAD=0.5 | Current irrigation practice vs. simulated demand with all existing setup (SCN1) |
| SCN4 | Pumping increased by 100%         | Impact on the water table gradient and return flow                              |
| SCN5 | Canal not coupled                 | Assumed fully lined and zero seepage. To see the impact on water table          |

### 6.5.1 Water table

The simulated groundwater table contour maps for pre-monsoon and post monsoon are presented in Figure 8. The map shows that the general groundwater flow direction is from north to south towards the Musi River and the existing pumping wells have not changed the overall flow pattern. This is mainly because of the steep topography slope like rolling terrain and also low pumping in the catchment.

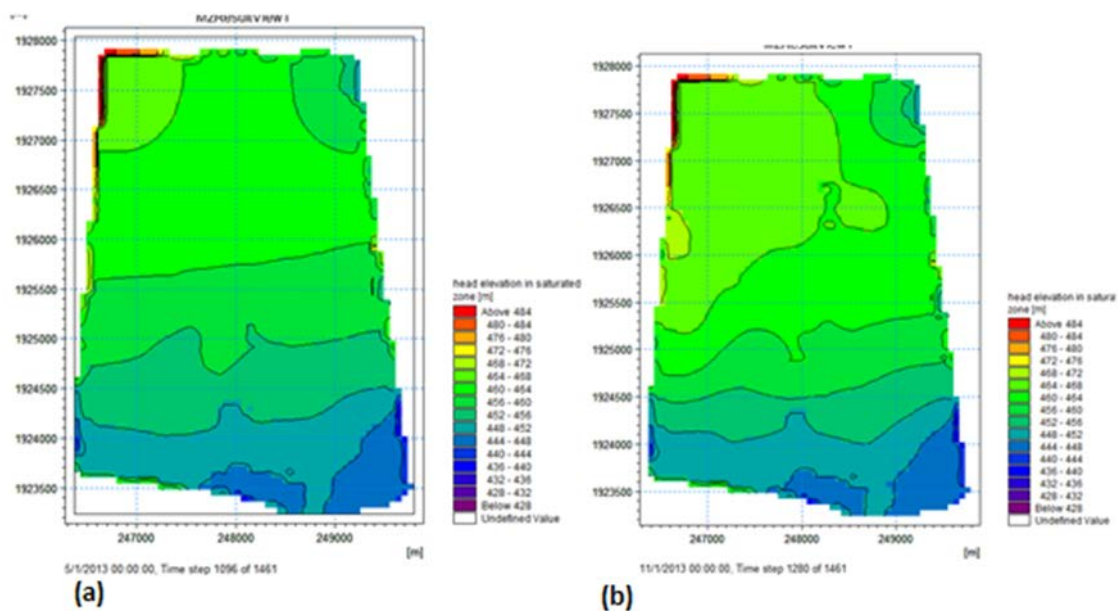


**Figure 8 Groundwater table contour during pre-monsoon (a) and post-monsoon (b)**

However, with the increase in pumping (Scenario SCN4) in the middle part of the domain, the groundwater table gradient reversed locally from MW4/MW) towards MW3, Figure 9. The impact of increased pumping on the groundwater table is not significant near the riparian zone, i.e., near Musi river which shows riparian zone /flood plain is dominated by the boundary (ponding level in the river). However, if a high and continuous pumping takes place then with time the influence of pumping (inverse groundwater gradient) may reach to the canal and the Musi River and waste water will start migrating towards inland side.

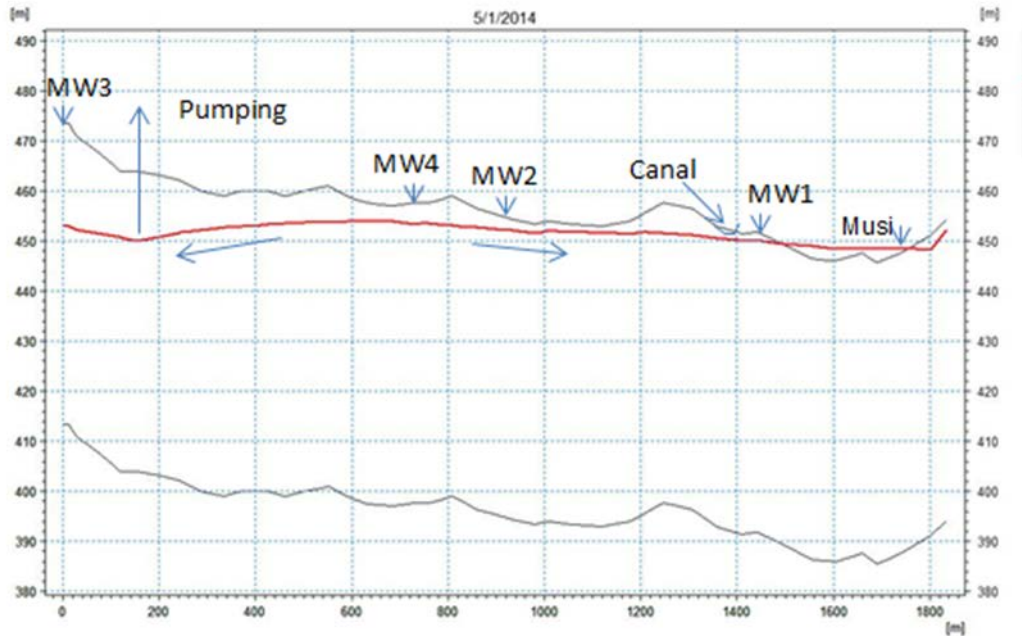


**Figure 9 Water table profile along the line joining monitoring wells and the river**

The combined impact of irrigation, canal, weirs and pumping on water table regime is illustrated through water table analysis as presented in Table 6, which presents the water table analysis where the water table is found within 2 m and 6 m from the ground surface. The analysis criteria of 2 m and 6 m depths have been chosen based on the definition of waterlogged area and wetland area. The table presents the areas with respect to cultivation area (1.7 Km<sup>2</sup>) as well as for the entire model domain (12.6828Km<sup>2</sup>) and differentiated between the pre monsoon and the post monsoon periods. In the irrigated part, the land area with water table within at 2 m (i.e., water logged area) from ground surface, has increased significantly from 0.112 km<sup>2</sup> (SCN2, pristine condition) to 0.842km<sup>2</sup> (SCN3) during the pre-monsoon period. Similarly, the wetland area, where the groundwater table is within 6 m, has also expanded from 0.742 km<sup>2</sup> to 1.472 km<sup>2</sup>. The Table 6 shows the impact of pumping (SCN4) and canal seepage (SCN5) on the water table.

The water table in the upland area away from the Musi River has gone down decreased, due to an increase in pumping (SCN 4) which is shown by the fact that the area with groundwater table within 6m from ground surface has been reduced from 4.446 Km<sup>2</sup> (SCN3) to 3.650 Km<sup>2</sup>(SCN4) during pre-monsoon. Here the gradient has become steeper and reversed locally from MW2-MW4 zone towards MW3 due to pumping action, Figure 9. In the riparian zone near the river, the groundwater table is primarily governed by the ponding levels and canal seepage.

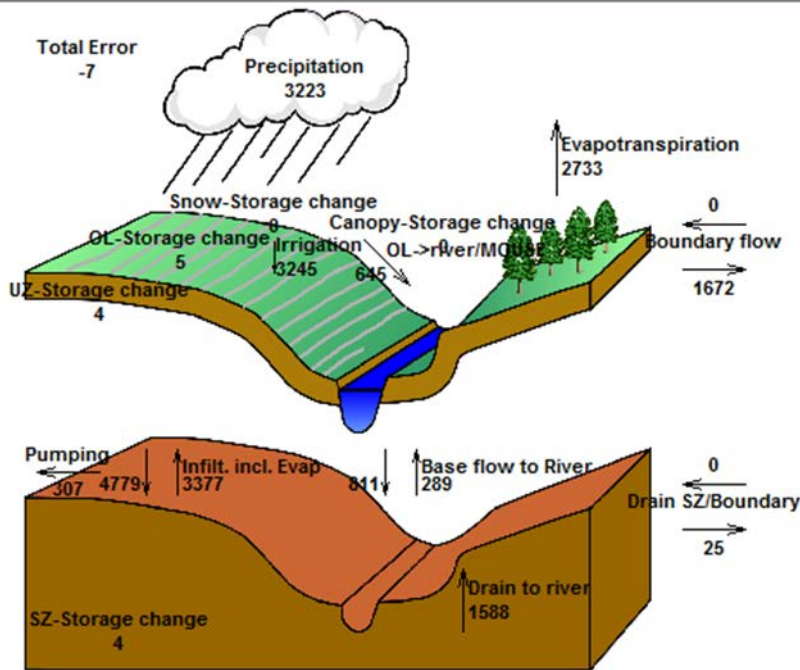
**Table 6 Area (km<sup>2</sup>) with groundwater table within 2m and 6m from ground surface**

| Scenario | Irrigated area (1.7 km <sup>2</sup> ) |       | Model domain (12.68km <sup>2</sup> ) |       | Period                |
|----------|---------------------------------------|-------|--------------------------------------|-------|-----------------------|
|          | ≤ 2 m                                 | ≤ 6 m | ≤ 2 m                                | ≤ 6 m |                       |
| SCN3     | 0.835                                 | 1.469 | 2.610                                | 5.160 | Post monsoon<br>(Nov) |
| SCN5     | 0.760                                 | 1.404 | 2.264                                | 4.738 |                       |
| SCN4     | 0.662                                 | 1.303 | 1.958                                | 4.104 |                       |
| SCN2     | 0.169                                 | 0.853 | 1.166                                | 3.179 |                       |
| SCN3     | 0.842                                 | 1.472 | 2.070                                | 4.446 | Pre Monsoon<br>(May)  |
| SCN5     | 0.774                                 | 1.422 | 1.937                                | 4.237 |                       |
| SCN4     | 0.724                                 | 1.318 | 1.757                                | 3.650 |                       |
| SCN2     | 0.112                                 | 0.742 | 0.785                                | 1.282 |                       |

### 6.5.2 Water balance

The MIKE SHE's water balance tool presents water balance results in depth-integrated terms.. The total water balance results are presented in a pictorial form showing various zones and the accumulated quantity of water in depth (mm) over the entire model domain area. To assess the water in volumetric terms, the depth has to be multiplied with the model domain area or sub area. Figure 10 presents the overall total water balance for the period from 5/1/2010 to 5/1/2014.

The above total water balance results could be further analysed at individual zone level. In MIKE SHE, the negative and positive sign has been considered for inflow and outflow respectively for a particular zone. For example, water leaving the canopy interception zone is positive and becomes negative for the overland, similarly, leaving overland as outflow (positive) and entering unsaturated zone as inflow (negative) . The detailed water balance analysis was done for the period 2010-2014 (4 years), covering the entire domain and the results are presented as an annual mean (in Mm<sup>3</sup>/year) as presented in Table 7.



Accumulated waterbalance from 5/1/2010 to 5/1/2014. Data type : Storage depth [millimeter].

**Figure 10 Total water balance output (depth integrated) showing movement and exchange**

The Table 7 presents the water balance in terms of mean annual (Mm<sup>3</sup>/year) for the baseline condition for the entire model domain of area 12.6828 Km<sup>2</sup> in terms of inflow, outflow, and change in storage, i.e. in book keeping approach, for each component. The water balance is presented as an mean annual of 4 years simulation results (5/1/2010 to 5/1/2014). The Table 7 shows the MIKE SHE's overall ability to simulate all the processes in sequential integrated manner and quantify the exchange of water among various zones. It shows the hydrodynamic characteristic of the area in relation to the movement of water flux from one zone to another. The direct exchange of water between saturated zone to overland and evaporation from saturated zone, confirms that the study area is a wetland type. In Table 7 below, the unsaturated zone (UZ) deficit of 0.03 Mm<sup>3</sup> is actually amount of air in the soil matrix /profile. It is opposite of UZ storage. Decreasing UZ deficit means soil is getting wetter. Similarly, water balance correction of -0.01 Mm<sup>3</sup> in unsaturated zone is to account for changing thickness of the UZ as the groundwater table rises and fall. The positive correction is for the falling groundwater table and negative corrections for the rising groundwater table. This water balance corrections of -0.01 Mm<sup>3</sup> in UZ is reflected in saturated zone storage (Table 7).

**Table 7 Detailed mean annual water balance statement in terms of inflow, outflow and storage (Mm<sup>3</sup>/year) for period 2010-2014 for scenario (SCN3)**

| Zone | Inflow | Outflow | Storage | Error |
|------|--------|---------|---------|-------|
|------|--------|---------|---------|-------|

|                  |   |        |       |       |       |
|------------------|---|--------|-------|-------|-------|
| Canopy           | Precipitation   | -10.22 |       |       |       |
|                  | Interception and evaporation  |        | 0.62  |       |       |
|                  | Error   |        |       | 0.00  | 0.00  |
| Overland         | Canopy through fall to OL   |        | 9.60  |       |       |
|                  | OL ponding  | -9.60  |       |       |       |
|                  | Irrigation  | -10.29 |       |       |       |
|                  | Direct evaporation from OL  |        | 5.26  |       |       |
|                  | Direct flow up from SZ to OL  | -10.68 |       |       |       |
|                  | Direct flow down from OL to SZ  |        | 10.55 |       |       |
|                  | Outflow from OL across the boundary   |        | 5.30  |       |       |
|                  | OL outflow to MIKE 11   |        | 2.04  |       |       |
|                  | OL Storage  |        |       | 0.02  | -0.02 |
|                  | Infiltration to UZ  |        | 7.37  |       |       |
| Unsaturated Zone | Infiltration from OL  | -7.37  |       |       |       |
|                  | Direct evaporation from top UZ node   |        | 0.64  |       |       |
|                  | Transpiration from root zone  |        | 2.11  |       |       |
|                  | UZ deficit.   |        |       | 0.03  |       |
|                  | Water balance correction to account for changing thickness of the UZ as the groundwater table rises and fall. |        |       | -0.01 |       |
| Saturated Zone   | Error   |        |       |       | 0.00  |
|                  | Recharge from UZ to SZ  |        | 4.61  |       |       |
|                  | Recharge from UZ  | -4.61  |       |       |       |
|                  | Direct upward flow from SZ to OL  |        | 10.68 |       |       |
|                  | Direct downward flow from OL ponded water to SZ   | -10.55 |       |       |       |
|                  | Evapotranspiration from SZ  |        | 0.03  |       |       |
|                  | Groundwater abstraction   |        | 0.97  |       |       |
|                  | SZ drainage out from boundary   |        | 0.08  |       |       |
|                  | SZ drainage to MIKE SHE river link  |        | 5.04  |       |       |
|                  | Infiltration MIKE SHE river link to SZ  | -2.57  |       |       |       |
|                  | Base flow from SZ to MIKE SHE River   |        | 0.92  |       |       |
|                  | Error   |        |       |       | 0.00  |
|                  | Storage   |        |       | 0.01  |       |

Overflowing weirs on the Musi River have raised the river water level and as a consequence, the water exchange pattern with surface water has also been altered. The impact of weirs on outflow was examined by simulating the model without weirs. The results show that weirs have reduced outflow from aquifer/sub surface to river resulting in rise in groundwater level and increase in residences time which in turn has a positive aspect in terms of water quality improvement. However, here it must be noted that in the current situation, the river is also polluted; therefore, the rise in river stage due to weirs



could be counter-productive if very huge pumping takes place in the catchment near riparian zone resulting in reversal of direction of groundwater gradient.

#### 6.5.1 Irrigation

The scenario SCN1 was simulated applying irrigation demand as per the time series developed based on field survey (Perrin, 2010). In the time series, it was assumed that there was no irrigation demand during monsoon period (August and September). Later, the scenario SCN3 was simulated assuming maximum allowable deficit (MAD) equal to 0.5 and irrigation demand was estimated intrinsically by the MIKE SHE. The average annual irrigation demand from field survey and simulated are 6.05 Mm<sup>3</sup> and 10.29 Mm<sup>3</sup> respectively. The RMSE values for the scenario SCN3 (simulated irrigation demand for maximum allowable deficit to 0.5 before applying water) was less than the RMSE values for the scenario SCN1 (user specified irrigation demand time series was supplied to the model as an input). This suggests that the current irrigation practice is to allow maximum deficit up to 0.5 (50%) before applying irrigation.

#### 6.5.2 Return flow

In general, return flow is defined (Langbein and Iseri, 1960) as the part of artificially applied irrigation water that was not lost by evapotranspiration and that either drains to the groundwater reservoir or runs off as overland and interflow to a surface-water body. Water that enters a saturated zone also eventually either discharges to a surface-water body, such as a lake, stream as base flow or may be pumped from a well. It also includes sewage / effluent discharged on land surface. The partitioning of aquifer recharge and direct runoff to surface-water bodies depends on the application rates and properties of soil profile. In the current case, as per above definition, the return flow is the summation of precipitation, irrigation and infiltration from canal and river minus total evapotranspiration from all the zones as:

Return flow= precipitation+irrigation+canal & river seepage-evapotranspiration

The total inflow, loss and return flow from different zones are presented in Table 8 below.

**Table 8 Total inflow, loss and return flow for different scenarios**

| Components   | SCN1  | SCN2   | SCN3   | SCN4   | SCN3*  |
|--|-------|--------|--------|--------|--------|
| <b>Inflow</b>  |       |        |        |        |        |
|  | -     |        |        |        |        |
| Precipitation(Mm <sup>3</sup> /year)                         | 10.22 | -10.22 | -10.22 | -10.22 | -2.14  |
| Irrigation (Mm <sup>3</sup> /year)                           | -6.05 | 0.00   | -10.29 | -10.52 | -10.17 |
| Infiltration from canal & Musi river (Mm <sup>3</sup> /year) | -2.85 | 0.00   | -2.57  | -2.61  | -2.56  |
|  | -     |        |        |        |        |
| <b>Total (Mm<sup>3</sup>/year)</b>                           | 19.12 | -10.22 | -23.08 | -23.35 | -14.87 |
| <b>Loss</b>  |       |        |        |        |        |
| Canopy evaporation (%)                                       | 3.13  | 5.41   | 2.70   | 2.67   | 1.03   |
| Overland evaporation (%)                                     | 27.90 | 23.84  | 22.78  | 22.18  | 19.84  |
| Soil evaporation (%)   | 3.41  | 6.93   | 2.77   | 2.76   | 0.85   |
| Saturated zone evaporation (%)                               | 0.11  | 0.19   | 0.13   | 0.13   | 0.18   |
| Plant transpiration (%)                                      | 10.03 | 23.50  | 9.16   | 9.19   | 3.21   |
| <b>Total loss (%)</b>  | 44.58 | 59.87  | 37.55  | 36.93  | 25.12  |
| <b>Return flow</b>   |       |        |        |        |        |
| Direct surface return flow (%)                               | 22.83 | 15.26  | 31.83  | 29.57  | 38.51  |
| Sub surface (interflow) flow (%)                             | 22.79 | 1.54   | 22.16  | 21.02  | 28.69  |
| Base flow-through aquifer (%)                                | 4.43  | 13.71  | 3.97   | 3.93   | 6.38   |
| Groundwater recovery (%)                                     | 5.08  | 9.51   | 4.21   | 8.32   | 1.13   |
| Storage (%)  | 0.17  | 0.00   | 0.18   | 0.15   | -0.05  |
| <b>Total return flow (%)</b>                                 | 55.30 | 40.01  | 62.35  | 62.99  | 74.66  |
| Error  | -0.12 | -0.12  | -0.10  | -0.08  | -0.22  |

**SCN\* represents irrigated area part of the domain**

The result for the current condition (SCN3) shows that about 38 % of water is due to consumptive loss and the total return flow is 62 %. The base flow contribution to the river is about 4-5 %. The water balance analysis was also done further for the sub area of the domain i.e. for the irrigated area. (Shown in column SCN3\* of Table 8). In the irrigated area part of the domain, the total loss and return flow accounted about 25 % and 75 % of the inflow respectively.

**6.5.3 Groundwater recharge**

The integrated modelling has confirmed that the area under study has wetland characteristics. Therefore, as expected the water table is very high and the exchange of water flux is taking place directly from saturated zone to overland flow and from overland to saturated zone and some evaporation is taking place from the saturated zone as well. Considering this, the water balance analysis has been done to estimate the net groundwater recharge for different scenarios as presented in Table 9. The groundwater recharge through unsaturated zone for SCN3 is 4.4 Mm<sup>3</sup>/year (20 % of total inflow to domain), Table . Since the overland and saturated zone is interacting water with each other, therefore, the net groundwater recharge has also been estimated to be about 19.26 %. However, the change in saturated zone storage is 0.01 Mm<sup>3</sup> (0.04 %) which means

that whatever amount of water that is added to the groundwater table is drained out as base flow or drainage and the saturated zone appears to be in equilibrium condition, i.e., neither rising nor depleting.. The groundwater recharge in the irrigated area (SCN3\*) is also not much different from the entire model domain average.

**Table 9 Groundwater recharge**

| Flow   | SCN1  | SCN2  | SCN3  | SCN4  | SCN3* |
|--|-------|-------|-------|-------|-------|
| Inflow (Mm <sup>3</sup> )                    | -19.1 | -10.2 | -23.1 | -23.3 | -14.8 |
| Recharge through UZ to SZ (Mm <sup>3</sup> ) | -4.7  | -2.5  | -4.6  | -5.1  | -2.8  |
| Direct flow from OL to SZ (Mm <sup>3</sup> ) | -7.9  | -2.4  | -10.5 | -9.0  | -7.7  |
| Direct flow from SZ to OL (Mm <sup>3</sup> ) | 9.2   | 2.4   | 10.7  | 8.9   | 7.6   |
| Evaporation from SZ (Mm <sup>3</sup> )       | 0.0   | 0.0   | 0.0   | 0.0   | 0.0   |
| Recharge (Mm <sup>3</sup> )                  | -3.3  | -2.5  | -4.4  | -5.2  | -2.8  |
| Recharge (%)                                 | 24.4  | 24.6  | 20.0  | 21.7  | 18.7  |
| Net recharge (%)                             | 17.5  | 24.7  | 19.3  | 22.1  | 19.0  |

#### 6.5.4 Groundwater exchange with MIKE 11- Musi river and wastewater canal

The canal and the Musi River are exchanging water with the groundwater zone. The entire coupled reach of the canal is in a losing state, i.e. due to canal seepage. However, the coupled reach of the Musi River is divided in two sub reaches by the second weir (Weir 2 in Figure 5). The coupled reach of the Musi River upstream of the Weir 2 is in ponding with raised river stage whereas the river stage downstream of the Weir 2 is very low. Since, the exchange of water takes place due to the water level difference between the channel water and the saturated zone cell water level, the coupled Musi river reach upstream of the Weir 2 is in losing state and infiltration is taking place from the river to the groundwater. The downstream of the Weir 2 in the coupled reach is in gaining state and is receiving groundwater as base flow, Figure 11 below. The negative values show that the river and canal are losing water, whereas positive values shows that the river is receiving water. The quantification of exchange of water between groundwater and surface water (influent or effluent) using Water balance tool for different reaches and branches directly is not supported in the current version of the water balance tool. This version gives the collective total exchange with groundwater from entire MIKE 11 coupled branches (Figure 10 and Table 7). The quantification of exchange of water between groundwater and surface water for each individual coupled reach or branch is important to understand the groundwater surface water interaction in many problems like, water logging due to canal seepage, contribution of water to a well from nearby river or unlined canal, conjunctive use of groundwater-surface water etc.

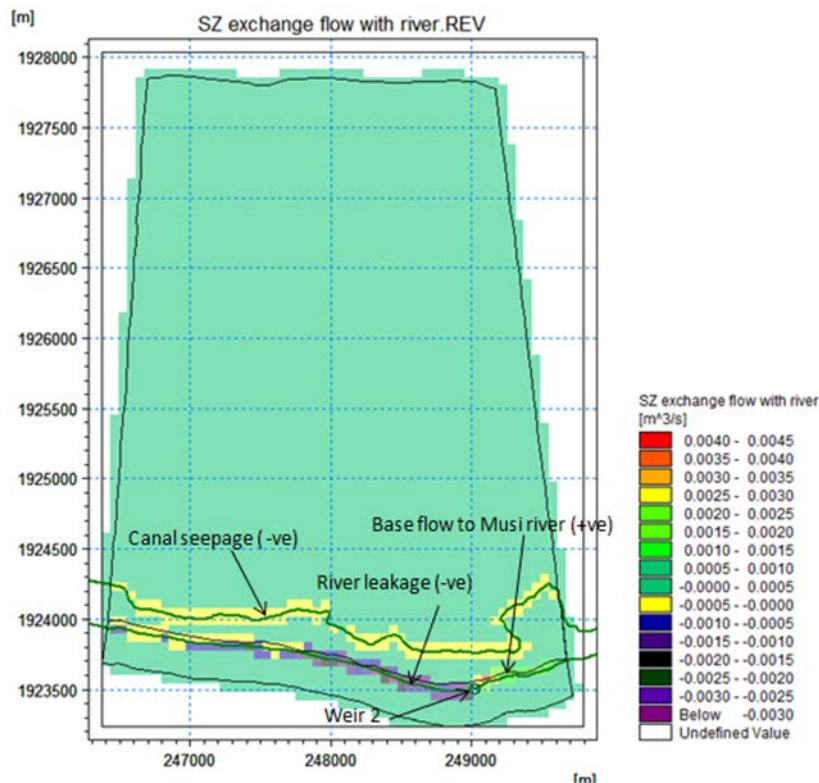


**Figure 11. Saturated zone exchange with MIKE 11-Canal and Musi River**

## 6.6 Conclusions and recommendations

The study area under consideration is a natural wetland influenced by anthropogenic activities. Since the irrigation infrastructures (human intervention) like the cascade of overflowing diversion weirs and the unlined canal system with year-round irrigation in the riverine zone have caused the area to function like a wetland, it can also be said that the study area is a man-made wetland in a natural setting. The study shows that both surface and sub-surface are represented based on the hydrodynamic characteristics. The basic difference between a constructed wetland and a natural wetland influenced by human activities like in the case of the Musi River wetland is that the boundary settings such as the inflow–outflow, and other parameters most of the time are unclear and not fully controlled. It is challenging to develop a physics-based distributed model for a natural system like the Musi wetland, which includes different perturbations like precipitation, canal inflow, river infiltration, modified boundary conditions (raised river water level) pumping, ponds etc.. However, a flexible, distributed and modular and user-friendly tool like MIKE SHE was able to accommodate multi-variant parameters that exist in nature to a reasonable extent.

The most important observation and recommendation from this study is that if a wetland is to be fed with wastewater, then hydrodynamic characteristics must be considered for design, operation and management. The key parameters of the system to be considered would be topography, well locations, withdrawal and boundary conditions. Further, surface and sub-surface flows should always be designed to occur towards the recipient river as outflow

system. In the present case, the action of wells have reversed the natural groundwater flow gradient slightly; however, the entire system appears to be in equilibrium condition in terms of the groundwater table flow direction. If the well density and the withdrawal increase for irrigation, domestic or commercial purposes, one can expect a change in the hydrodynamic behaviour of the existing system. Since the system is being fed with wastewater due to surface irrigation as well as sub surface canal and river seepage, further increase in agriculture command in the upland area does not appear to be a feasible scenario. The natural attenuation of contamination through soil and aquifer is also governed by the wastewater load and dry and wet cycles and the exact user specified time series of irrigation application. These parameters are important considerations that are often difficult to collect in real-time. The next modelling scenario can be on water quality modelling, which will be a separate study requiring a different modelling approach.

## 6.7 Application of the model

The MIKE SHE integrated hydrological modelling system was capable of demonstrating the highly complex flow processes that occur within the Musi River wetland. The analyses revealed that the area under study could be described as a wetland that has surface and subsurface flows, which is an important finding. The model utilized data arising from different studies for the same site for over 3 years (2012-2014). Usually, large data requirements of the modelling systems are a potential problem for the construction of models of wetland sites. While in general extensive site specific databases are required for integrated modelling, the experience gained in the development of the Musi model helped develop some recommendations that could be useful in the future, as ideal situations do not exist in nature. .

## 6.8 Acknowledgements

This research was conducted within the framework of the Saph Pani project and co-financed by the European Commission within the Seventh Framework Programme Grant agreement No. 282911.

## 6.9 References

- Amerasinghe, P., Weckenbrock, P., Simmons, R., Acharya, S., Drescher, A and Blummel, M., 2009. An atlas of water quality, health and agronomic risks and benefits associated with "Wastewater" irrigated agriculture, A study from the banks of the Musi River, India.
- Biggs, T.W. and Jiang, BinBin (2009). Soil Salinity and Exchangeable Cations in a Wastewater Irrigated Area, India. *Journal of Environmental Quality*, Volume 38, May–June.
- Crites, R.W., Middlebrooks, J, Reed, S.C., 2006. Natural wastewater treatment systems. Taylor and Francis.

- Daan J. Rooijen V, Turrall H. and Biggs T. W. (2005). "Sponge City: Water balance of mega city water use and wastewater use in Hyderabad, India", *Irrig. and Drain.* 54: S81–S91
- Dai Z., Trettin C. C., Li, C., Amatya, D.M., Sun G., and Li, H. 2010. Sensitivity of stream flow and water table depth to potential climatic variability in a coastal-forested watershed. Vol. 46, No. 5, *Journal of the American water resources association*,
- Demetriou C., Punthakey J.F., 1999. Evaluating sustainable groundwater management options using the MIKE SHE integrated hydrogeological modelling package. *Environmental Modelling & Software*, 14, 129–140
- DHI, 2014. MIKE SHE Technical reference, version 2014. DHI Water and Environment, Denmark
- Water Resources Institute (WRI), 2005. Ecosystems and Human Well-being: Wetland and Water, Synthesis*, Water Resources Institute, Washington, DC
- Hytteborn, J.2005. Irrigation with wastewater in Andhra Pradesh, India, A water balance evaluation along Peerzadiguda canal. Department of Soil Sciences, Swedish University of Agricultural Sciences, Ulls väg 17, SE 756 51 UPPSALA... Master thesis
- Hofstedt C., 2005. Wastewater use in Agriculture in Andhra Pradesh, India. An evaluation of irrigation water quality in reference to associated health risks and agricultural suitability. Department of Soil Sciences, Swedish University of Agricultural Sciences, Ulls väg 17, SE 756 51 UPPSALA... Master thesis
- Jensen, Jens Raunso (2005). Climate, water balance, irrigation, and nutrient loads. Technical Report of the Project Wastewater Reuse in Agriculture in Vietnam -A Case study on wastewater irrigated rice at Nam Dinh, Red River Delta, Vietnam. The Royal Veterinary and Agricultural University (KVL), Copenhagen, Denmark
- Jeroen H. J. Ensink, Christopher A. Scott, Simon Brooker, and Sandy Cairncross (2009). "Sewage disposal in the Musi-River, India: water quality remediation through irrigation infrastructure" *Irrig Drainage Syst*, DOI 10.1007/s10795-009-9088-4
- Langbein, W. B. and Iseri, K. T., 1960. "General Introduction and Hydrologic Definitions Manual of Hydrology: Part 1. General Surface-Water Techniques, USGS Water supply paper, 1541-A
- McCartney M., Scott, C. Ensink J., Jiang, B. and Biggs, T. 2008. Salinity Implications of Wastewater Irrigation in the Musi River Catchment in India. *Cey. J. Sci. (Bio. Sci.)* 37 (1): 49-59.
- Perrin, J, Ahmed, S, Dinis, L, Aellen, V.P., Amerasinghe, P, Pavelic, P and Schmitt,R, 2010. Groundwater processes in a micro-watershed influenced by wastewater in irrigation, peri urban Hyderabad, Scientific report.
- Rasmussen, T. 2008. Wetland hydrology, EPA, 822-R-08-024
- Refsgaard, J. C., Storm, B., Refsgaard, A., 1995. Recent developments of the Système Hydrologique Européen (SHE) towards the MIKE SHE, Modelling and

- Management of Sustainable Basin-scale Water Resource Systems (Proceedings of a Boulder, Symposium,). IAHS Publ. No. 231, 1995.
- Singh R., Subramanian, K., Refsgaard, J.C., 1999, Hydrological modelling of a small watershed using MIKE SHE for irrigation planning, *Agricultural Water Management*, 41, 149-166
- Schmitt, R 2010. "Wastewater reuse in Indian peri urban agriculture: Assessment of irrigation practices in a small, peri urban catchment in Hyderabad, Andhra Pradesh, India". M.Sc Thesis, ETHZ, Zurich.
- The Ramsar Convention Manual, 6th edition, 2013, Ramsar convention secretariat
- Thompson, J.R., Sørensen, H. R., Gavin, H., Refsgaard, A. 2004. "Application of the coupled MIKE SHE/MIKE 11 modelling system to a lowland wet grassland in southeast England". *Journal of Hydrology*, 293,151–179
- International water management institute (IWMI), 2001. *Wastewater Reuse in Agriculture in Vietnam: Water Management, Environment and Human Health Aspects* Proceedings of a Workshop held in Hanoi, Vietnam, 14 March 2001, working paper 30,
- Wijesekara, G.N., Farjad, B., Gupta, A. I, Qiao, Y., Delaney, P. and Danielle J. A, 2014. Comprehensive Land-Use/Hydrological Modelling System for Scenario Simulations in the Elbow River Watershed, Alberta, Canada, *Environmental Management* February 2014, Volume 53, Issue 2, pp 357-381